ACKNOWLEDGMENTS

The bulk of this work was undertaken during 6 months' leave of absence from the E.T.H. as a guest at the Oak Ridge National Laboratory, for which reason sincere thanks are extended to innumerable colleagues at both institutions. At the E.T.H. thanks are due principally to Professor P. Marmier and to the members of the Zürich group who generously permitted inclusion of their results prior to publication, B. Gobbi, T. Niewodniczanski, R. E. Pixley, M. P. Steiger, and R. Szostak; whereas at ORNL thanks are due principally to G. R. Satchler, D. E. Arnurius, R. H. Bassel, B. Buck, K. Denning, R. Drisko and F. Perey. Among the outstanding facilities at ORNL which were greatly appreciated, special mention must be made of the assistance in coding and computation on an IBM 7090 computer, and also of the preparation and photography of the many figures whose excellence is eloquent testimony to the Graphic Arts Department. Apart from the theoretical support of ORNL and the experimental support of ETH, the author finally wishes to acknowledge his gratitude for the realization of this project through financial support from the Swiss National Science Foundation and the patient support of his wife.

REVIEWS OF MODERN PHYSICS VOLUME 35, NUMBER 4 OCTOBER, 1963

Spherical Nuclei with Simple Residual Forces*

LEONARD S. KISSLINGER
Western Reserve University, Cleveland, Ohio
AND
RAYMOND A. SORENSEN
Carnegie Institute of Technology, Pittsburgh, Pennsylvania

CONTENTS

* Supported in part by the National Science Foundation, the United States Army Research Office, Durham, and the United States Office of Naval Research.

I. INTRODUCTION

THE large accumulation of data on the low-energy spectra of many nuclei has made it possible to study systematically and in detail the variation from nucleus to nucleus of various nuclear properties, such as level energies, moments, transition rates, and reaction rates. In many cases it has been possible to identify, in the low-energy spectrum, states which seem to correspond to the motion of a single particle

or quasi-particle in an effective field and states corresponding to collective vibrations or rotation of the nucleus. Moreover, there is now accumulating more information determining in which regions nuclei are spherical or deformed and which cases seem to correspond to the transformation between a spherical and a deformed equilibrium shape.

It has thus been useful to utilize a nuclear model from which the nuclear properties may be computed in detail for many nuclei over a large region of the periodic table. Such a model was that first studied in some detail by Belyaev[1] in which particles interact with a particularly simple two-body force. The force is represented by two simple components, the pairing force suggested by work in superconductivity and first discussed in relation to the nuclear problem by Bohr, Mottelson, and Pines,[2] and a long-range part represented by a quadrupole force as suggested by the work of Elliot.[3] Belyaev showed that the model contained the main qualitative features of nuclear spectra, including in particular the transition from the regions of spherical nuclei with their quadrupole vibrational spectra[4] to the regions of deformed nuclei with their associated vibrational and rotational modes of excitation.[5]

The first quantitative comparison of the model with experimental data was made by the authors[6] in a study of nuclei for which either the neutrons or protons completely fill a major shell. (This work is referred to here as I.) There have also been a number of calculations applying this model to deformed nuclei, with the result that one now believes that an important part of nuclear structure effects can be accounted for by these simple interactions.[7] The present work carries out a detailed study of nuclei from Ni to Pb in order to try to learn to what extent methods essentially the same as those used in I can be applied to the other spherical nuclei. Also some phenomena such as β decay, not treated previously owing to the restriction there to single closed-shell nuclei, are included.

The main assumption of the work is that the low-lying states of spherical nuclei can be treated in terms of two basic excitations, quasi-particles and phonons. For the most part these are treated as separate modes of motion. For even–even nuclei the lowest excitations are the phonons, and only these are treated in detail. For the odd-mass nuclei both of these modes of excitation are low in energy and must be considered, as well as their interactions. We trace the states of quasi-particles and phonons to see to what extent systematic trends of the experimental data can be followed.

While in I the shell-model levels (single-particle levels) were chosen separately in each of the nuclear regions considered, i.e., the Pb region, the Sn region, etc., in the present work these levels must be chosen once for all the nuclei in a large region of the isotope table, since all these nuclei are considered together. To obtain agreement with experimental results it is found necessary to include a smooth variation of the single-particle level spacings with A, and to use different level spacings for the neutrons and the protons. Because the neutrons and protons are filling different levels, the pairing force, which is effective only for shell-model pairs coupled to zero angular momentum, is assumed to exist only for protons and neutrons separately and is described by two strength parameters G_p and G_n. The quadrupole force is effective for protons, neutrons, and for proton–neutron pairs as well and so is described by three coupling constants χ_p, χ_n, χ_{np}.

With the chosen set of levels and coupling constants, the interaction is treated in the following manner. First, the pairing Hamiltonian is approximately diagonalized by the use of the quasi-particle transformation for neutrons and protons separately. The quadrupole force is then described as an interaction between the proton and neutron quasi-particles. The effect of this force is determined by the quasi-particle random-phase approximation, through which the phonons are introduced. Finally, for certain nuclear properties the effects of an additional short-range interaction are derived by the use of perturbation theory applied to the pairing plus quadrupole wave functions.

In Chap. II the quasi-particle transformation is described and results used here are derived. The proton–neutron short-range force is also discussed. The quasi-particle random-phase approximation as ap-

[1] S. T. Belyaev, Kgl. Danske Videnskab. Selskab. Mat-Fys. Medd. **31**, No. 11 (1959).

[2] A. Bohr, B. R. Mottelson, and D. Pines, Phys. Rev. **110**, 936 (1958). B. R. Mottelson, Notes from Cours de L'Ecole d'Ete de Physique Theorique des Houches, 283 (1958).

[3] J. P. Elliott, Proc. Roy. Soc. (London) **A245**, 128, 562 (1958).

[4] G. Scharff-Goldhaber and J. Wenesser, Phys. Rev. **98**, 212 (1955).

[5] A. Bohr, Kgl. Danske Videnskab. Selskab. Mat-Fys. Medd. **26**, No. 1 (1952). A. Bohr and B. R. Mottelson, Kgl. Danske Videnskab. Selskab. Mat-Fys. Medd. **27**, No. 16 (1953).

[6] L. S. Kisslinger and R. A. Sorensen, Kgl. Danske Videnskab. Selskab. Mat-Fys. Medd. **32**, No. 9 (1960), referred to hereafter as I.

[7] D. Bes, Kgl. Danske Videnskab. Selskab. Mat-Fys. Medd. **33**, No. 2 (1961). D. R. Bes and Z. Szymanski, Nucl. Phys. **28**, 42, 63 (1961). J. J. Griffen and M. Rich, Phys. Rev. **118**, 850 (1960). S. G. Nilsson and O. Prior, Kgl. Danske Videnskab. Selskab. Mat-Fys. Medd. **32**, No. 16 (1960). V. G. Soloviev, Kgl. Danske Videnskab. Selskab. Mat-Fys. Skrifter. **1**, No. 11 (1961). C. J. Gallagher and V. G. Soloviev, Kgl. Danske Videnskab. Selskab. Mat-Fys. Skrifter **2**, No. 2 (1962).

plied to the quadrupole force is then outlined, and the results compared with those of adiabatic perturbation theory. The results are compared with experimental energy level systematics in Chap. III. In Chap. IV, the systematic binding energy data is discussed. In Chaps. V and VI the static electromagnetic moments of the ground state and some excited states of nuclei are considered. Chapter VII treats the electromagnetic transition rates and Chap. VIII, the systematic data concerning beta decay.

II. DESCRIPTION OF HAMILTONIAN AND WAVE FUNCTIONS

A. The Hamiltonian

Starting from a shell model with a two-body interaction, we derive various single-particle and collective properties and compare the results with systematic data. Only the particles outside of the closed shells are treated explicitly, the particles in the core being neglected, except in so far as they give rise to the single-particle potential and renormalize certain properties of the nuclear particles, such as the charge.

The residual interaction consists of two components, a short-range part, which leads to an approximate seniority spectrum, plus a quadrupole interaction, which is mainly associated with the collective states. The pairing force used to approximate the short-range component in this work has the property that for two particles in a j level only the state of zero angular momentum (seniority zero) is affected. In the regions in which detailed comparison with experiments are attempted the neutrons and protons are for the most part being placed in different shell-model levels. This tends to make a force which acts most strongly in states with all particles coupled two-by-two to spin zero less effective between neutrons and protons than between like particles. For this reason, we use a pairing force only between neutrons and between protons separately, and neglect the neutron–proton, short-range interaction (except the spherical field producing part, as is described in the next section).

The notation is the same as in I, with $b^{\dagger\xi}_{jm}$ (b^{ξ}_{jm}) the creation (destruction) operators for shell-model particles of type (p,n)ξ, angular momentum j and z component m, with the time-reversed phases for the states $|j\ -\ m\rangle = b^{\dagger}_{j-m}|0\rangle$. Thus, the Hamiltonian is

$$\begin{aligned} H' = &\sum_{\substack{jm \\ \xi=\text{protons, neutrons}}} \epsilon^{\xi}_{j} b^{\dagger\xi}_{jm} b^{\xi}_{jm} - \tfrac{1}{4} \sum_{\substack{jj' \\ mm' \\ \xi}} G_{\xi} b^{\dagger\xi}_{j'm'} b^{\dagger\xi}_{j'-m'} b^{\xi}_{j-m} b^{\xi}_{jm} \\ &- \tfrac{1}{2}\chi_{\mathrm{p}} \hat{Q}^{\mathrm{p}} \cdot \hat{Q}^{\mathrm{p}} - \tfrac{1}{2}\chi_{\mathrm{n}} \hat{Q}^{\mathrm{n}} \cdot \hat{Q}^{\mathrm{n}} \\ &- \tfrac{1}{2}\chi_{np} (\hat{Q}^{\mathrm{p}} \cdot \hat{Q}^{\mathrm{n}} + \hat{Q}^{\mathrm{n}} \cdot \hat{Q}^{\mathrm{p}}) , \end{aligned} \tag{1}$$

in which $\hat{Q}$ is the quadrupole operator

$$\hat{Q}^{\xi}_{\mu} = \sum \langle j'm' | r^2 Y^2_{\mu} | jm \rangle b^{\dagger\xi}_{j'm'} b^{\xi}_{jm} , \tag{2}$$

the ϵ are the single-particle energies, and G_{p}, G_{n}, χ_{p}, χ_{n}, and χ_{np} are force constants which must be determined. The choice of these constants is limited by the calculation in the single closed-shell regions. From I one knows approximate values for G_{n}, G_{p}, χ_{n} and χ_{p}, however, one does not know the magnitude of χ_{np} from that work.

The only neutron–proton interaction which occurs explicitly in this Hamiltonian is via the quadrupole force. With this assumption the energy spectrum is extremely simple. The particlelike states are separated from the ground state by the smaller of the proton or neutron gap, the one-phonon vibrational state occurs in the gap (except in the few cases, when there is a low-lying 0+ first excited state), and the vibrational states with more than one phonon lie either in the gap or among the excited particle states. This work studies the solutions to this system in order to learn to what extent systematic nuclear data can be fit by such a model.

B. The Pairing Solutions

The first two terms of the Hamiltonian (1) constitute the pairing Hamiltonian, which is used to represent the short-range force because of the ease with which fairly accurate solutions can be found regardless of the number of particles involved. Since there exist rather complete descriptions of the method of solution based on the work in the theory of superconductivity[8] and of the accuracy of the results (including the effect of spurious states) for nuclear problems in the regions studied in the present work,[9] we limit ourselves to a brief discussion of the procedure in order to define the various quantities and to try to make the paper more self-contained. Since the neutron–proton pairing interaction is neglected, the procedure which is described below is applied to neutrons and protons separately and the index ξ is dropped.

First, a Bogolyubov–Valatin canonical transformation is carried out to introduce the "quasi-particle" creation and annihilation operators

$$\begin{aligned} \alpha_{jm} &= U_j b_{jm} - V_j b^{\dagger}_{j-m} , \\ \beta_{jm} &= U_j b_{j-m} + V_j b^{\dagger}_{jm} , \\ U_j^2 &+ V_j^2 = 1 , \end{aligned} \tag{3}$$

[8] J. Bardeen, L. N. Cooper, and J. R. Schrieffer, Phys. Rev. **108**, 1175 (1957), N. N. Bogoliubov, Zh. Eksperim. i Teor. Fiz. **34**, 58, 73 (1958) [English transl.: Soviet Phys—JETP **7**, 41, 51 (1958)]; Nuovo Cimento **1**, 794 (1958), J. G. Valatin, Nuovo Cimento **1**, 843 (1958).

[9] A. K. Kerman, R. D. Lawson, and M. H. Macfarlane, Phys. Rev. **124**, 162 (1961).

in which V_j^2 (U_j^2) is the probability of occupation (nonoccupation) of the j level. Since the seniority coupling scheme is specified, one needs to know only these quantities to specify the wave functions. The chemical potentials λ, introduced as Lagrangian multipliers to adjust the average number of protons and neutrons to correspond to the isotope under consideration, serve as the Fermi energies of the proton and neutron systems. The coefficients U_j and V_j are determined by the solution of the equations

$$\frac{G}{4}\sum_j \frac{2j+1}{E_j} = 1$$
$$\textstyle\sum_j (j+\frac{1}{2})[1-(\epsilon_j-\lambda)/E_j] = n\,, \qquad (4)$$

where n is the particle number, and the quantities

$$E_j = [(\epsilon_j-\lambda)^2+\Delta^2]^{\frac{1}{2}} \qquad (5)$$

are the quasi-particle energies. These are the energies of the elementary excitations from the ground state, which in turn depend upon the quantity Δ, defined by

$$\Delta = \tfrac{1}{2} G \textstyle\sum_j (2j+1)U_jV_j\,, \qquad (6)$$

which is approximately one-half the gap in the even proton or neutron spectrum. Having selected λ and Δ to satisfy Eq. (4) for protons and neutrons, one can obtain the occupation coefficients from the relationships

$$U_j^2 = \tfrac{1}{2}[1+(\epsilon_j-\lambda)/E_j]\,,$$
$$V_j^2 = \tfrac{1}{2}[1-(\epsilon_j-\lambda)/E_j]\,. \qquad (7)$$

The Hamiltonian (1) can be then approximately written as

$$H \cong E_0^{(0)} + \textstyle\sum_\xi \sum_{jm} E_j^\xi \alpha_{jm}^{\xi\dagger}\alpha_{jm}^\xi - \frac{1}{2}\sum_\xi \chi_\xi \hat{Q}^\xi\cdot\hat{Q}^\xi$$
$$- \tfrac{1}{2}\chi_{pn}(\hat{Q}^p\cdot\hat{Q}^n + \hat{Q}^n\cdot\hat{Q}^p)\,. \qquad (8)$$

The approximation made in Eq. (8) is the dropping of terms in the scattering of quasi-particles due to the pairing force and the neglect of the change of the quantities λ and Δ in the excited states. Although these latter effects are sometimes large, especially for the calculation of the states of odd-mass nuclei in the deformed region (e.g., see Soloviev[7]), in the region in which we calculate they are generally small [for an extensive study of the so-called blocking effect, see S. G. Nilsson (to be published)]. In the quasi-particle representation a single-particle operator of rank L,

$$\mathcal{O}_\mu^L = \sum \langle j'm'|\mathcal{O}_\mu^L|jm\rangle b_{j'm'}^\dagger b_{jm}$$

has the form

$$\mathcal{O}_\mu^L = \textstyle\sum_{jj'}\langle j||\mathcal{O}^L||j'\rangle(2L+1)^{-\frac{1}{2}}\{\frac{1}{2}(U_jV_{j'}\pm U_{j'}V_j)$$
$$\times[A_{jj'}^{L\mu\dagger}+(-1)^\mu A_{jj'}^{L-\mu}] + (U_jU_{j'}\mp V_jV_{j'})\eta_{jj'}^{L\mu}\}$$
$$+\delta_{L0}\textstyle\sum_j (2j+1)^{\frac{1}{2}}V_j^2\langle j||\mathcal{O}^L||j\rangle\,\frac{1}{2}(1\pm 1)\,, \qquad (9)$$

with the upper (lower) sign holding for an operator which does not (does) change sign upon time reversal. For convenience, two operators have been introduced in Eq. (9), the double quasi-particle creation operator

$$A_{jj'}^{LM\dagger} = [\alpha_j^\dagger\alpha_{j'}^\dagger]_M^L(-1)^{l+l'}\,, \qquad (10)$$

representing two quasi-particle creation operators vector coupled to form a tensor of rank L [with a phase $(-1)^{l+l'}$], and

$$\eta_{jj'}^{LM} = [\alpha_j^\dagger\alpha_{j'}]_M^L \qquad (11)$$

a tensor of rank L corresponding to the transition of a quasi-particle from state j to state j'. The explicit forms for these operators in terms of the quasi-particles with time-reversed phases are given in Appendix I, Eqs. (A1) and (A2). The two quasi-particles which are coupled to form $A_s^\dagger$ are always either both protons or both neutrons, and the notation $[\alpha_p^\dagger\alpha_n^\dagger]_m^L$ is used when we wish to consider a proton and a neutron quasi-particle vector coupled.

The eigenfunctions corresponding to the pairing part of the Hamiltonian are the quasi-particle states. For an even–even nucleus the (unnormalized) states are ψ_0^0, $A_{12}^{LM\dagger}\psi_0^0$, $[A_{12}^{L\dagger}A_{34}^{\lambda\dagger}]^{JM}\psi_0^0$, etc., with energies E_0^0, $E_0^0+E_1+E_2$, $E_0^0+E_1+E_2+E_3+E_4$, etc., respectively, the quasi-particle vacuum, the two quasi-particle states, the four quasi-particle states, etc. In each state there are an even number of proton and neutron quasi-particles. The ground state ψ_0^0 is the quasi-particle vacuum defined by

$$\alpha\psi_0^0 = 0\,. \qquad (12)$$

For an odd-mass nucleus the eigenfunctions are the one quasi-particle states $\alpha_{lm}^\dagger\psi_0^0$, the three quasi-particle states $[\alpha_1^\dagger A_{23}^{L\dagger}]^{JM}\psi_0^0$, etc., with energies $E_0^0+E_1$, $E_0^0+E_1+E_2+E_3$, etc. In each odd proton (neutron) state there are an odd number of proton (neutron) quasi-particles and an even number of the other type. The states of an odd–odd nucleus consist of odd numbers of both neutron and proton quasi-particles with an energy spectrum $E_0^0+E_1^n+E_2^p$, etc.

Since the gap separates the zero quasi-particle states from the two quasi-particle states, the low-lying states for the even–even nuclei are the zero and two quasi-particle states, and for odd–odd nuclei are the coupled one proton and one neutron quasi-particles. Therefore, insofar as the quadrupole terms can be neglected, the low-lying states of odd-mass nuclei have the simplicity of a single particle in several j levels, and the low-lying states of even–even (except for the ground state) and odd–odd nuclei appear as two-particle spectra in those same levels regardless of the number of nucleons involved. This

enables one to compare systematically the theoretical calculations to the experimental spectroscopic information with little difficulty. There is now good experimental evidence that there is a smooth and gradual variation of the particlelike states as one proceeds through the major shells, in agreement with the basic assumptions of this picture. In the next section, the effects of the quadrupole interaction are discussed, but first the neutron–proton short-range force will be considered.

The neutron–proton short-range force is expected to play an increasingly larger role as one treats nuclei of lighter mass. For the investigation of the role of this force in nuclear structure, the nuclei with one particle added to or removed from one closed shell and various numbers of nucleons outside of the other closed shell seem to give the most direct information. Silverberg, who has carried out extensive calculations for these isotopes, concludes that he must include a neutron–proton short-range force to account for the level systematics of these nuclei; he finds that he can successfully account for the general features of these systematics by calculating the radial overlap integrals between the neutron and proton[10] wave functions.

Let us consider the case of one proton outside of the proton closed shell and a δ-function interaction between the proton and various numbers of neutrons

$$V = \sum_{nn'} \langle p'n'|g\delta(r_p - r_n)|np\rangle b_p^\dagger b_n^\dagger b_n b_p . \quad (13)$$

A spin-dependent part gives no contribution for the δ-function force. Evaluating the energy shift due to this force in perturbation theory for the states with one proton and an even number of neutrons

$$\psi_{jp} = b_{jp}^{\dagger p}\psi_0^{(n)} = b_{jp}^{\dagger p} \prod_{jnm_n} (U_n + V_n b_{jnm_n}^{\dagger n} b_{jn-m_n}^{\dagger n})|0\rangle , \quad (14)$$

one finds for the energy shifts of these states

$$\Delta E_{jp} = \sum_{nn_l n j_n} (2j_n + 1) V_{jn}^2 g \int_0^\infty R_{np l_p}(r) R_{nn l_n}(r) r^2 dr . \quad (15)$$

The $R_{nl}(r)$ are the radial wave functions. Since the energy shifts ΔE_{jp} of the different proton levels are unequal, these can be interpreted as additional shifts in the single-particle levels as a function of A. However, the interpretation is complicated by the fact that there are other phenomena which can cause effective level shifts. For example, the particle interacts with the phonon (see next section), and the level spacings depend upon the parameters ϵ_j, G, and χ. Moreover, the addition of other long-range forces to the quadrupole force, to change the composition of the phonon, can alter the energy levels of the odd-mass isotopes without changing the systematics of the collective states.[11] In Chap. III systematic studies with these energy shifts ΔE are discussed.

Similarly, one can evaluate the interaction, Eq. (13), in pure quasi-particle states. Introducing the quasi-particle transformation (3), one finds that only the P_0 part of the force contributes and that, e.g., in proton one quasi-particle states $\alpha_p^\dagger \psi_0$, the energy shifts of the quasi-particle states ΔE^{qp} are[10]

$$\Delta E_{jp}^{qp} = (U_{jp}^2 - V_{jp}^2)\Delta E_{jp} . \quad (15')$$

For the lowest quasi-particle states $U^2 \approx V^2$ so these effects would tend to be reduced, and one would expect the maximum energy shifts at the single closed shell plus one nuclei.

There are also contributions which arise from the admixture of higher quasi-particle states. Because of the low-lying phonon states which can be accounted for by the quadrupole interaction, one can expect that the quadrupole part of the neutron–proton force might play an especially important role. This part is included in our Hamiltonian, as is described in the next section.

C. The Long-Range Force

1. *Even–Even Nuclei, QRPA Approximation*

The general experimental systematics[4] for the even–even nuclei in the regions which are treated in this work are that the first excited state is almost always a single 2+ state (at energy $\hbar\omega$ above the ground state) with a fast reduced E2 transition to the ground state. The next excited states, which are 2+, 4+, and 0+ states, are at roughly $2\hbar\omega$ excitation energy with a reduced E2 transition rate to the first 2+ state of the same order as that of the latter to the ground state, while the reduced M1 transitions from the second 2+ to the first 2+ state and the reduced E2 crossover transition to the ground state is much weaker. Although these systematics are not so regular or so striking as the analogous ones in the rotational region, these data strongly suggest that the lowest states of the even–even nuclei in this region are not properly described as two quasi-particle or other simple-particle states, but more nearly as quadrupole vibrational states.

Starting from the pairing force with its approximate quasi-particle solutions, one can see that the

[10] L. Silverberg, Arkiv Fysik **22**, 289 (1962); and work to be published.

[11] L. S. Kisslinger, Nucl. Phys. **35**, 114 (1962).

simplest additional force which gives rise to such adiabatic motions is the quadrupole interaction. Therefore, for the long-range-force component we use the quadrupole force. Whereas this force is important for particles in different orbits, it cannot be assumed to be effective only among proton pairs and neutron pairs as is the pairing force, but must also be effective as a proton–neutron interaction. There are then three coupling strength parameters χ_n, χ_p, and χ_{np}, and the Hamiltonian Eq. (8) including the effect of pairing and quadrupole forces may be written out in terms of the quasi-particle operators as

$$H - E_0^0 = \sum_p E_p(\alpha_p^\dagger\alpha_p + \beta_p^\dagger\beta_p) + \sum_n E_n(\alpha_n^\dagger\alpha_n + \beta_n^\dagger\beta_n) - \tfrac{1}{2}\chi_p\hat{Q}^p\cdot\hat{Q}^p - \tfrac{1}{2}\chi_n\hat{Q}^n\cdot\hat{Q}^n - \tfrac{1}{2}\chi_{np}(\hat{Q}^p\cdot\hat{Q}^n + \hat{Q}^n\cdot\hat{Q}^p), \tag{16}$$

where the subscript p, n refers to proton, neutron quasi-particle operators, and energies, respectively, and $\hat{Q}$ is the proton or neutron quadrupole-moment operator:

$$\hat{Q}_\mu = \sum_{\nu\nu'>0} q^\mu_{\nu\nu'}(U_\nu U_{\nu'} - V_\nu V_{\nu'})(\alpha_\nu^\dagger\alpha_{\nu'} + \beta_{\nu'}^\dagger\beta_\nu) \sum_{\nu\nu'>0} q^\mu_{\nu\nu'}(U_\nu V_{\nu'} + V_\nu U_{\nu'})(\alpha_\nu^\dagger\beta_{\nu'}^\dagger + \beta_\nu\alpha_{\nu'}) \tag{17}$$

and

$$q^\mu_{\nu\nu'} = \langle\nu|r^2Y^2_\mu|\nu'\rangle\,, \quad \nu = jm\,. \tag{18}$$

The lowest excited states of an even–even nucleus are the two quasi-particle states, where both are protons or neutrons. (A state of one neutron and one proton quasi-particle corresponds to an odd–odd nucleus.) The quadrupole force has its most pronounced effect on the states, in which the proton or neutron quasi-particle pair is coupled to 2+. The approximation of linearized equation of motion in terms of quasi-particle pairs called the quasi-particle random-phase approximation, referred to hereafter as QRPA, is used to treat this force.[12] The result is that only the 2+ states among the many two quasi-particle states are affected. In the absence of χ_{np}, the neutron and proton states remain independent and two 2+ states are lowered into the energy gap. One is a linear combination of neutron 2+ states and the other of proton 2+ states. In the presence of a large χ_{np} a single 2+ level, which is a linear combination of both proton and neutron 2+ states, is lowered into the energy gap. In the QRPA approximation, that 2+ level is the first excited state of a quadrupole harmonic oscillator in the sense that it is followed by an 0+ 2+ 4+ triplet at twice the energy, and by the other well-known levels at integral multiples of the energy $\hbar\omega$ of the lowest 2+ states. The previous calculations for single closed-shell nuclei (Ref. I) for which only one kind of particle is free to utilize the two-body force show that $\chi_n \approx \chi_p$. The experimental observation of only one low 2+ (and not a doublet) shows furthermore that χ_{np} must at least be a sizable fraction of χ_n and χ_p.

For even nuclei the QRPA approximation consists in dropping the first sum in Eq. (17). The justification for this is that the effect of this term is spread over many pair states of various angular momenta, and its matrix elements are small since they are proportional to the number of quasi-particles in the state. The second term of Eq. (17), the one which is retained, has its effect concentrated entirely on the 2+ pairs, and its matrix element is proportional to the number of participating particles rather than quasi-particles. The other approximations necessary for the solution of Eq. (16) all involve dropping terms of single-quasi-particle type spread over many angular momenta and so are consistent with the central approximation above.

We may approximate the independent quasi-particle Hamiltonian as

$$\sum_{\nu>0} E_\nu(\alpha_\nu^\dagger\alpha_\nu + \beta_\nu^\dagger\beta_\nu) \cong \tfrac{1}{2}\sum_{j_1j_2JM} \mathcal{E}(j_1j_2)A_{12}^{JM\dagger}A_{12}^{JM}\,, \tag{19}$$

since both sides of Eq. (19) have approximately the same commutator with all of the A and $A^\dagger$. In Eq. (19)

$$\mathcal{E}(j_1j_2) = E_{j_1} + E_{j_2}\,, \tag{20}$$

and $A_{12}^{JM\dagger}$ is the vector coupling of j_1 and j_2 quasi-particle creation operators to a total angular momentum of J, M defined by Eq. (A1).

The $A^\dagger$ have the commutation relation,

$$[A_{12}^{JM}, A_{1'2'}^{J'M'\dagger}] = \delta_{JJ'}\delta_{MM'}(\delta_{j_1j_1'}\delta_{j_2j_2'} - (-1)^{j_1+j_2+l_1+l_2}\delta_{j_1j_2'}\delta_{j_2j_1'}) + \text{single-quasi-particle scattering terms spread over many angular momenta.} \tag{21}$$

With the omission of the last term in Eq. (21), Eq.

[12] The approximation used here was applied to the electron gas by K. Sawada, Phys. Rev. **106**, 372 (1957); G. Wentzel, Phys. Rev. **108**, 1593 (1957). Application to the nuclear problem was made by R. Arvieu and M. Veneroni, Compt. Rend. **250**, 992, 2155 (1960), T. Marumori Prog. Theoret. Phys. (Kyoto) **24**, 331 (1960), and by M. Baranger, Phys. Rev. **120**, 957 (1960). Application to E2 systematics has been made by T. Tamura and T. Udagawa, Progr. Theoret. Phys. (Kyoto) **25**, 1051 (1961), and with the adiabatic approximation by J. Bro-Jorgensen and A. Haatuft, to be published. Octupole systematics have been considered by S. Yoshida, to be published. Shell-model calculations using a particle–hole interaction have been carried out for the dipole state by G. Brown and M. Bolsterli, Phys. Rev. Letters **3**, 472 (1959), and G. Brown, L. Castillejo, and J. Evans, Nucl. Phys. **22**, 1 (1961).

(19) describes a set of independent harmonic oscillators.

With the Wigner–Eckart theorem on Eq. (18), the retained term of Eq. (17) may be written in terms of the "A" operators

$$\hat{Q} = \sum_{jj'} Q_{jj'}[A^{2\mu\dagger}_{jj'} + (-1)^{\mu} A^{2-\mu}_{jj'}] , \qquad (22)$$

where

$$Q_{jj'} = \tfrac{1}{2}\, 5^{-\frac{1}{2}} \langle j||r^2 Y^2||j'\rangle (U_j U_{j'} + V_j V_{j'}) . \qquad (23)$$

In this approximation, the quadrupole terms of Eq. (16) produce a harmonic coupling among the otherwise independent harmonic oscillators described by the first two terms. The problem is simply to find the normal modes. The modes described by A^{JM}_{12}, $J \neq 2+$ are already normal and retain the energies $\varepsilon(j_1 j_2)$. Because of the commutation relation Eq. (21) only the $J = 2+$ modes are coupled. Since the coupling terms are themselves harmonic, the Hamiltonian Eq. (16) expressed in terms of its normal mode creation operators will be a set of uncoupled harmonic oscillators. Calling the creation operators for these oscillators $B^{\dagger}_{\omega}$ and their energies ω, and letting ψ_0 and E_0 be the ground state and ground-state energy of the Hamiltonian such that $B_{\omega}\psi_0 = 0$ one has (with the μ index suppressed)

$$(H - E_0)B^{\dagger}_{\omega}\psi_0 = [H, B^{\dagger}_{\omega}]\psi_0 = \omega B^{\dagger}_{\omega}\psi_0 . \qquad (24)$$

Since $[\hat{Q}, A^{J\neq 2\dagger}] = 0$, the $A^{J\neq 2\dagger}$ do form normal modes. For $J = 2$, one also wishes to consider higher excitations of the lowest mode oscillator, hereafter referred to as the phonon, which requires

$$[H, B^{\dagger}_{\omega}] = \omega B^{\dagger}_{\omega} \qquad (25)$$

as an operator equation. Let us define the commutators (which are c numbers in our approximation)

$$[A_{\xi}, B^{\dagger}_{\omega}] = r_{\omega}(\xi) , \qquad (26a)$$

$$[A^{\dagger}_{\xi}, B^{\dagger}_{\omega}] = s_{\omega}(\xi) , \qquad (26b)$$

where ξ stands for a proton or neutron pair $j_{p_1} j_{p_2}$ or $j_{n_1} j_{n_2}$ (with the two angular momenta coupled to $2+$). Taking the commutator of Eq. (25) with $A_{\xi=p}$ and $A^{\dagger}_{\xi=p}$ one obtains with the use of (16), (17), (19), and (21):

$$[\varepsilon(\mathrm{p}) - \omega] r_{\omega}(\mathrm{p}) = 2Q_{\mathrm{p}}\{\chi_{\mathrm{p}} \textstyle\sum_{\mathrm{p}'} Q_{\mathrm{p}'}[r_{\omega}(\mathrm{p}') + s_{\omega}(\mathrm{p}')] + \chi_{\mathrm{np}} \sum_{\mathrm{n}'} Q_{\mathrm{n}'}[r_{\omega}(\mathrm{n}') + s_{\omega}(\mathrm{n}')]\} , \qquad (27a)$$

$$[\varepsilon(\mathrm{p}) + \omega] s_{\omega}(\mathrm{p}) = 2Q_{\mathrm{p}}\{\chi_{\mathrm{p}} \textstyle\sum_{\mathrm{p}'} Q_{\mathrm{p}'}[r_{\omega}(\mathrm{p}') + s_{\omega}(\mathrm{p}')] + \chi_{\mathrm{np}} \sum_{\mathrm{n}'} Q_{\mathrm{n}'}[r_{\omega}(\mathrm{n}') + s_{\omega}(\mathrm{n}')]\} , \qquad (27b)$$

and two similar equations may be obtained using $A_{\xi=n}$ and $A^{\dagger}_{\xi=n}$. One may combine Eqs. (27a), (27b) to obtain

$$(\chi_{\mathrm{p}} S_{\mathrm{p}} - 1) \textstyle\sum_{\mathrm{p}'} Q_{\mathrm{p}'}[r_{\omega}(\mathrm{p}') + s_{\omega}(\mathrm{p}')] + \chi_{\mathrm{np}} S_{\mathrm{p}} \sum_{\mathrm{n}'} Q_{\mathrm{n}'}[r_{\omega}(\mathrm{n}') + s_{\omega}(\mathrm{n}')] = 0 , \qquad (27c)$$

and the two similar equations to obtain

$$\chi_{\mathrm{np}} S_{\mathrm{n}} \textstyle\sum_{\mathrm{p}'} Q_{\mathrm{p}'}[r_{\omega}(\mathrm{p}') + s_{\omega}(\mathrm{p}')] + (\chi_{\mathrm{n}} S_{\mathrm{n}} - 1) \sum_{\mathrm{n}'} Q_{\mathrm{n}'}[r_{\omega}(\mathrm{n}') + s_{\omega}(\mathrm{n}')] = 0 , \qquad (27d)$$

where

$$S_{\mathrm{p}} = 4 \textstyle\sum_{\mathrm{p}} (Q_{\mathrm{p}})^2 \varepsilon(\mathrm{p}) / [\varepsilon(\mathrm{p})^2 - \omega^2] , \qquad (28)$$

and a similar equation defines S_{n}. Since Eqs. (27) are linear and homogeneous in the sums on $r_{\omega} + s_{\omega}$ they will have solutions only for certain values of ω, namely, those satisfying the relation

$$(\chi_{\mathrm{p}} S_{\mathrm{p}} - 1)(\chi_{\mathrm{n}} S_{\mathrm{n}} - 1) - \chi^2_{\mathrm{np}} S_{\mathrm{p}} S_{\mathrm{n}} = 0 . \qquad (29)$$

The nature of the solutions ω satisfying Eq. (29) is easily seen. If $\chi_{\mathrm{np}} = 0$ we get solutions when either $\chi_{\mathrm{p}} S_{\mathrm{p}} = 1$ or $\chi_{\mathrm{n}} S_{\mathrm{n}} = 1$. Each of these equations has as the number of solutions the number of proton (neutron) pair states coupling to $2+$. For $\chi_{\mathrm{p}} > 0$, $\chi_{\mathrm{n}} > 0$ the lowest proton ω will lie below $\varepsilon(\mathrm{p})$ minimum and the lowest neutron ω below $\varepsilon(\mathrm{n})$ minimum. The larger the χ, the lower the state is (until for sufficiently large χ, ω^2 passes zero and becomes negative corresponding to a permanent deformation). There may thus be two low-energy $2+$ states in this case. The effect on these states of changing χ_{np} from zero is also easily seen. The product $(\chi_{\mathrm{p}} S_{\mathrm{p}} - 1)(\chi_{\mathrm{n}} S_{\mathrm{n}} - 1)$ must now be positive. Thus, the lower of the two $\chi_{\mathrm{np}} = 0$ levels must be lowered farther making each factor above positive, while the higher energy is raised making each factor negative. For sufficiently large χ_{np} there will be essentially only one ω left in the energy gap. In particular, for $\chi^2_{\mathrm{np}} = \chi_{\mathrm{n}}\chi_{\mathrm{p}}$, Eq. (29) becomes

$$\chi_{\mathrm{n}} S_{\mathrm{n}} + \chi_{\mathrm{p}} S_{\mathrm{p}} = 1 . \qquad (30)$$

For Eq. (30) to be satisfied it is clear that the lowest ω is below the lowest $\varepsilon(\xi)$ while the other ω's are spaced with one ω between each adjacent pair of energies $\varepsilon(\xi)$. The spectrum in this case is similar to that of the single closed-shell case.

The reduced electromagnetic transition rate from the lowest $2+$ to $0+$ may easily be computed. We have

$$B(\mathrm{E2}) = |\langle\psi_0|\hat{Q}_e|B^{\dagger}_{\omega}\psi_0\rangle|^2 = |\textstyle\sum_{\mathrm{p}} Q_{\mathrm{p}}[r_{\omega}(\mathrm{p}) + s_{\omega}(\mathrm{p})] e^{\mathrm{p}}_{\mathrm{eff}} + \sum_{\mathrm{n}} Q_{\mathrm{n}}[r_{\omega}(\mathrm{n}) + s_{\omega}(\mathrm{n})] e^{\mathrm{n}}_{\mathrm{eff}}|^2 \qquad (31)$$

where e^{ξ}_{eff} are the total effective charge for protons and neutrons, respectively. From Eq. (26) we see that

$$B^{\dagger}_{\omega} = \tfrac{1}{2} \sum_{\xi} [r_{\omega}(\xi) A^{\dagger}_{\xi} - s_{\omega}(\xi) A_{\xi}] , \tag{32}$$

so the normalization condition on B_{ω} requires

$$[B_{\omega}, B^{\dagger}_{\omega}] = \tfrac{1}{2} \sum [|r_{\omega}(\xi)|^2 - |s_{\omega}(\xi)|^2] = 1 . \tag{33}$$

Aside from this over-all normalization Eqs. (27a)–(27d) show that for positive χ_{np}

$$r_{\omega}(\mathrm{p}) = [S_{\mathrm{n}}(1 - \chi_{\mathrm{n}} S_{\mathrm{n}})]^{\frac{1}{2}} Q_{\mathrm{p}} / [\mathcal{E}(\mathrm{p}) - \omega] , \tag{34a}$$

$$s_{\omega}(\mathrm{p}) = [S_{\mathrm{n}}(1 - \chi_{\mathrm{n}} S_{\mathrm{n}})]^{\frac{1}{2}} Q_{\mathrm{p}} / [\mathcal{E}(\mathrm{p}) + \omega] , \tag{34b}$$

$$r_{\omega}(\mathrm{n}) = [S_{\mathrm{p}}(1 - \chi_{\mathrm{p}} S_{\mathrm{p}})]^{\frac{1}{2}} Q_{\mathrm{n}} / [\mathcal{E}(\mathrm{n}) - \omega] , \tag{34c}$$

$$s_{\omega}(\mathrm{n}) = [S_{\mathrm{p}}(1 - \chi_{\mathrm{p}} S_{\mathrm{p}})]^{\frac{1}{2}} Q_{\mathrm{n}} / [\mathcal{E}(\mathrm{n}) + \omega] . \tag{34d}$$

Thus, we have

$$B(\mathrm{E2}) = \frac{|[S_{\mathrm{n}}(1 - \chi_{\mathrm{n}} S_{\mathrm{n}})]^{\frac{1}{2}} S_{\mathrm{p}} e^{\mathrm{p}}_{\text{eff}} + [S_{\mathrm{p}}(1 - \chi_{\mathrm{p}} S_{\mathrm{p}})]^{\frac{1}{2}} S_{\mathrm{n}} e^{\mathrm{n}}_{\text{eff}}|^2}{8\omega\{S_{\mathrm{n}}(1 - \chi_{\mathrm{n}} S_{\mathrm{n}}) \sum_{\mathrm{p}} (Q_{\mathrm{p}})^2 \mathcal{E}(\mathrm{p}) / [\mathcal{E}(\mathrm{p})^2 - \omega^2]^2 + S_{\mathrm{p}}(1 - \chi_{\mathrm{p}} S_{\mathrm{p}}) \sum_{\mathrm{n}} (Q_{\mathrm{n}})^2 \mathcal{E}(\mathrm{n}) / [\mathcal{E}(\mathrm{n})^2 - \omega^2]^2\}} . \tag{35}$$

For the numerical results, the effective charge for protons and neutrons have been taken as $2e$, and e, respectively. The majority of the computations were performed with the parameters of quadrupole coupling all chosen equal, i.e., $\chi_{\mathrm{p}} = \chi_{\mathrm{n}} = \chi_{\mathrm{np}}$. In that case the $B(\mathrm{E2})$ value takes the simpler form

$$\underset{\chi,\mathrm{s\ equal}}{B(\mathrm{E2})} = \frac{|S_{\mathrm{p}} e^{\mathrm{p}}_{\text{eff}} + S_{\mathrm{n}} e^{\mathrm{n}}_{\text{eff}}|^2}{8\omega\{\sum_{\mathrm{p}} (Q_{\mathrm{p}})^2 \mathcal{E}(\mathrm{p}) / [\mathcal{E}(\mathrm{p})^2 - \omega^2]^2 + \sum_{\mathrm{n}} (Q_{\mathrm{n}})^2 \mathcal{E}(\mathrm{n}) / [\mathcal{E}(\mathrm{n})^2 - \omega^2]^2\}} . \tag{36}$$

2. Even–Even Nuclei, the Adiabatic Limit

Condition (29) may be rewritten

$$\begin{vmatrix} \chi_{\mathrm{p}} - 1/S_{\mathrm{p}} & \chi_{\mathrm{np}} \\ \chi_{\mathrm{np}} & \chi_{\mathrm{n}} - 1/S_{\mathrm{n}} \end{vmatrix} = 0 . \tag{37}$$

In the adiabatic limit, i.e., for any ω such that

$$\omega^2 \ll \mathcal{E}^2(\xi)_{\text{minimum}} , \tag{38}$$

we may write

$$S^{-1}_{\xi} = \tfrac{1}{2} \mathfrak{A}^{-1}_{\xi} (1 - \omega^2 \mathfrak{B}_{\xi} / \mathfrak{A}_{\xi}) , \tag{39}$$

where

$$\mathfrak{A}_{\xi} = 2 \sum_{\xi} (Q_{\xi})^2 / \mathcal{E}(\xi) , \tag{40a}$$

$$\mathfrak{B}_{\xi} = 2 \sum_{\xi} (Q_{\xi})^2 / \mathcal{E}(\xi)^3 . \tag{40b}$$

In this limit Eq. (37) may be written

$$\begin{vmatrix} (\tfrac{1}{2} \mathfrak{A}^{-1}_{\mathrm{p}} - \chi_{\mathrm{p}}) - \tfrac{1}{2} \omega^2 \mathfrak{B}_{\mathrm{p}} \mathfrak{A}^{-2}_{\mathrm{p}} & \chi_{\mathrm{np}} \\ \chi_{\mathrm{np}} & (\tfrac{1}{2} \mathfrak{A}^{-1}_{\mathrm{n}} - \chi_{\mathrm{n}}) - \tfrac{1}{2} \omega^2 \mathfrak{B}_{\mathrm{n}} \mathfrak{A}^{-2}_{\mathrm{n}} \end{vmatrix} = 0 . \tag{41}$$

There are two values of ω^2 which satisfy Eq. (41). Either one or both of these roots may satisfy the inequality (38). In the first case only that lowest root will be an approximate solution to the original relation Eq. (29). In the latter case (which will hold only for relatively small χ_{np}), both roots are approximate solutions of Eq. (29).

It is easy to show that Eq. (41) is also the result of adiabatic perturbation theory. The quadrupole force is replaced by the interaction of each particle with two quadrupole fields—a neutron and a proton field. The self-consistency conditions are applied that each field have the same quadrupole moment as the corresponding particles. The inertial parameters are calculated as in I. The resulting collective Hamiltonian written in terms of the collective parameters $\overline{Q}$ is derived in the same fashion as in I.

$$H = \tfrac{1}{2} \overline{C}_{\mathrm{p}} \overline{Q}^2_{\mathrm{p}} + \tfrac{1}{2} \overline{C}_{\mathrm{n}} \overline{Q}^2_{\mathrm{n}} - \chi_{\mathrm{np}} \overline{Q}_{\mathrm{n}} \overline{Q}_{\mathrm{p}} + \tfrac{1}{2} \overline{B}_{\mathrm{p}} (d\overline{Q}_{\mathrm{p}}/dt)^2 + \tfrac{1}{2} \overline{B}_{\mathrm{n}} (d\overline{Q}_{\mathrm{n}}/dt)^2 \tag{42}$$

with

$$\overline{C}_{\xi} = \tfrac{1}{2} \mathfrak{A}^{-1}_{\xi} - \chi_{\xi} , \tag{43a}$$

$$\overline{B}_{\xi} = \tfrac{1}{2} \mathfrak{B}_{\xi} \mathfrak{A}^{-2}_{\xi} . \tag{43b}$$

It is then easy to show that the normal mode energies of Eq. (42) are just given by Eq. (41).

In the special case $\chi_{\mathrm{n}} = \chi_{\mathrm{p}} = \chi_{\mathrm{np}} = \chi$ the adiabatic limit to Eq. (29) takes the particularly simple form

$$\omega^2 = (\mathfrak{B}_{\mathrm{p}} + \mathfrak{B}_{\mathrm{n}})^{-1} [(2\chi)^{-1} - (\mathfrak{A}_{\mathrm{p}} + \mathfrak{A}_{\mathrm{n}})] . \tag{44}$$

Equation (44) is also the result of an adiabatic-perturbation theory calculation. In this case a single-quadrupole field is introduced which acts with equal strength, given by the parameter χ, on protons and neutrons. A single self-consistency condition is applied that the field have the same quadrupole moment as that of all the neutrons and protons taken together. The resulting collective Hamiltonian describes harmonic vibrations with a frequency given in the adiabatic limit by Eq. (44).

The adiabatic limit to the $B(E2)$ value Eq. (35) is also obtained by adiabatic-perturbation theory, with the assumption that the lowest 2+ state of Eq. (42) contain the entire quadrupole matrix element with the ground state. Thus, in the adiabatic limit, QRPA and the harmonic oscillating quadrupole field model are identical. For weaker quadrupole coupling, the QRPA has the advantage of going to the correct limit while in the oscillator model, the vibration is introduced as an extra degree of freedom which persists to zero coupling.

It should be emphasized that the QRPA requires a large effective degeneracy and a domination of pairing effects. If Δ/G is not sufficiently large, the η terms can be as important as the $A^\dagger$ terms and, for example, the ground state can be lowered in energy more than the 2+ state by the $P^{(2)}$ force.[13]

3. *Odd-Mass Nuclei*

In odd-mass nuclei, the low states (in the absence of quadrupole coupling) are the states of one quasi-particle. With quadrupole coupling there will be in addition some number of phonons. Considering only the degrees of freedom associated with the phonons and the quasi-particle we may obtain the approximate Hamiltonian for the odd-mass system by simply adding to the phonon Hamiltonian $H_{\text{phonon}} = \omega B_\omega^\dagger B_\omega$ [which comes from Eq. (24)], the energy of the quasi-particle given by $\sum_\nu E_\nu(\alpha_\nu^\dagger\alpha_\nu + \beta_\nu^\dagger\beta_\nu)$, and the interaction between the quasi-particle and the phonons. The ω is the phonon energy, i.e., the energy of the lowest oscillator. The phonon operators B_ω and the quasi-particle operators α, β are treated as independent variables, i.e., the equality $[B_\omega,\alpha^\dagger] = 0$ is assumed. This is justified by the fact that a phonon contains only a small amplitude for the presence of any particular quasi-particle. The interaction referred to above, between the quasi-particle and the phonon, arises from terms in the quadrupole part of the original Hamiltonian obtained from the first sum of Eq. (17). Specifically, from the term $\hat{Q}\cdot\hat{Q}$ the cross term is retained in which one of the $\hat{Q}$ is approximated by Eq. (22), and the other retains the scattering term $\sum q^\mu_{\nu\nu'}(U_\nu U_{\nu'} - V_\nu V_{\nu'})(\alpha_\nu^\dagger\alpha_{\nu'} + \beta_{\nu'}^\dagger\beta_\nu)$. Although this term is dropped for even–even nuclei, for odd-mass nuclei it must be retained since it can scatter the odd quasi-particle causing energy shifts comparable to the original single-particle separations. This interaction term may be written in terms of η and $A^\dagger$ of Eqs. (10) and (11), for a proton quasi-particle as

$$\begin{aligned} H_{\text{int}} = {} & \textstyle\sum_\mu (-1)^\mu \sum_{jj'} 5^{-\frac{1}{2}}\langle j||r^2Y^2_\mu||j'\rangle \\ & \times (U_jU_{j'} - V_jV_{j'})\eta^{2\mu}_{jj'} \\ & \times \{-\chi_{\text{p}} \textstyle\sum_{\text{p}} Q_{\text{p}}[A_{\text{p}}^{2-\mu\dagger} + (-1)^\mu A_{\text{p}}^{2\mu}] \\ & - \chi_{\text{np}} \textstyle\sum_{\text{n}} Q_{\text{n}}[A_{\text{n}}^{2-\mu\dagger} + (-1)^\mu A_{\text{n}}^{2\mu}]\}\,, \end{aligned} \tag{45}$$

and a similar expression occurs for a neutron quasi-particle. By the use of the inverse transformation to Eq. (32),

$$A_\xi^\dagger = \textstyle\sum_\omega [r_\omega(\xi)B_\omega^\dagger + s_\omega(\xi)B_\omega]\,, \tag{46}$$

the interaction term Eq. (45) may be written in terms of B_ω and $B_\omega^\dagger$. If only the phonon and odd-quasi-particle degrees of freedom are considered the odd-proton Hamiltonian may be written

$$\begin{aligned} H_{\text{odd}} = {} & \sum_{\substack{\nu=\\ \text{proton}}} E_\nu(\alpha_\nu^\dagger\alpha_\nu + \beta_\nu^\dagger\beta_\nu) + \omega\sum_\mu B_\omega^{\mu\dagger}B_\omega^\mu - \sum_\mu (-1)^\mu 5^{-\frac{1}{2}}\langle j||r^2Y^2||j'\rangle(U_jU_{j'} - V_jV_{j'})\eta^{2\mu}_{jj'} \\ & \times [B_\omega^{-\mu\dagger} + (-1)^\mu B_\omega^\mu] \\ & \times \frac{\chi_{\text{p}}[S_{\text{n}}(1-\chi_{\text{n}}S_{\text{n}})]^{\frac{1}{2}}S_{\text{p}} + \chi_{\text{np}}[S_{\text{p}}(1-\chi_{\text{p}}S_{\text{p}})]^{\frac{1}{2}}S_{\text{n}}}{(8\omega)^{\frac{1}{2}}\{S_{\text{n}}(1-\chi_{\text{n}}S_{\text{n}})\sum_{\text{p}}(Q_{\text{p}})^2\varepsilon(\text{p})/[\varepsilon(\text{p})^2-\omega^2]^2 + S_{\text{p}}(1-\chi_{\text{p}}S_{\text{p}})\sum_{\text{n}}(Q_{\text{n}})^2\varepsilon(\text{n})/[\varepsilon(\text{n})^2-\omega^2]^2\}^{\frac{1}{2}}}\,. \end{aligned} \tag{47}$$

In writing Eq. (47) we have included, for the quadrupole interaction, part but not all of the contributions from the three or more quasi-particle states. In some cases the effects of the P_2 force on the quasi-particle states are not properly described in this manner, e.g., in the V^{51} calculation of I, the low-lying 5/2 state, which is associated mainly with the seniority three state of the $(f_{7/2})^3$ configuration, is predicted by an exact solution of the pairing plus quadrupole interactions, while this state would remain high in energy if one used the Hamiltonian (47). Although the phonon–quasi-particle interaction does not always reproduce accurately the quadrupole effects, in the regions included in this work the phonon states are much lower in energy than the two and more quasi-particle states (in the even–even nuclei) whenever the quadrupole effects are large, so one can expect that the Hamiltonian (47) will include the largest quadrupole effects for the states arising from the one quasi-particle states in the absence of a

[13] I. Hamamoto and A. Arima, Nucl. Phys. **37**, 457 (1962).

quadrupole interaction. However, for the states which arise from the seniority three states, e.g., the low-lying states of spin $j-1$ for pure j configurations such as in the V^{51} case, one would not expect that the interaction will properly treat the effect of the three quasi-particle states.

This Hamiltonian Eq. (47) which is in the form of an intermediate coupling between quasi-particles and phonons[14] is diagonalized including the quasi-particle states together with all admixed states containing up to two phonons. The matrix elements for this calculation aside from the U, V factor and the r, s factor are just those given by Chaudhury.[14] The no-phonon and one-phonon matrix elements are

$$\langle\alpha_j|H_{\rm odd}|(B^\dagger\alpha_{j'})_j\rangle = -\bar{\chi}(5/4\pi)^{\frac{1}{2}}\langle j|r^2|j'\rangle C^{2jj'}_{0\frac{1}{2}\frac{1}{2}} \times (U_jU_{j'}-V_jV_{j'}) . \quad (48)$$

As the two-phonon states are weakly admixed in low states, the fact that $[B^\dagger B^\dagger]_I\psi_0$ may not describe them very well does not introduce much error. The one-phonon to two-phonon elements are

$$\langle(B\alpha_j)_J|H_{\rm odd}|[(B^\dagger B^\dagger)_I\alpha^\dagger_{j'}]_J\rangle = -\bar{\chi}(5/2\pi)^{\frac{1}{2}}\langle j|r^2|j'\rangle \times C^{2jj'}_{0\frac{1}{2}\frac{1}{2}}\cdot[(2I+1)(2j+1)]^{\frac{1}{2}} \times W(22Jj';Ij)(U_jU_{j'}-V_jV_{j'}) . \quad (49)$$

The effective coupling constant $\bar{\chi}$ is

$$\bar{\chi} = \frac{\chi_{\rm p}[S_{\rm n}(1-\chi_{\rm n}S_{\rm n})]^{\frac{1}{2}}S_{\rm p} + \chi_{\rm np}[S_{\rm p}(1-\chi_{\rm p}S_{\rm p})]^{\frac{1}{2}}S_{\rm n}}{(8\omega)^{\frac{1}{2}}\{S_{\rm n}(1-\chi_{\rm n}S_{\rm n})\sum_{\rm p}(Q_{\rm p})^2\mathcal{E}({\rm p})/[\mathcal{E}({\rm p})^2-\omega^2]^2 + S_{\rm p}(1-\chi_{\rm p}S_{\rm p})\sum_{\rm n}(Q_{\rm n})^2\mathcal{E}({\rm n})/[\mathcal{E}({\rm n})^2-\omega^2]^2\}^{\frac{1}{2}}} . \quad (50)$$

The equations for an odd-neutron nucleus are the same type. The diagonalization of Eq. (47) was performed on an electronic computer and the wave functions and energies of all levels up to 1 MeV and higher in some cases were retained. The results of this diagonalization are presented in the following section, together with the results on energy systematics for even nuclei and a few comments on odd–odd nuclei.

III. ENERGY-LEVEL SYSTEMATICS

Since in the systematic studies of even–even, odd–odd, and odd-mass nuclei for the spherical region one is generally concerned with quite different aspects of nuclear structure, we shall treat these systems separately. For the even–even nuclei the main energy-level systematics concern the positions of the vibrational levels, while for the odd-mass nuclei one has information both about the positions of the quasi-particle states and the states of quasi-particles and phonons, and these states are often strongly admixed. For the odd–odd nuclei the experimental data is not so extensive, and seems mainly to give information about the states of proton and neutron quasi-particles.

[14] This kind of coupling was suggested by the work of J. Rainwater, Phys. Rev. **79**, 432 (1950), and L. L. Foldy and F. J. Milford, Phys. Rev. **80**, 751 (1950). Detailed calculations were then made by A. K. Kerman, Phys. Rev. **92**, 1176 (1953); D. C. Choudhury, Kgl. Danske Videnskab. Selskab. Mat.-Fys. Medd. **28**, No. 4 (1954); K. Ford and C. Levenson, Phys. Rev. **100**, 1 (1955), and more recently by N. K. Glendenning, Phys. Rev. **119**, 213 (1960). The formalism of the present work was applied to the single closed-shell nuclei by R. A. Sorensen, Nucl. Phys. **25**, 674 (1961).

A. The Parameters and Description of Method of Calculation

1. *The Interaction Strength Parameters*

The parameters which enter into the determination of the energy levels, and the wave functions which are used subsequently to calculate the other properties, are the two pairing force strength parameters, $G_{\rm p}$ and $G_{\rm n}$, the three long-range-force parameters, $\chi_{\rm n}$, $\chi_{\rm p}$, and $\chi_{\rm np}$, and the single-particle energy-level parameters ϵ_j. A fourth parameter g, defined in Eq. (13), is used for studies to try to determine the ϵ_j's, but does not actually enter into any part of the calculation directly.

The most accurate information for the determination of the strength parameters of the pairing force comes from the single closed-shell data. As we discussed in I, the main experimental information which goes into the choice of these parameters is the even–odd mass differences, the gap, and the position of certain states of high angular momentum and odd parity in even–even nuclei. However, to the extent that the calculated values of these quantities depend upon the details of the single-particle spacing, there is some uncertainty in the choice of the best value of these parameters even in the single closed-shell regions. We estimate that the over-all accuracy is approximately 20% for these isotopes.

It is surprising how little additional direct information on these pairing force parameters can be extracted from the remaining isotopes, which constitute the great majority of the nuclei included in this work. First of all, there are not many of these isotopes in which one can clearly identify the lowest excited quasi-particle states because the multiple phonon

states are always in the gap or mixed in with the lowest lying two-quasi-particle states. Secondly, because of the increased complexity in the spectrum as soon as one leaves the single closed-shell isotopes, it has been difficult for many determinations of states of high spin and odd parity to be made in even–even nuclei. Moreover, although there are some excellent mass data, the theoretical uncertainties due to increased importance of the long-range force do not allow the even–odd mass data to be so clearly interpreted, as is discussed in Chap. IV.

For this reason, we have used the force parameters which are obtained from the single closed-shell regions. Although there is some evidence for G_p to be slightly larger than G_n in the deformed region,[7] and one might expect this to be the case because of the smaller Fermi energy for protons than neutrons in heavy nuclei,[15] we were unable to justify the use of two different force parameters in our calculation. In a rather extensive survey in various regions we could not find an over-all systematic improvement in the various states by using different values. Thus we chose

$$G_p = G_n = G\,, \tag{51}$$

for each isotope, and allowed G to have a mass dependence of $G \sim 1/A$, where A is the mass number.

As discussed more fully in Sec. B, there is nothing in the systematics on the vibrational states which contradicts the simple picture of the vibration being formed by a force equivalent to the interaction of the quadrupole moments of the particles with the quadrupole moment of the entire nucleus; i.e., in all of these nuclei the spacing of the vibrational levels is essentially that of a single-quadrupole vibrator. As can be seen from Eq. (44) and the earlier discussion, this suggests that the three-quadrupole force parameters are approximately equal. Since there was nothing found in the calculations using different force strengths to suggest that systematic improvements could be obtained by using different force strengths, we have made the choice that

$$\chi_p = \chi_n = \chi_{np} = \chi \tag{52}$$

for all of the calculations which are discussed hereafter.

In the even–even nuclei we attempt to determine the best over-all values for this χ parameter and its A dependence. However, for the odd-mass nuclei we do not directly use this value, as explained below.

[15] V. Weisskopf (unpublished notes).

2. *The Single-Particle Parameters*

The greatest uncertainty in the numerical results comes from the uncertainty in the values of the single-particle energy parameters, ϵ_j. From the single closed-shell nuclei and from the isotopes with one particle away from a single closed shell one can often obtain rather good information about two or three levels, but usually one can only have reasonably good values for the levels which are most important for a particular isotope. However, because of the large changes in the mass numbers, even in one region, which are involved in these calculations, this is not always easy to do in practice.

The most important aspect of this difficulty seems to be effective changes which are produced by the neutron–proton short-range force. In any calculation with a phenomenological residual force, the simplest correction which one can make, to take into account the parts of the interaction which have been neglected, is that of altering the effective potential for the particles. In doing this, one effectively takes into account the P_0 (spherically symmetric) part of the interaction. We have done this here in a phenomenonological manner in a few cases where there seemed to be clear evidence that it is necessary.

Although this adds a certain amount of arbitrariness to the numerical results, such a device cannot alter the essential picture which results from the coupling schemes which are employed. When the coupling schemes break down, low-lying states appear of character different from those which we can obtain. Also, the limitations imposed by the necessity of fitting so many of the low-energy properties considerably reduce this arbitrariness. The main reasons for these adjustments are to better test the validity of the methods which are being employed and to make the results more useful.

In order to try to estimate the energy shifts which would be needed to incorporate the spherical field part of the short-range neutron–proton force, we calculated the energy shifts for one particle in all of the levels used in the various regions, interacting with the particles of the other type by the method described in Chap. II. For the single closed shell plus one isotope one does obtain over-all improvement,[10] however, there are a number of difficulties which make it impossible to apply the method consistently. For example, using a force parameter of sufficient strength to account for the 1/2–3/2 spacing in the Tl isotopes, the change in the spacing which occurs for the Hg isotopes causes the gap to get extremely small or vanish for the protons which contradicts the data;

and although the changes in the 1/2–9/2 separation in the In isotopes are in good agreement with the experiments, the resulting values for the $p_{1/2}$–$g_{9/2}$ spacing in the lighter isotopes in that region are not satisfactory.

On the other hand, from these studies we can see which levels are most strongly altered and can estimate the energy shifts which might be reasonable. The results of the calculation mentioned above are not given.

We also incorporate the energy shifts which are known to occur in nuclei; the separation of all of the ϵ_j vary as $A^{-\frac{1}{3}}$ and in addition change with the spin–orbit splitting dependence $A^{-\frac{2}{3}}$.

Having decided upon the parameters, the occupation numbers V_j and the quasi-particle energies E_j are determined from Eqs. (4). The even- and odd-mass calculations are carried out independently. For the even-mass nuclei we determine the phonon energy ω with several choices of the quadrupole parameter, while for the odd-mass nuclei we attempt to carry out a more nearly accurate calculation by using the experimental value of the phonon energy and fit the force strength from the neighboring even–even nuclei.

B. Energy Levels of Even–Even Nuclei

Although most of the calculations were performed using the QRPA approximation and $\chi_n = \chi_p = \chi_{np}$, a number of preliminary studies were made of the effect of using different coupling constants and of the relation of the QRPA approximation to the adiabatic approximation. With the exception of a few nuclei, the adiabatic approximation to QRPA is quite good for the calculation of the vibration of spherical nuclei. Most of the exceptions are among the nuclei with a closed proton or neutron shell and thus a particularly high energy for the 2+ vibrational level. A few other cases occur for nuclei at a subshell such as $Z = 40$ for which the energy gap is particularly small. In the worst cases, the QRPA energy and B(E2) can differ from the adiabatic approximation by as much as a factor of 2. In all other cases the energy and B(E2) agree within a few percent for the two methods of calculation. This indicates that the nuclear vibration is indeed adiabatic and that it is correct to picture the motion as a vibration of the nuclear shape of low enough frequency that the individual particle orbits can follow the motion.

The same values were used for the proton and neutron long-range strength parameters χ_n and χ_p for most of the studies, in agreement with the results found for the single closed proton shell and single closed neutron shell nuclei. The value of χ_{np} in relation to χ_p and χ_n has two main effects. Firstly, a very small value of χ_{np} leads to two low-lying 2+ states (except for the single closed-shell nuclei) contrary to the experimental fact. Secondly, its value determines the 2+ energies and B(E2)'s of the nuclei away from closed shells as compared with those quantities for the closed-shell or near-closed-shell nuclei. This is because the value of χ_{np} has no effect on a single closed-shell nucleus in the approximation used here. One might, for example, choose χ_n and χ_p to fit the 2+ energies of the single closed-shell cases, and then choose χ_{np} so that the nuclei just two particles away from the single closed shell would have the right energy. Although these latter 2+ levels are much lower in energy than the former, the above procedure leads to a rather small χ_{np}. In each region of isotopes only a limited number of proton (and neutron) single-particle levels are considered; namely, those of a major shell. Thus, for example, for the nuclei below Sn the protons are in the $28 \leqslant Z \leqslant 50$ shell while for the nuclei above Sn they are in the $50 \leqslant Z \leqslant 82$ shell. For Sn itself, the protons do not exist for the calculation. Since different numbers of levels are used in the different cases the effective coupling constant may be a little different due to renormalization effects. In particular, it may be a little extreme to eliminate the protons entirely for $Z = 50$. The effect of the inclusion of the levels of two shells has been examined and found to suggest that the closed shells are probably not completely inert. For example, the inclusion of the $f_{7/2}$ level below, for protons and neutrons in the $28 \leqslant Z \leqslant 50$ shell, has quite noticeable effects (softens the vibrator), particularly for the Ni isotopes. The inclusion of this $f_{7/2}$ gives more than just a renormalization effect, since it changes the shape of the 2+ curve for the Ni isotopes, lowering the predicted energy much more for Ni^{58} than for the heavier Ni isotopes. The shape of this curve could be corrected again by bringing the $g_{9/2}$ neutron level more into the picture. With the single closed-shell vibrators softened somewhat, the previously described prescription would give a larger χ_{np} since χ_p and χ_n could be chosen smaller.

While many of the detailed variations of the 2+ energy seen in a particular sequence of isotopes could be reproduced by a particular choice for χ_p, χ_n, and χ_{np}, it was not possible, with a single set of parameters, to fit all these details for all the spherical nuclei. However, a reasonably good compromise is possible. It is found that the choice $\chi_p = \chi_n = \chi_{np}$ seems to give over-all results as good as any. This choice together with a judicious choice of the single-

particle energies and pairing strength reproduces the variation of 2+ energy fairly well.

The exact values of ω near the point at which ω^2 becomes negative for a particular isotope series are extremely sensitive to the value of χ because ω is increasingly sensitive to χ for increasingly small ω. This can be seen from the adiabatic limit Eq. (44). For $\omega \approx 0$,

$$\omega \propto (\chi_0 - \chi)^{\frac{1}{2}}, \tag{53}$$

where χ_0 is the value of χ for which $\omega = 0$. Thus, it is not surprising that while the fit is reasonable if ω is not too small, for those isotopes for which E_{2+} is less than about one-fourth of the pairing gap, the smallest change in χ or isotope number can mean the difference between $E_{2+} = \frac{1}{4}$ gap and a predicted deformation. On the other hand near mass number 150 the point in the isotope table at which ω^2 becomes negative is such a general feature of nuclear structure that for any reasonable choice of parameters one can only change this point by about one isotope. In order to use the model for nuclei as far toward the deformed region as possible, the value of χ used in the calculation of other properties was chosen to fit the experimental 2+ level energy. Such a set of χ values is plotted in Fig. 1.

Nevertheless, considerable detailed agreement with experimental 2+ energies is obtained with fixed χ in each region as can be seen in Figs. 2(a) and 2(b). The shape is right in the Pb isotopes, as observed in Ref. I; in addition the lower energies in Hg and Pt are well fit if not in fine detail. Then for all of the lighter nuclei of the so-called deformed region with the exception of Os, which is just on the edge and can be made to vibrate or not with slight parameter adjustments, the $\omega^2 < 0$ indicating a theoretical deformation. From the other side, starting with the good Sn results, the decrease of the 2+ energy for heavier nuclei Te, Xe, Ba, etc., and the increase at $N = 82$ is well represented (only the most neutron deficient Xe and Ba isotopes have $\omega^2 < 0$). Above $N = 82$ the deformation quickly sets in in agreement with experiment on energy-level systematics as well as the photonuclear experiments[16] which show a double dipole resonance as one enters the deformed region near mass number 150. Presumably our result that the prediction of spherical symmetry in the 0s isotopes is uncertain within the range of our parameters is in agreement with the experiments which show a

[16] See G. H. Fuller and E. Hayward, Nucl. Phys. **30**, 613 (1962) for other references.

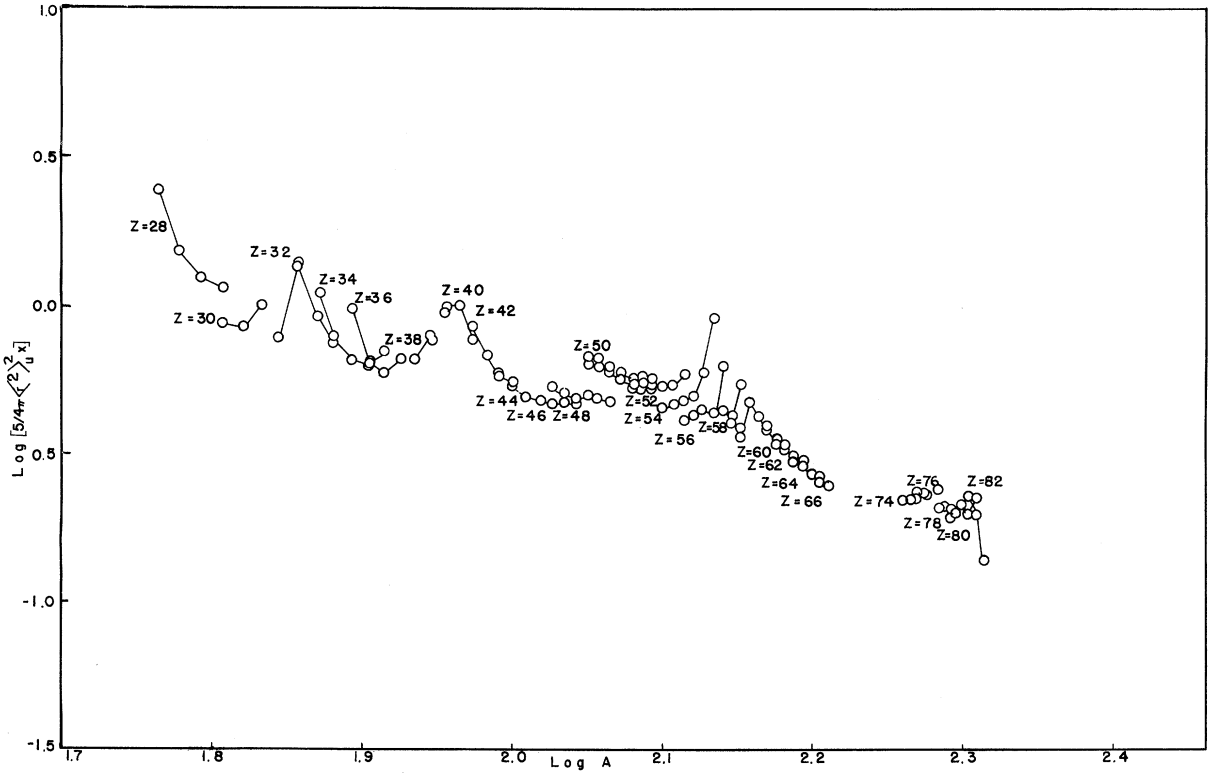

FIG. 1. The coupling parameter $X = 5/4\pi\langle r^2\rangle_\mu^2\chi$ chosen to bring E_{2+} into agreement with the experimental data; $\langle r^2\rangle_\mu$ is the matrix element of r^2 in the most usual orbit of the shell under consideration.

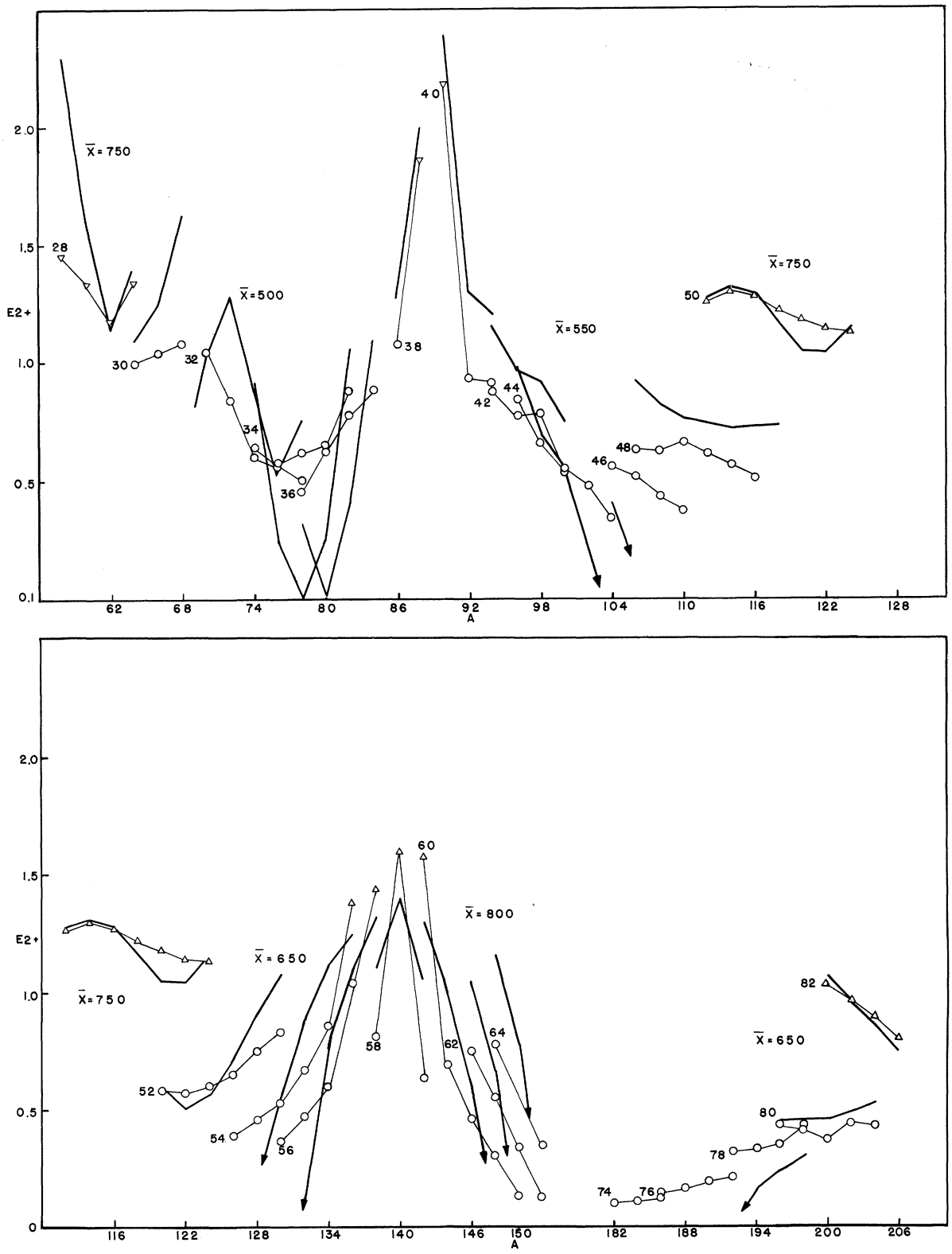

FIG. 2. The experimental E_{2+} compared to $\hbar w$ computed with a fixed $\overline{X}$ in each region. Semiclosed shell nuclei are indicated by triangles. Isotopes of the same Z (indicated on the figure) are connected by light lines. In each region X is given a dependence of $A^{-5/3}$ for which we define $\overline{X}A^{-5/3} = \frac{1}{2} X$. The value of $\overline{X}$ used for each region is indicated on the figure.

gradual transition from spherical to deformed shape in the Os region.[17]

The rapid drop of the 2+ energy as one moves away from closed shells for nuclei lighter than Sn is also well represented with she same parameters. However, these parameters lead to negative ω^2 values for some regions away from closed shells, in which the nuclei do not exhibit the extremely low E_{2+} values and the clear-cut rotational spectra characteristic of the rare-earth nuclei. In particular, the region of isotopes with $N \sim 42$, $32 \leqslant Z \leqslant 36$ and the heavy isotopes for $Z = 44$, 46 are predicted to be deformed. Although these nuclei do not exhibit rotational spectra, they are the ones with lowest E_{2+} values in the vicinity, and in several cases the odd–mass nuclei have low states corresponding to anomalous coupling which might indicate incipient deformation. For example, these are cases for which the simplest interpretation of a low $\frac{7}{2}+$ state is that it is a seniority three configuration of $(g_{9/2}^3)_{7/2+}$. This is essentially the configuration which would be predicted by the Nilsson model and is thus suggestive of deformation.

Nevertheless, in the rest of the discussion, the value of ω for these isotopes is taken from experiment and the computations are performed as if the 2+ was a vibrational state of a spherical nucleus.

[17] W. R. Kane, G. T. Emery, G. Scharff-Goldhaber, and M. McKeown, Phys. Rev. **119**, 1953 (1960), and G. T. Emery, W. R. Kane, M. McKeown, M. L. Perlman, and G. Scharff-Goldhaber, *Electromagnetic Lifetimes and Properties of Nuclear States* N.A.S., N.R.C. Nuclear Science Series Rept. No. 37.

C. Energy Levels of Odd-Mass Nuclei

In states of one quasi-particle with zero, one, and two phonons

$$\psi_j = C^j_{j00}\alpha^\dagger_j\psi_0 + \sum_{j'} C^j_{j'12}[\alpha^\dagger_{j'}B^\dagger]_j\psi_0 + \sum_{j'J} C^j_{j'2J}[\alpha^\dagger_{j'}[B^\dagger B^\dagger]_J]_j\psi_0 , \quad (54)$$

the Hamiltonian (47) with the interaction term (45) is diagonalized. Since we are using force parameters $\chi = \chi_p = \chi_n = \chi_{np}$, this interaction has the simple form

$$H_{\text{int}} = \chi K(\omega,G,\epsilon_j) \sum_{jj'} f_{jj'}\eta_{j'j}(B^\dagger + B) , \quad (55)$$

in which the $f_{j'j}$ represent the coefficients in the sum in Eq. (47) and K is a quantity which only depends upon the single-particle energy levels, the pairing parameter, and the phonon energy. In this work we have used the experimental value for the phonon energy from the neighboring even–even nuclei for both the unperturbed energies and K for each odd-mass isotope, and fit the value of χ from experimental phonon data. This allows us to proceed with the important odd-mass data without the necessity of a selection of parameters so accurate as to fit the very sensitive phonon energy, as was described above. The parameters used and the results of the calculations are presented in the figures and in Appendix II.

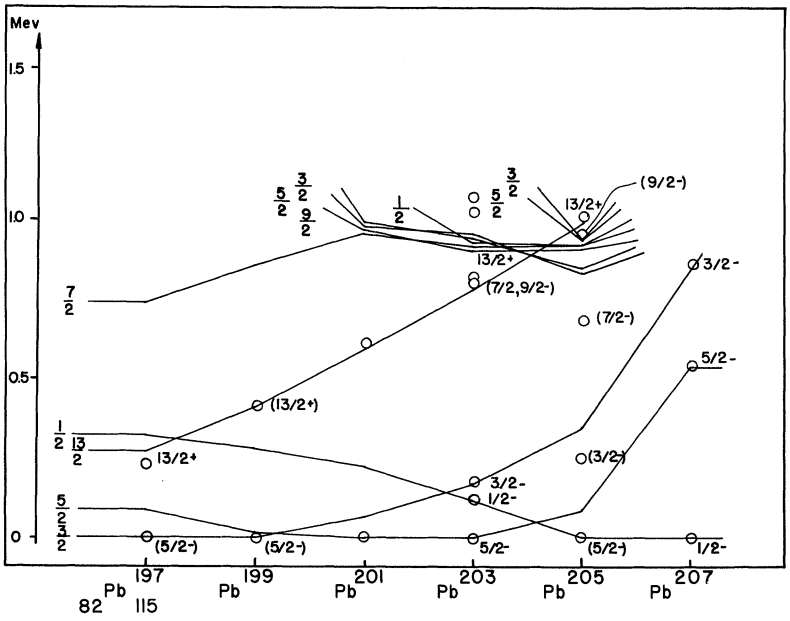

FIG. 3. Energy levels of odd-mass Pb isotopes. The pairing and single-particle energy parameters are given in Appendix II; the long-range force is chosen to fit the even–even spectra. The experimental points are given as open circles and the theoretical results as solid lines.

1. *The Region* $50 \leqslant Z \leqslant 82$; $82 \leqslant N \leqslant 126$

This is the region in which there is probably the least uncertainty in the parameters. From the Pb^{207}

isotopes one knows the neutron energies for the 82–126 shell in the region below Pb and from the Tl isotopes one has quite a good idea of the important proton levels. The results for the odd-mass Pb isotopes are so similar to I and the work of Sorensen, Ref. 14, that we shall not discuss them.

Let us first discuss the nuclei above the deformed region, Figs. 3–7. For the odd-neutron nuclei as one proceeds from the Pb isotopes to the deformed nuclei at mass number 190 one is removing neutrons from the $p_{1/2}$, $f_{5/2}$, and $p_{3/2}$ levels and the $i_{13/2}$ quasi-particle state is dropping just as in the odd-Pb isotopes. In the Hg isotopes, where the no-phonon and one-phonon states generally remain well separated one can see this effect. Since the "opposite" parity states in any region are generally not so strongly admixed by the quadrupole force, in Hg the mixing is still weak enough for the $13/2^+$ quasi-particle to move through the one-phonon state. The comparison with experiment shows good agreement for this state and the fact that one does not see the isomeric state after Hg^{199} is predicted by the fact that the 13/2 level is

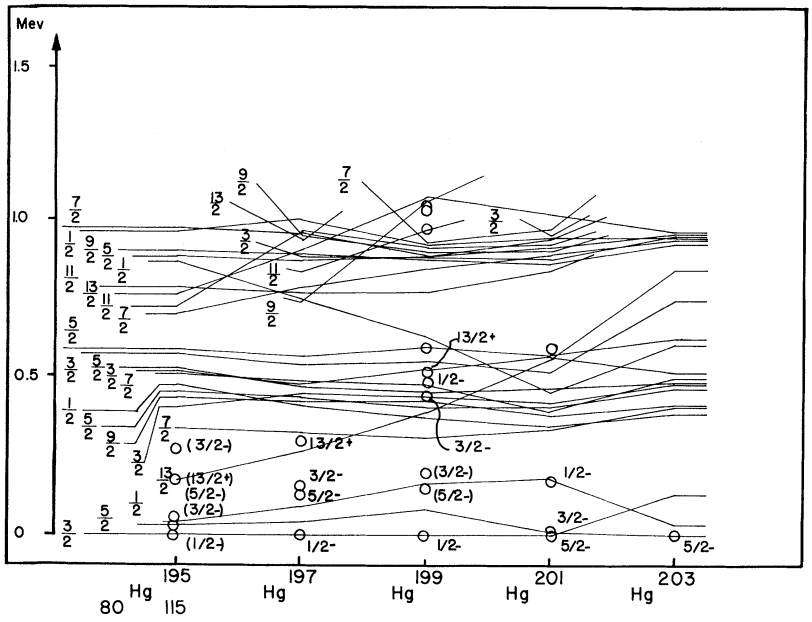

FIG. 4. Energy levels of odd-mass Hg isotopes.

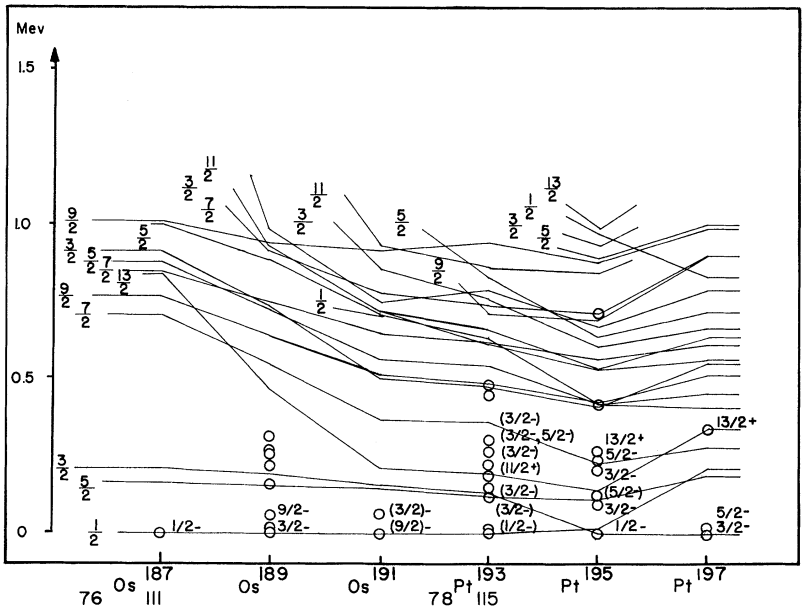

FIG. 5. Energy levels of odd-mass Os and Pt isotopes.

moving into the one-phonon levels of higher spin for Hg^{201} and Hg^{203}. The other one quasi-particle states are affected by the long-range force much more than in the Pb cases, and the results are in reasonable agreement with the experimental values. For the Pt isotopes the one-phonon states do not fall quite as low in energy as the experimental ones, while the occurrence of low-lying phonon states in the experimental data for the Os isotopes suggests that one is in a transition region where the methods employed here are beginning to be inadequate.

The $s_{1/2}$, $d_{3/2}$, and $h_{11/2}$ levels are the important ones for the pairing part of the odd-proton calculation. For the Tl and Au isotopes the theory and experiments show the phonon states separated from the no-phonon states, while the theoretical calculation does not seem so show the no-phonon state being sufficiently admixed into the one quasi-particle states for the Ir isotopes. An increase in the strength of the quadrupole interaction would markedly improve the results in the Tl isotopes, and then in Au the phonon states would fall lower, which would be more nearly consistent with the experimental data.

In order to describe better the effects of the quasi-

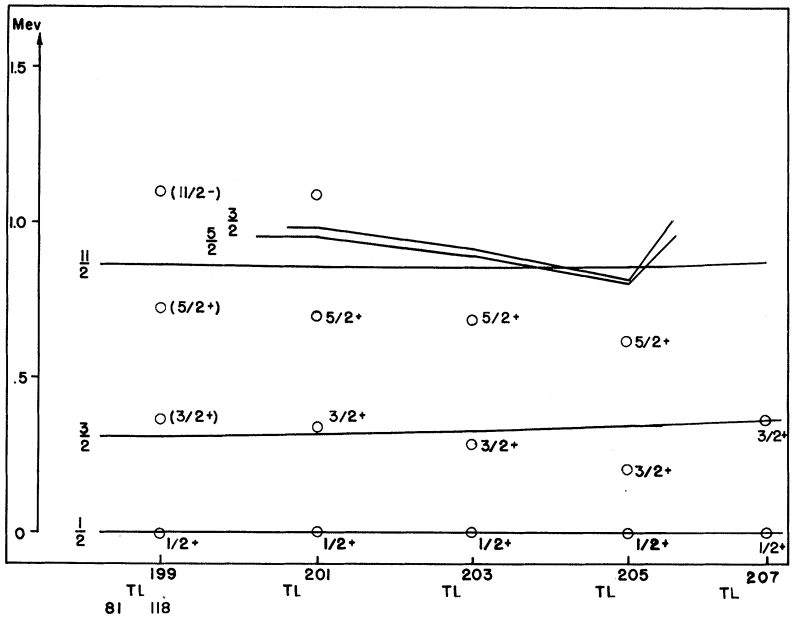

FIG. 6. Energy levels of odd-mass Tl isotopes.

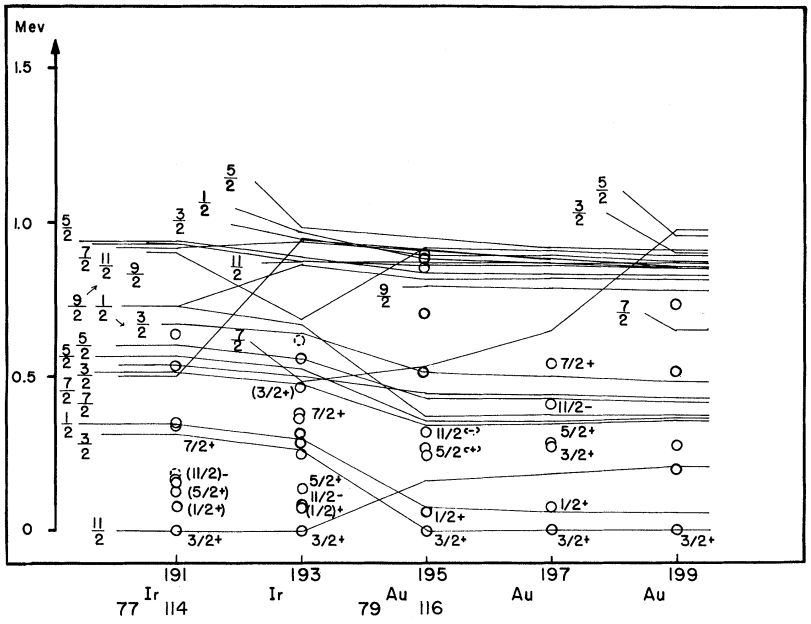

Fig. 7 Energy levels of odd-mass Ir and Au isotopes.

particle–phonon interaction we show the energies of the quasi-particle states and the states which arise from them in the presence of the quadrupole force in Fig. 8. The quadrupole force has little effect in the odd-Pb isotopes, while for the odd-Hg spectra one can see that the phonon effects are large and very

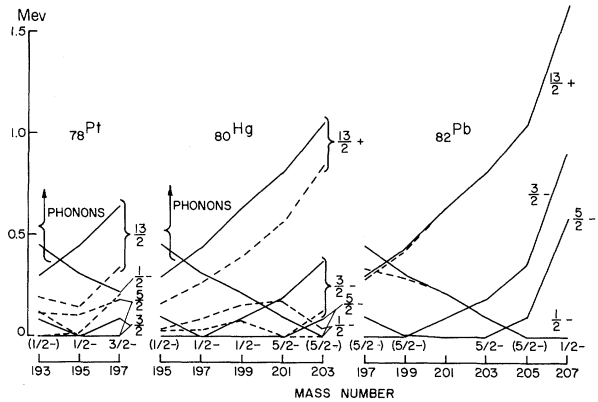

FIG. 8. The effect of quadrupole interaction on states of odd-neutron nuclei above the deformed region. The quasi-particle energy levels in the absence of the quadrupole interaction are given as solid lines while the low-lying states in the presence of the quadrupole interaction are given as dashed lines. The experimental ground-state spins are included.

An effect occurs here which seems to be present in all of the spherical nuclei, that of the compressing of the quasi-particle states due to the stronger interaction of the higher lying quasi-particles with the phonons [see Eq. (47)]. This is an important systematic feature of our coupling scheme which seems to be verified by the empirical data.

There are not much data below the deformed nuclei for this region, and one expects our methods to give rather inaccurate results for cases with even a few neutrons added to the 82 neutron shell because of the approaching deformed region. The only systematic data concern the odd-proton nuclei shown in Fig. 17 in which one sees the 7/2 and 5/2 states with relative motion due to both the change of the quasi-particle energies as one adds protons, and the effect of the quadrupole force. However, the density of states does not seem to be in agreement even as the phonon states begin to fall low in energy as one can see in Figs. 13 and 17.

2. *The Region* $50 \leqslant Z \leqslant 82; 50 \leqslant N \leqslant 82$

In this region the protons are being placed into the $g_{7/2}$ and $d_{5/2}$ levels and the neutrons into the $h_{11/2}$, $s_{1/2}$, and $d_{3/2}$ levels (see Figs. 9–17). Insofar as the single-particle level shifts can be neglected, the two important proton levels are accurately known from the $N = 82$ isotopes. Referring to Fig. 14, one sees that the Sb energy levels give clear indication that, in fact, the relative motion of these levels occurs

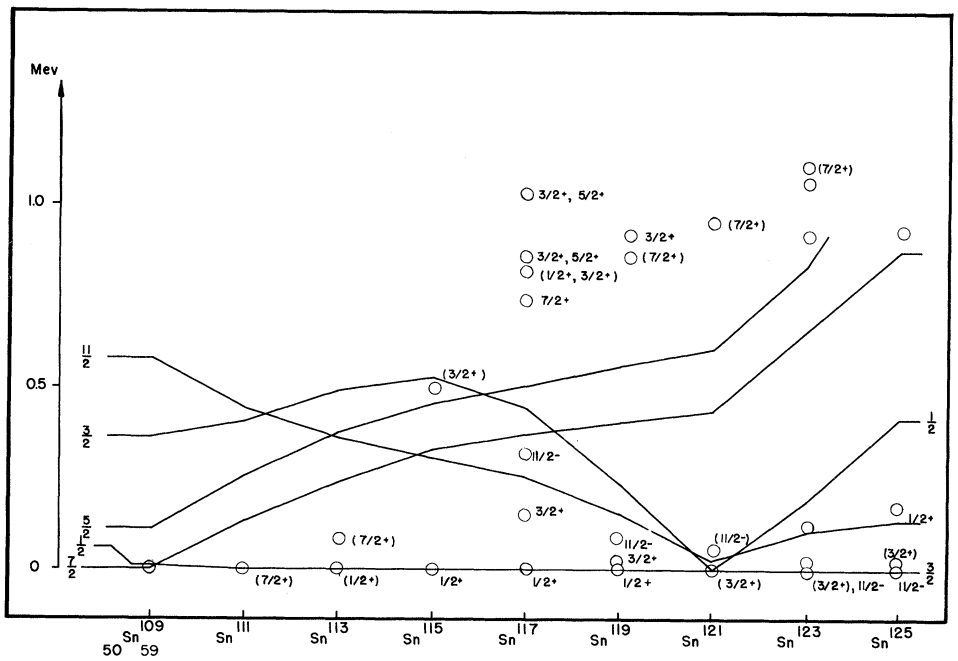

FIG. 9. Energy levels of odd-mass Sn isotopes.

much improve the agreement with experiment, since the $\frac{1}{2}-$ state is lowered with respect to the $3/2-$ and $5/2-$ states. In fact, a moderate increase in the quadrupole strength would make $1/2-$ be the ground state in Hg^{195} and Hg^{197}, and perhaps in Hg^{199}.

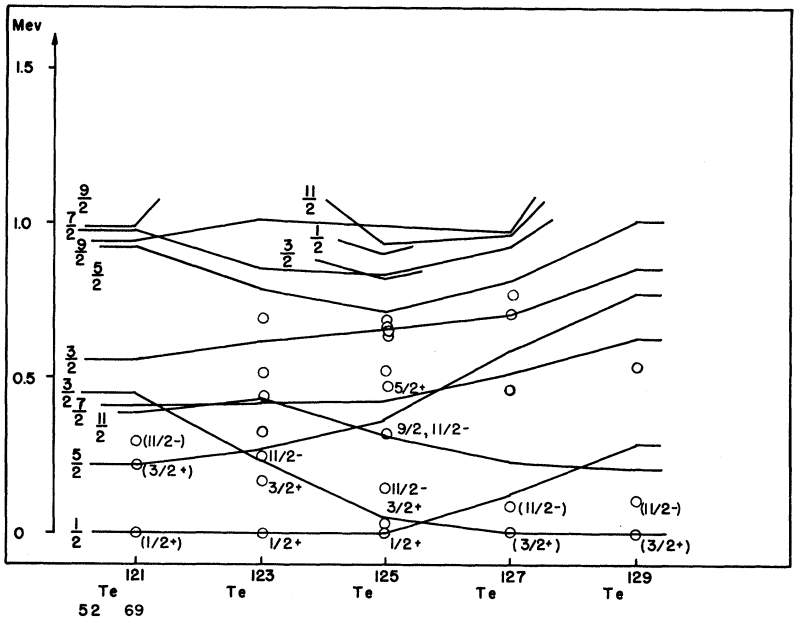

FIG. 10. Energy levels of odd-mass Te isotopes.

more rapidly with changing neutron number than can be accounted for by the phonon interaction of the strength used here. In Fig. 14 the calculation is shown with dashed lines including the energy shifts due to a delta interaction between the single proton in Sb and neutrons. This effect is smaller for the other odd-proton isotopes, since one is approaching the $N = 82$ shell closing.

A very interesting phenomenon which is occurring in the odd-proton isotopes is the important role of one particular state. Both in the theoretical calculations and in the experiments, one can see a spin-1/2 state moving quite rapidly with respect to the other states, Figs. 14–16, and even becoming the ground state in Cs^{129}. This state is mainly of phonon character according to the theoretical calculations. It

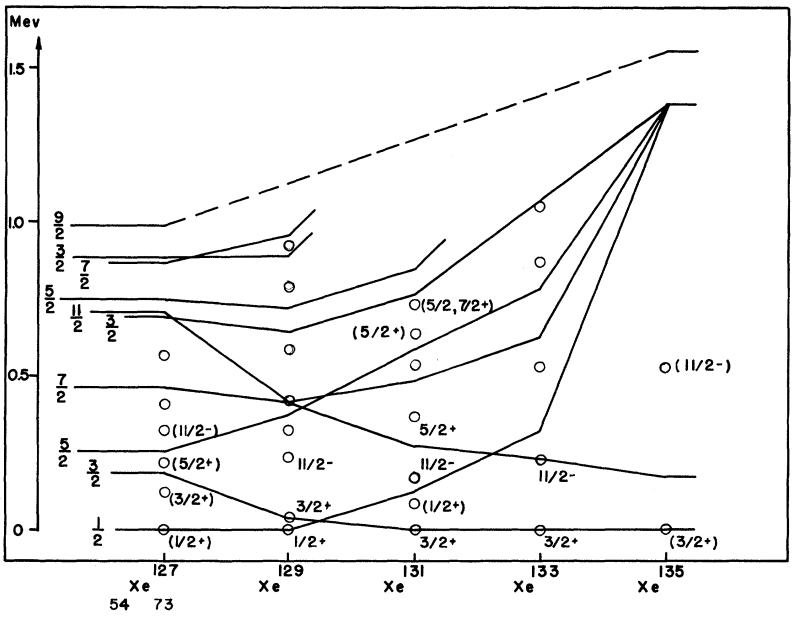

FIG. 11. Energy levels of odd-mass Xe isotopes.

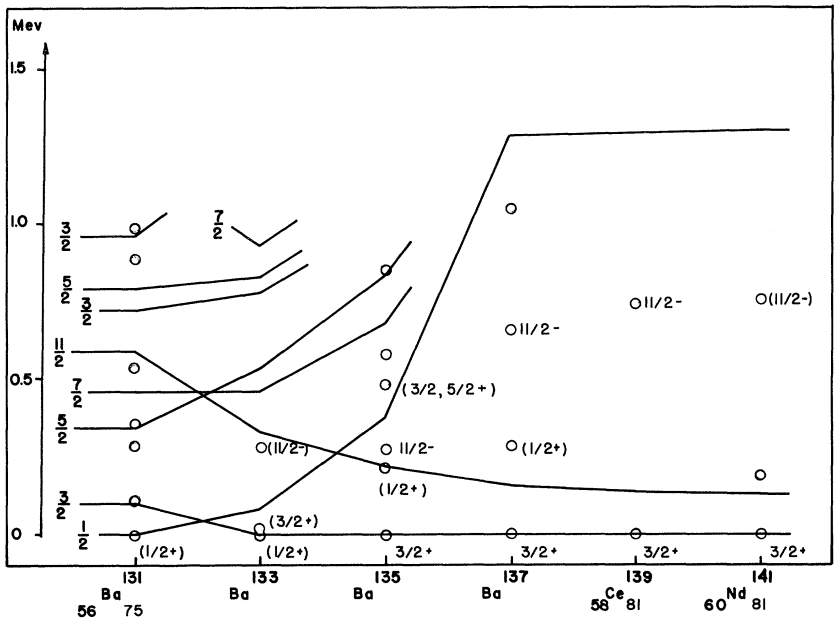

FIG. 12. Energy levels of odd-mass Ba, Ce, and Nd isotopes.

would be nice to obtain information about the transition rates for this state, since we would predict that E2 transitions to, say, the 5/2 state would be highly enhanced.

The odd-neutron isotopes are also interesting, with very good systematic data. The Sn results differ from the results in I mainly in that it was found that a different ordering of the single-particle levels could account for the systematics of the 2+ first excited states in the even Sn isotopes and give much better fits away from the closed proton shell. The positions of the 1/2, 3/2, and 11/2 states are fit adequately in the Te, Xe, and light Ba isotopes. However, as one approaches the case of one particle away from the closed shell at Ba^{137}, Ce^{139}, and Nd^{141} there are errors either in handling the effect of the quadrupole force or of the neglected neutron–proton force. Because of the special nature of a calculation with one particle

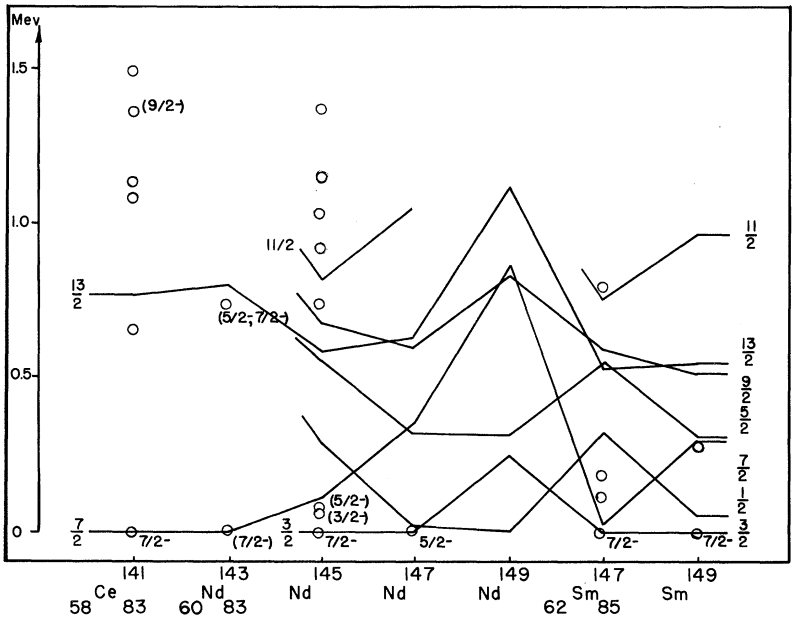

FIG. 13. Energy levels of odd-mass Ce, Nd, and Sm isotopes.

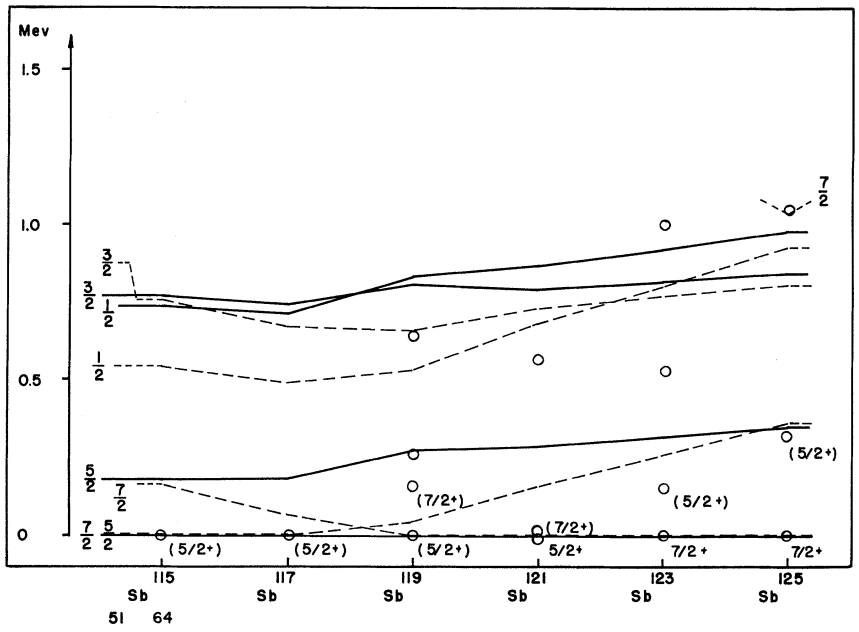

FIG. 14. Energy levels of odd-mass Sb isotopes.

away from the closed shell, the phonon calculation might be particularly inaccurate for those cases. As for the neutron–proton interaction, because of the dependence upon the occupation numbers of the states [see Eq. (15)] and the sudden decrease in the pairing effects as one reaches one particle outside of a closed shell, there might occur a marked difference in the shifts in the 11/2–3/2 and 11/2–1/2 separations as one goes from 79 to 81 particles.

In Figs. 18 and 19 are shown the effects of the quadrupole interaction on the quasi-particles for the odd-proton and odd-neutron isotopes, respectively. For the odd-proton cases in the absence of the quadrupole force one would have only the 7/2 and 5/2 low-lying levels. First one sees that the relative motion of the experimental 5/2 and 7/2 levels in I, Cs, La, and Pr is much larger than could be explained by the motion of the Fermi level. Also, the neutron–

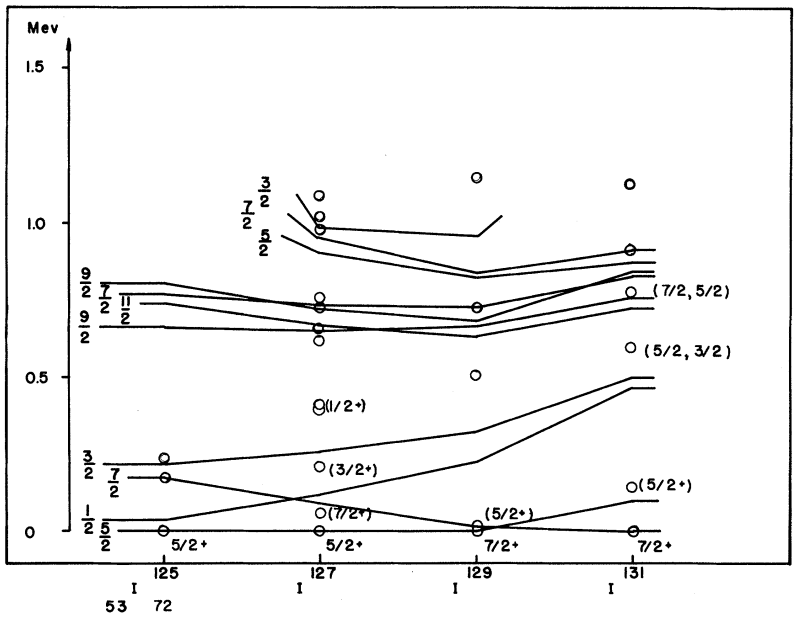

FIG. 15. Energy levels of odd-mass I isotopes.

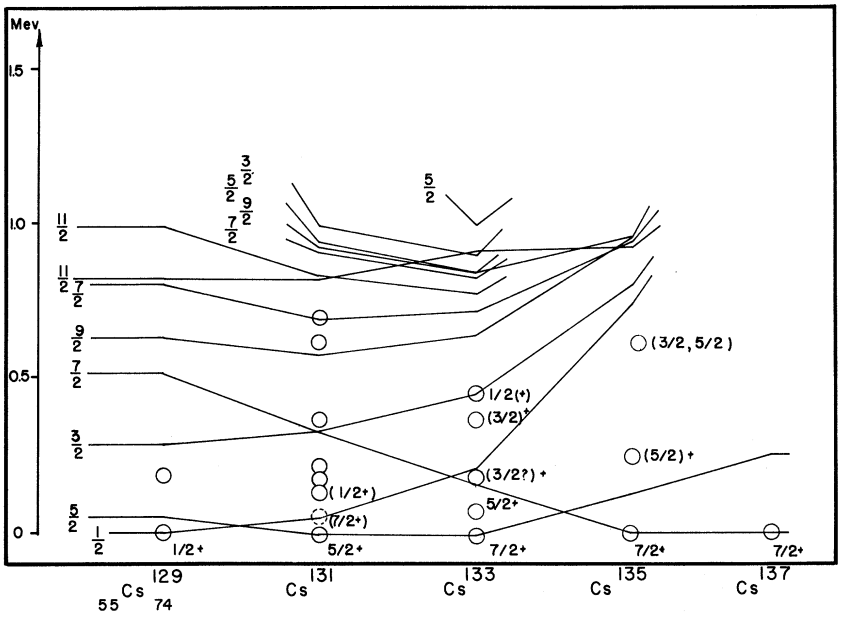

FIG. 16. Energy levels of odd-mass Cs isotopes.

proton short-range interaction gives very small contributions since one is near the 82 closed shell at which the energy levels have been determined. The quadrupole force thus not only brings down the 1/2 state and other one-phonon states, but semiquantitatively accounts for the 5/2–7/2 relative motion.

In Fig. 19 one can see that there are large effects of the quadrupole force which generally give important improvements when compared to the quasiparticle levels. The main effects are to keep the 1/2 level as the ground or low-lying level for high neutron numbers to give consistency to the spectra of Sn, Te, Xe, and Ba. It also tends to lower the 3/2 state, keeping the 11/2 level from being the ground state or very low-lying state in all of the isotopes with $N \geqslant 69$. In the light Sn isotopes one sees that the relative shifts

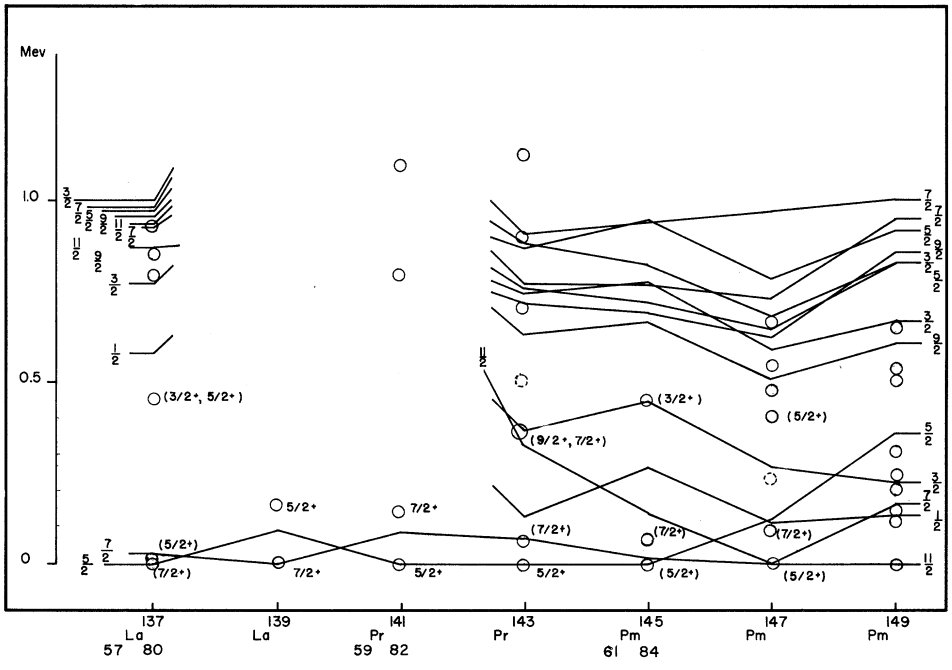

FIG. 17. Energy levels of odd-mass La, Pr, and Pm isotopes.

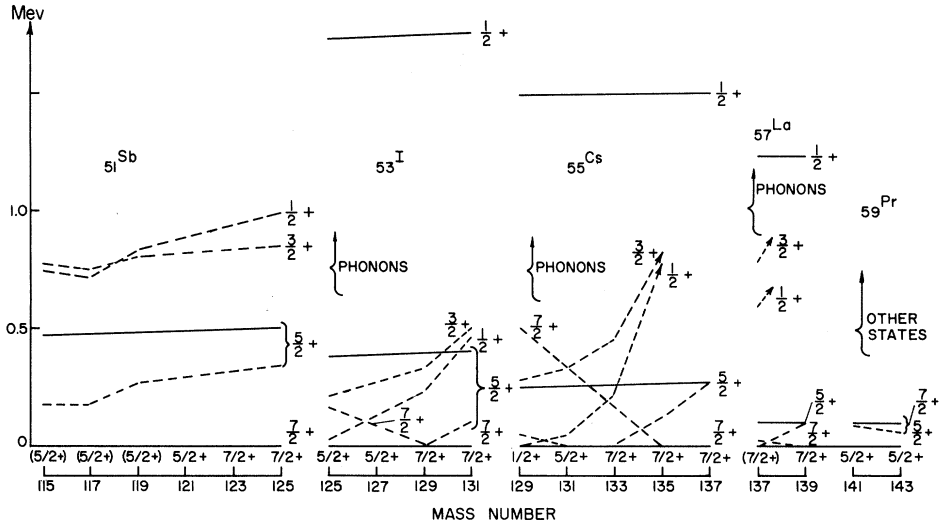

FIG. 18. The effect of quadrupole interaction on states of odd-proton nuclei for $51 \leq Z \leq 59$, $64 \leq N \leq 84$. The notation is the same as in Fig. 8.

in the 1/2–7/2 levels go in the wrong direction making the fit a little poorer, although the energy shifts involved are only 0.1 to 0.2 MeV. From all of the evidence it seems that the general description and approximations used in this work are adequate for all of the isotopes in this region.

3. *The Region* $28 \leqslant Z \leqslant 50; 50 \leqslant N \leqslant 82$

For the odd-proton isotopes in this region, the $p_{1/2}$ and $g_{9/2}$ levels are mainly involved, Figs. 20–23. Because of the great difference in the radial wave functions of these two states, their overlap integrals with the $g_{7/2}$ and $d_{5/2}$ neutrons are very different. For this reason one can expect these levels to change effectively their relative spacings as one changes the neutron number. In the calculation there is included a shift of the $g_{9/2}$ level of 0.1 MeV per neutron to account for this effect.

For the Tc, Rh, and Ag isotopes it seems almost certain that our coupling scheme is breaking down. The occurrence of the low-lying 7/2 and perhaps 5/2 positive parity states would have to be explained in our method by a coupling of the $g_{9/2}$ quasi-particle to the phonon. However, we are never able to bring that level nearly as low as required, and do not seem to have a mechanism for causing such rapid changes in these levels as do occur for the spin-1/2 states. If we were to include the three-quasi-particle states, important corrections would probably be introduced. This would be analogous to the type of calculation done for the configuration $(g_{9/2})^3$, which has been used by Talmi for calculations which do have a $7/2^+$

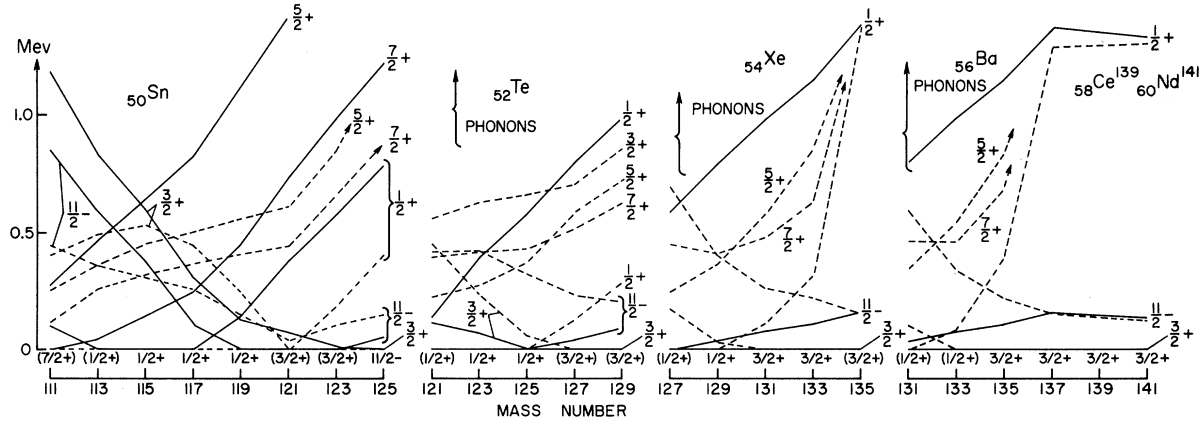

FIG. 19. The effect of quadrupole interaction on states of odd-neutron nuclei for $50 \leq Z \leq 60$, $61 \leq N \leq 81$. The notation is the same as in Fig. 8.

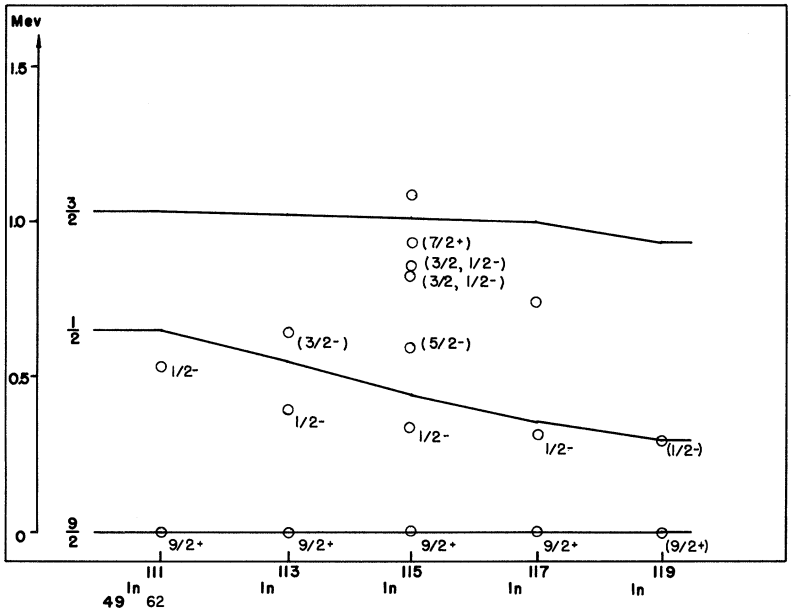

FIG. 20. Energy levels of odd-mass In isotopes.

state,[18] but it is not clear that such a modification would be adequate to handle this situation. The even–even isotopes in this region show great instability for the spherical shape.

A similar situation seems to be present in the odd-neutron isotopes, Figs. 24–27, where for the Ru and Pd isotopes there is obviously a strong admixing of

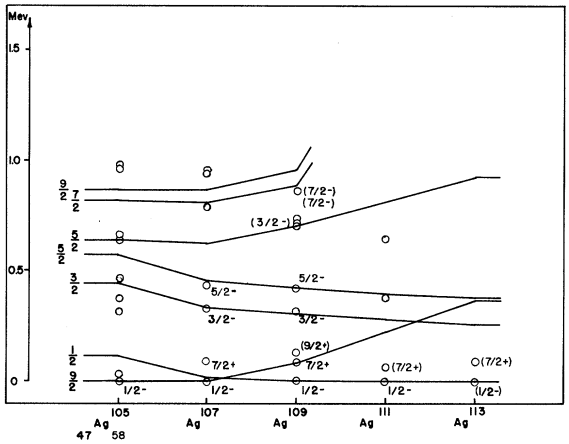

FIG. 21. Energy levels of odd-mass Ag isotopes.

phonon states in the low excited states. However, in these cases it is not clear that the coupling scheme is inadequate, although there is a tendency for the phonon states to remain too high to account for the density of low-lying states.

[18] I. Talmi and I. Unna, Nucl. Phys. 19, 225 (1960).

4. *The Region* $28 \leqslant Z \leqslant 50; 28 \leqslant N \leqslant 50$

In this region the protons and neutrons begin to have a large probability of being in the same j levels, so that one can expect the neutron–proton short-range interaction, which has been neglected except for its field producing parts, to become very important. Moreover, the inclusion of the $f_{7/2}$ levels in the calculation of the energy of the 2+ state considerably alters the relative positions of the 2+ states in the even–even Ni isotopes and indicates that at least for the lighter isotopes in this region the $f_{7/2}$ particles must be included—which makes the neutron–proton short-range force important even for such isotopes as Ni and Cu. In fact, the level spectra in this range cannot be understood in terms of the approximations used in this work.

In the odd-proton isotopes shown in Figs. 28 and 29 this is most evident in the As and Br isotopes for which the neutrons are filling the $g_{9/2}$ levels. Here one sees many low-lying levels which originate from the phonon states and other states of higher seniority. We can understand a little of this in our coupling scheme, such as the low-lying $9/2^+$ state in Br in spite of the $9/2^+$ quasi-particle being at 1.5 MeV, but since a number of the levels apparently originate from the seniority three states we cannot hope to account for them (see Chap. II).

Similar results hold for the odd-neutron isotopes, shown in Figs. 30, 31, and 32. Once again the $9/2^+$ state can be lowered by the quadrupole interaction while the $7/2^+$ state is not much affected, just as in

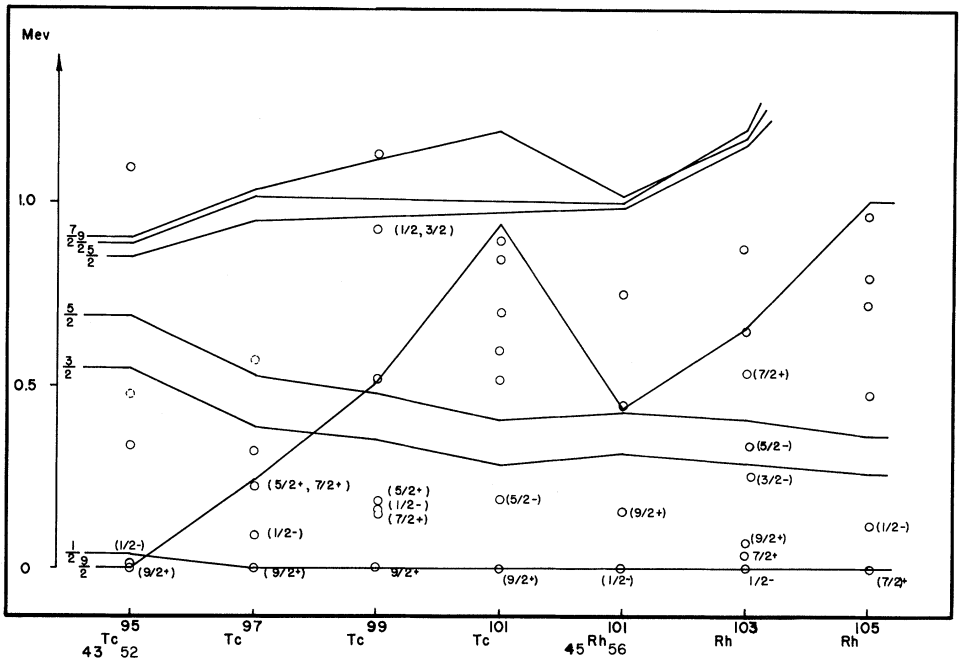

FIG. 22. Energy levels of odd-mass Tc and Rh isotopes.

the cases of the odd protons filling the $g_{9/2}$ levels discussed in the preceding section. Near $N = 50$ and to a lesser extent near Z or $N = 40$, the vibrations stiffen and the picture once again simplifies approximately into the quasi-particles. Because of the obvious inadequacies of the model, no attempt was made to obtain the best parameters in this region and only a few sample calculations were tried. Both a better treatment of the phonon–quasi-particle coupling and the introduction of the neutron–proton short-range will be needed for a semiquantitative treatment of this region.

D. Energy Levels of Odd–Odd Nuclei

Owing to the large number of low-lying levels, both theoretical and experimental, in odd–odd nuclei, it

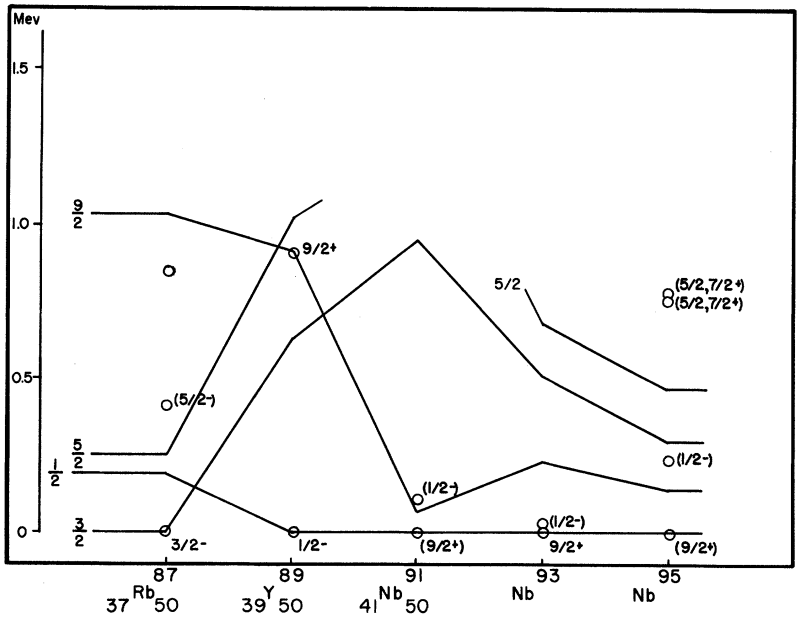

FIG. 23. Energy levels of odd-mass Rb, Y, and Nb isotopes.

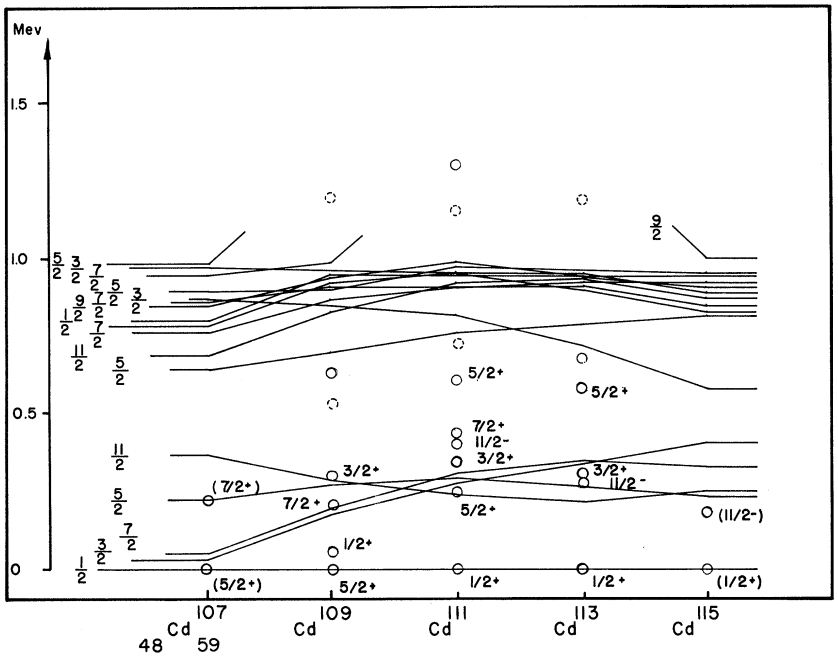

FIG. 24. Energy levels of odd-mass Cd isotopes.

would be difficult to use the energy-level systematics to help determine the parameters of the theory. However, the odd–odd levels can be shown to be consistent with the theory parameters determined from other data (particularly the odd-mass level energies). All the levels of odd–odd spherical nuclei of known spin and parity may be described consistently as a state of the lowest (or other low) proton quasi-particle coupled with the lowest (or other low) neutron quasi-particle. The effect of a coupling of the quasi-particles to a phonon vibrator is suggested in a few cases, discussed below, and the coupling force between the two quasi-particles (not discussed here) shows itself in the fact that only one or two of the angular momentum states arising from the proton–neutron quasi-particle pair are seen in the low-energy spectra. (No coupling force would imply a degenerate multiplet of levels which is not seen experimentally.)

Since the quasi-particle energies correspond to the odd-mass low-energy spectra, and since the param-

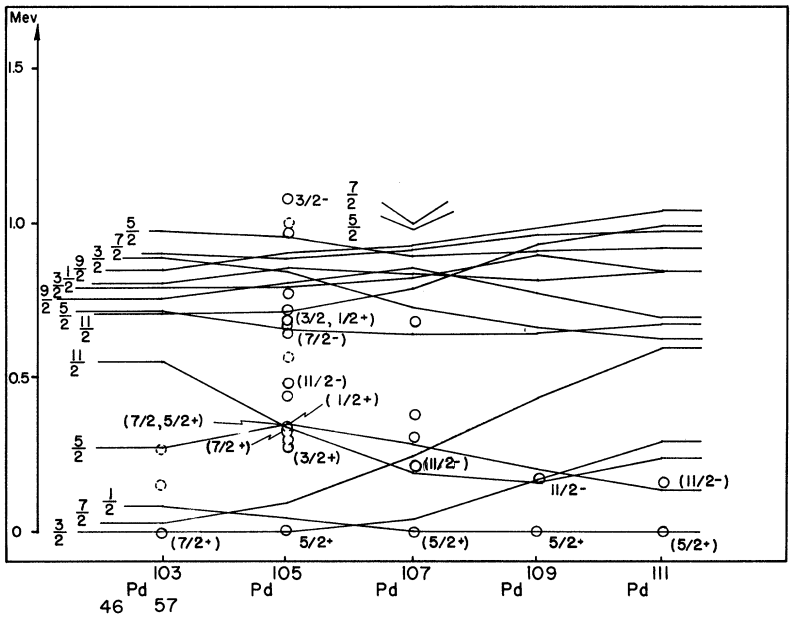

FIG. 25. Energy levels of odd-mass Pd isotopes.

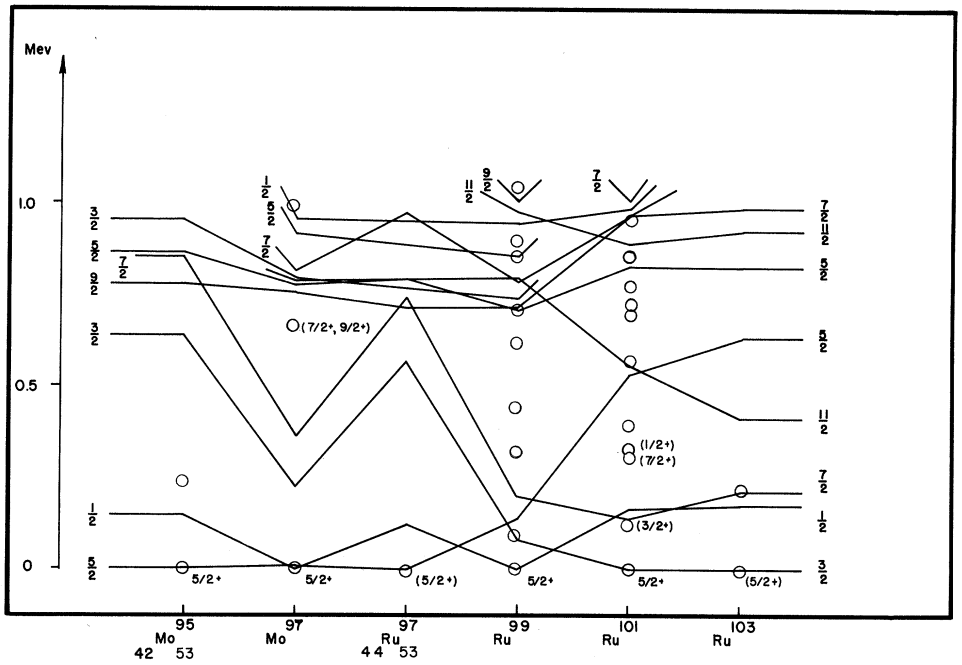

FIG. 26. Energy levels of odd-mass Mo and Ru isotopes.

eters were chosen to agree (as well as possible) with the experimental odd-mass spectra, the above description of the odd–odd states means that these states are made up of the angular momenta appearing near the ground state in the adjacent odd-mass nuclei.[19] This description is used by Brennan and Bernstein[20] who, in addition, deduce coupling rules. In general, we agree with their assignment of the proton–neutron configuration (proton–neutron quasiparticles in our case); however, we note a few exceptions.

For $P < 28$, $N > 28$ all the odd–odd levels of

[19] Such a scheme was used by L. W. Nordheim, Phys. Rev. **78**, 294 (1950); Rev. Mod. Phys. **23**, 322, (1951).

[20] M. H. Brennan and A. M. Bernstein, Phys. Rev. **120**, 927 (1960).

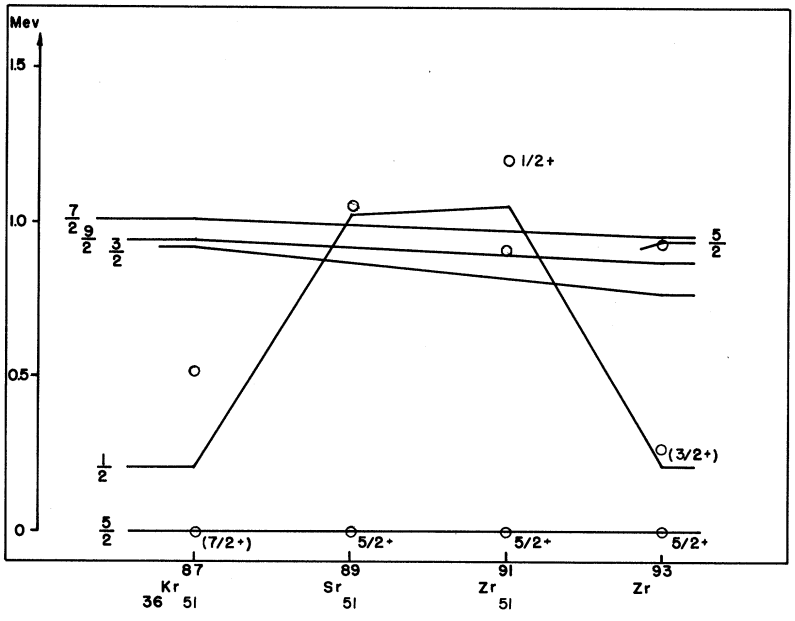

FIG. 27. Energy levels of odd-mass Kr, Sr, and Zr isotopes.

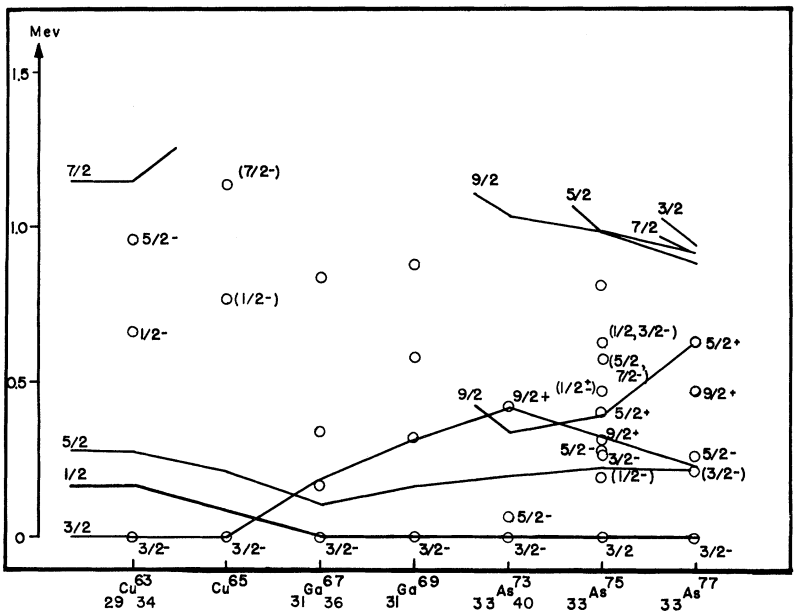

FIG. 28. Energy levels of odd-mass Cu, Ga, and As isotopes.

known spin and parity can be fitted with an $f_{7/2}$ proton quasi-particle and a $p_{3/2}$ or $f_{5/2}$ neutron quasi-particle. For $P > 28$ but $N < 42$ there are three cases for which Brennan and Bernstein make the P, N assignments $p_{3/2}, f_{5/2}$ for a $1+$ state. For ${}_{29}Cu_{37}^{66}$ and ${}_{31}Ga_{37}^{68}$ a more likely assignment would be $p_{3/2}$, $p_{1/2}$ as the β decay $(1+ \rightarrow 0+)$ rates have log ft values of about 5.2 (see the section on β decay of even-mass nuclei). In the neighboring odd-mass nuclei the β decay rate is known for six proton $-p_{3/2}$, neutron $-f_{5/2}$ transitions and the log ft values range from 5.7 to 7.4. We agree with their assignment for ${}_{35}Br_{41}^{76}$ for which the log ft of 8.4 suggests that it is l forbidden. It is a bit surprising to find the $f_{5/2}$ neutron quasi-particle so low for $N = 41$. For $42 < N < 50$ many of the levels have an $l = 1$ proton and a $g_{9/2}$ neutron. There are, however, four cases with $N = 43, 45$ where a $1+$ level has a fast β decay (log $ft \sim 4.6$) to the

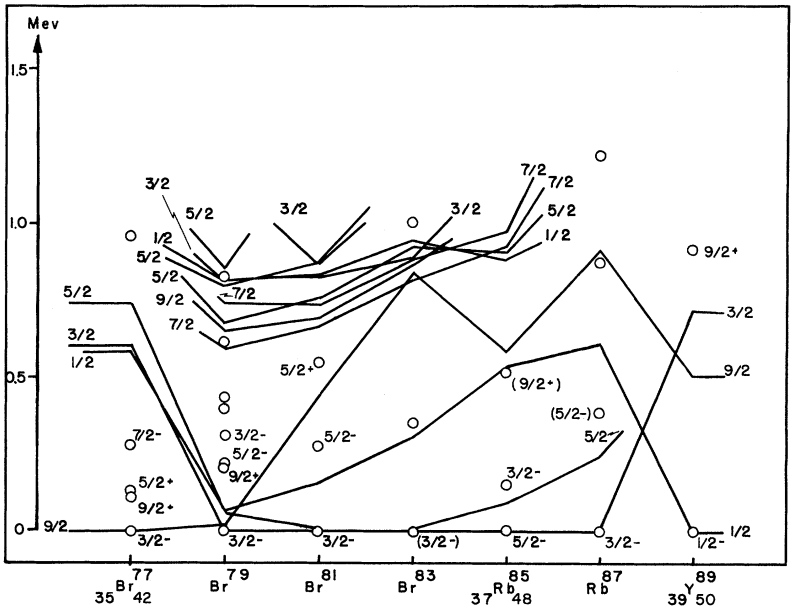

FIG. 29. Energy levels of the odd-mass Br, Rb, and Y isotopes.

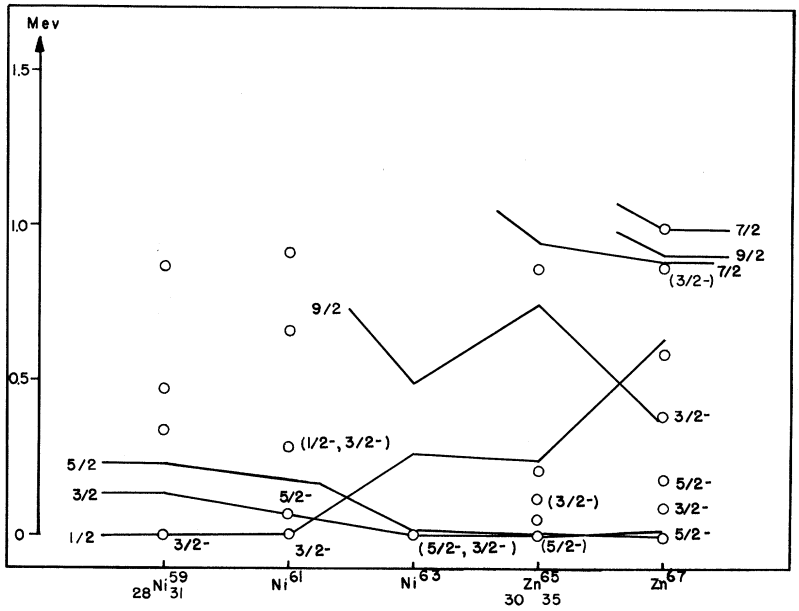

FIG. 30. Energy levels of the odd-mass Ni and Zn isotopes.

adjacent 0+ ground state. This must have the $p_{3/2}$ proton coupled to the $p_{1/2}$ neutron. For $N = 43, 45$ the $g_{9/2}$ neutron quasi-particle lies $\sim$0.2, 0.6 MeV below the $p_{1/2}$ quasi-particle, but the particularly strong coupling of the $p_{1/2}$ quasi-particle to the phonon vibrator lowers the $p_{1/2}$ level to an energy comparable with the $g_{9/2}$ energy. For $P < 50$, $N > 50$ the positive parity levels are explained as a $g_{9/2}$ proton and a $g_{7/2}$ or $d_{5/2}$ neutron. There are a number of negative parity states explained as $p_{1/2}$ protons with a $d_{5/2}$ neutron. Such levels occur, e.g., for $Z = 45$ where once again the phonon coupling is important in bringing down the $p_{1/2}$ proton level enough to compete with the $g_{9/2}$ proton level. Brennan and Bernstein assign $P = (g_{9/2}^{n})_{7/2}$, $N = d_{5/2}$ to four 1+ levels in this region. All of these have fast β transitions to the neighboring ground state 0+ the average log $ft = 4.7$. This would suggest $P = g_{9/2}$ $N = g_{7/2}$ to be more reasonable. Brennan and Bernsteins' assignment comes from the neighboring odd-mass ground states which are in

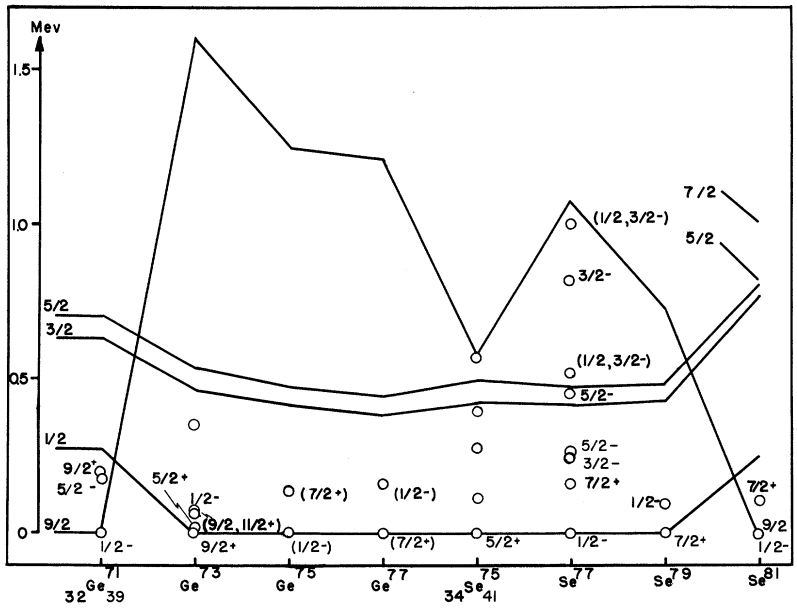

FIG. 31. Energy levels of the odd-mass Ge and Se isotopes.

some cases 7/2+ and 5/2+. The β decays between these levels are seen in several cases and have, in general, ft values an order of magnitude or two higher than the $1+ - 0+$ ft's. This argument is weakened somewhat by the occurrence of two fairly fast $7/2+ - 5/2+$ β decays in this region with $\log ft \sim 5.0$.

For $Z > 50$, $N < 82$ all the odd-odd levels of known spin may be obtained from a $d_{5/2}$ or $g_{7/2}$ proton quasi-particle coupled with a $s_{1/2}$, $d_{3/2}$, or $h_{11/2}$ neutron. Many of these states could be composed with the 1/2+ proton state which is often low lying in this region. For $N > 82$ up to the deformed region, the neutrons move in the $h_{9/2}$ and $f_{7/2}$ levels. The odd-odd nuclei with $186 \leqslant A \leqslant 206$ have mostly negative parity levels which can be explained among other possibilities as an $h_{11/2}$ proton and an $i_{13/2}$ neutron. The few positive parity levels for $A > 200$ can be formed from an $h_{11/2}$ proton and an $f_{5/2}$ neutron.

types of odd–even mass difference which are observed experimentally.[6,21] We define three odd–even mass differences

$$P_p(Z,N) = E(Z-1,N) + E(Z+1,N) - 2E(Z,N), \quad (56)$$

$$P_n(Z,N) = E(Z,N-1) + E(Z,N+1) - 2E(Z,N), \quad (57)$$

$$P_{np}(Z,N) = E(Z+1,N-1) + E(Z-1,N+1) - 2E(Z,N), \quad (58)$$

where in (56) Z is odd, N even; in (57) Z is even, N odd; and in (58) both N and Z are odd integers. $E(Z,N)$ is the binding energy of the Z,N nucleus. Aside from the effect of the long-range part of the force, which we ignore, these mass differences are simply related to the quasi-particle energies. P_p compares an odd-Z nucleus to the adjacent even–even nuclei and should thus just be equal to $2E_p$, twice the energy of the ground-state proton quasi-particle. Similarly, $P_n = 2E_n$ and $P_{np} = 2E_n + 2E_p$ where E represents in each case the ground-state quasi-particle energy.

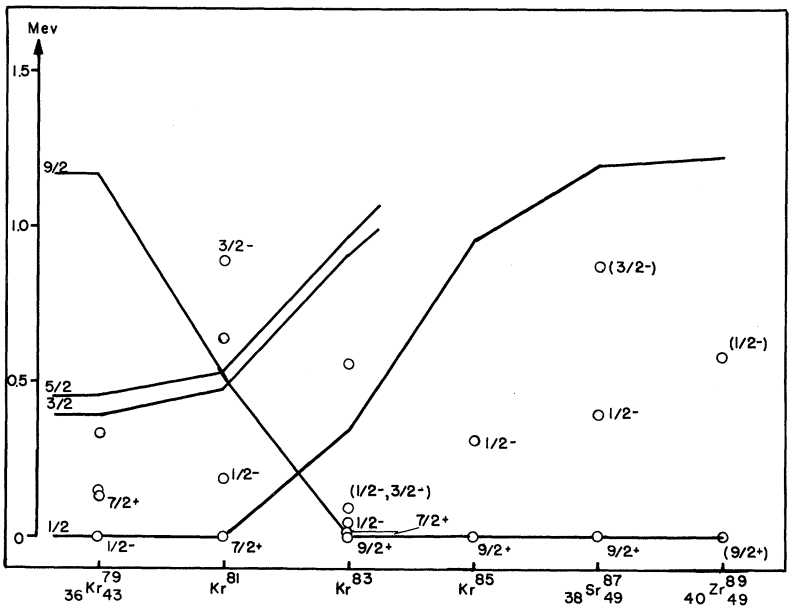

FIG. 32. Energy levels of the odd-mass Kr, Sr, and Zr isotopes.

It is seen that no difficulties arise in describing odd–odd nuclei on the quasi-particle basis, but to use the theory to predict level positions quantitatively, it would be necessary to include accurately residual interactions that have not been considered here.

IV. ODD–EVEN MASS DIFFERENCE

There is now available such a large body of data on nuclear masses of sufficient accuracy that it may be possible to see finer details of shell and interaction effects. The pairing force acting between pairs of protons and between pairs of neutrons produces the

To test the agreement between the theoretical E's and the experimental P's we plot all the experimental data for $P_p(Z,N)$ with Z as the abscissa, see Fig. 33.

[21] The experimental mass differences were obtained from F. Everling, L. A. Konig, J. H. E. Mattauch, and A. H. Wapstra, Nucl. Phys. **18**, 529 (1960) and the Nuclear Data Sheets.

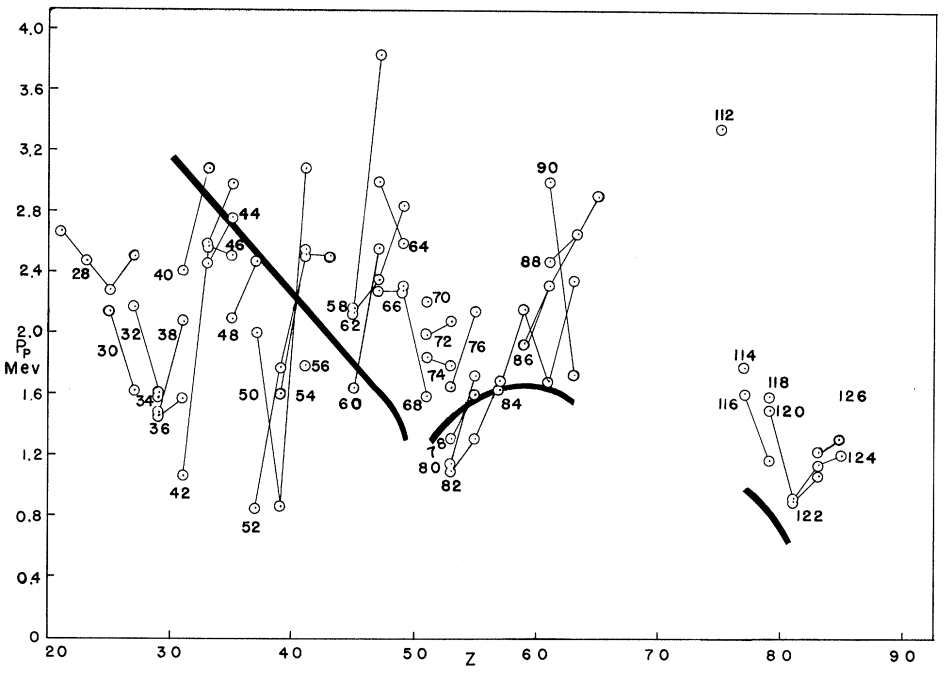

FIG. 33. The quantities $P_p(Z,N)$ vs $2E_p(Z)$. The curve $E_p(Z)$ is $E_p(Z,N)$, the proton quasi-particle energy averaged over N. The points are the experimental $P_p(Z,N)$.

On this same graph the heavy line is $2E_p(Z)$. Actually E_p depends on N as well as Z, but to make the plot readable we simply average over this small N dependence for each Z value. Similarly, on an N scale we plot all $P_n(Z,N)$ data against $2E_n(N)$ averaging over the small Z dependence of the theoretical energy, see Fig. 34. The theoretical curve $2E_n$ shows considerable structure including a sharp dip at $N = 50,82,126$, and a less marked one at $N = 40$. Each of these features is also seen in the data although there is considerable scatter of the points. Also, the over-all trend as a function of N is well represented

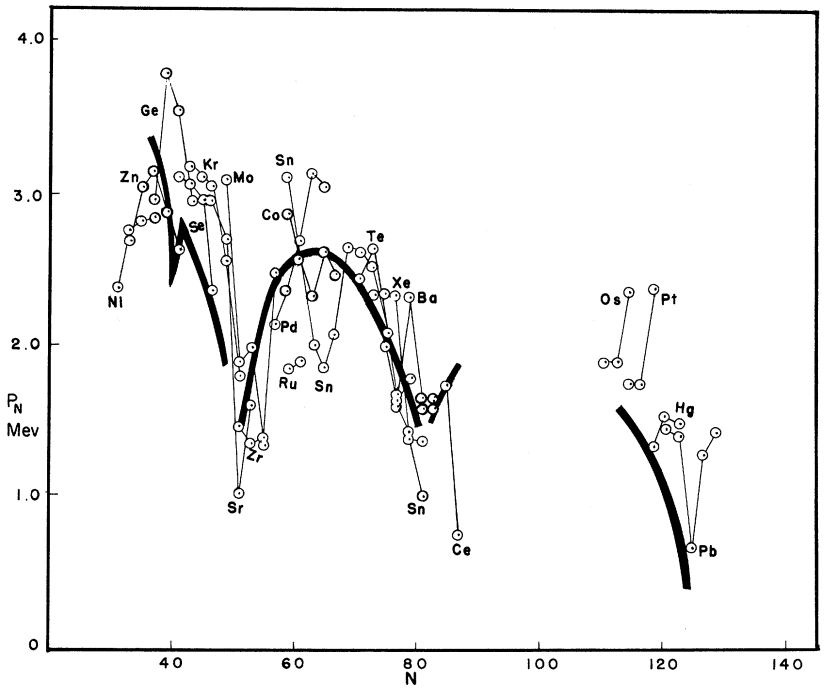

FIG. 34. The quantities $P_n(Z,N)$ vs $2E_n(N)$. The curve $E_n(N)$ is $E_n(Z,N)$, the neutron quasi-particle energy averaged over Z. The points are the experimental $P_n(Z,N)$.

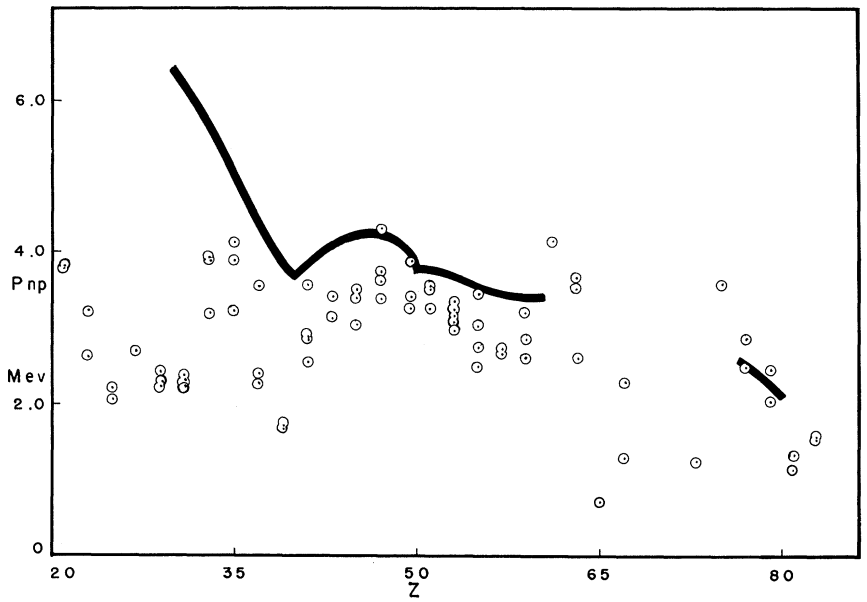

FIG. 35. The quantities $P_{np}(Z,N)$ vs $2E_p + 2E_n$. For the plot against Z, the curve for E_p and E_n are averaged over N. The experimental points $P_{np}(Z,N)$ are the same as in Fig. 36.

by this choice of parameters. The theoretical E_p curve has less noticeable structure showing a little dip at $Z = 50$ and otherwise being a decreasing function of Z to $Z = 82$. The experimental points show a large scatter with little structure. A general decrease in P_p is only seen in that the points above the deformed region $65 < Z < 75$ are lower than those below.

The quantity $2E_p + 2E_n$ depends equally strongly on Z and N. To show any possible structure of the data without resorting to a two-dimensional plot we show all of the P_{pn} data on each of two plots once against Z and once against N as the abscissa (see Figs. 35, 36). As the scatter of the data does not seem to justify a more detailed comparison the plots are compared to the theoretical curves averaged on N and Z, respectively, for the two plots. The main structure noticeable in the theoretical curves, the dip at $Z = 40$, $N = 50$, shows up even more strongly in the experimental points. The lowest points are for $Z = 39$ where the isolated $p_{1/2}$ level is filling giving a small effective degeneracy and thus a small energy gap, while the $Z = 41$ points are higher. This effect is also observed in P_p. The smaller dip at $N = 82$ can also be seen in the data and the rapid drop as N ap-

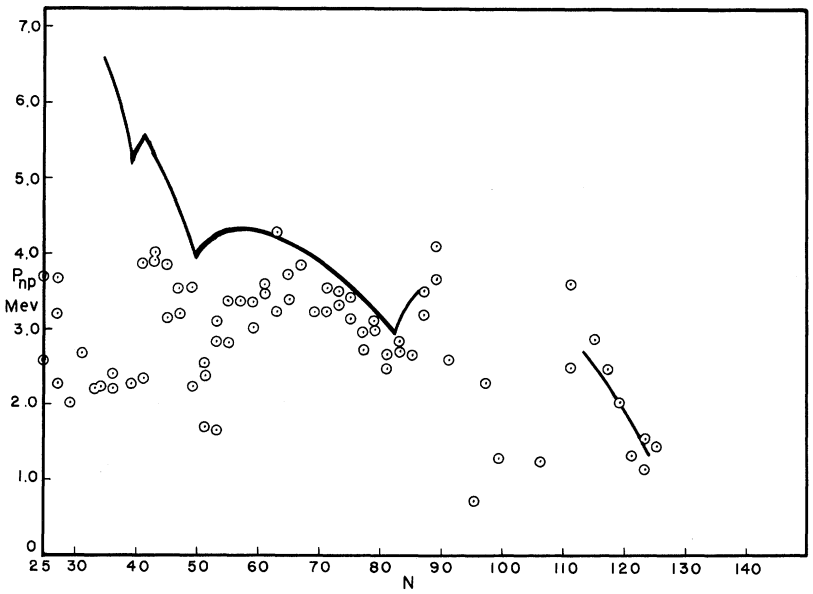

FIG. 36. The quantities $P_{np}(Z,N)$ vs $2E_p + 2E_n$. For the plot against N, the curve for E_p and E_n is averaged over Z.

proaches 126 is also reflected in the data. For $Z > 45$, $N > 60$ the magnitude of the theoretical curves and experimental points agree well, but for the lighter nuclei, while the theoretical curves rise higher, the experimental points have a constant average magnitude from $A \sim 50$ to $A \sim 130$. This is in opposition to the P_n data which show a steady rise with decreasing A in this region in agreement with the theoretical curves. Although there are some discrepancies, the pairing force model can account for shell and subshell effects in the even–odd mass differences in some detail. Forces other than the pairing force must be included to account for the large fluctuations.

V. MAGNETIC DIPOLE MOMENTS

A. Magnetic Dipole Moments of Odd-Mass Nuclei

The magnetic dipole moments have played an important role in the shell model since its earliest beginnings, and from them we have been able to derive important properties both of the nuclear coupling scheme and the nuclear forces. From the observation that in many instances the experimental values of these static moments for odd-mass nuclei tend to be associated with the value expected with a single particle in a level with the spin and orbital angular momentum of the state, one can conclude that the coupling scheme must be similar to that suggested by Mayer and Jensen ("simple" seniority) for these regions.[22] In other regions they provide evidence for the deformation and offer some quantitative information about the collective properties of the states.[23] For the spherical nuclei we attempt a detailed study to try to derive in terms of particle coordinates both the important particle and collective effects involved in producing deviations of these moments from the single-particle values.

1. *Quasi-Particle and Collective Contributions*

The operator for the magnetic dipole moment in the quasi-particle representation is

$$\mu_{\rm op} = \sum_{j'j} 3^{-\frac{1}{2}}\langle j'||\mu||j\rangle\{(U_{j'}U_j + V_{j'}V_j)\eta_j^{1m}{}_{j'} + \tfrac{1}{2}(U_{j'}V_j - U_jV_{j'})[A_{jj'}^{1m\dagger} + (-1)^m A_{j'j}^{1-m}]\} \quad (59)$$

in terms of the single particle operator $\mu = g_s S_z + g_l l_z$ with $g_s = 5.585$ (-3.826) and $g_l = 1(0)$ for protons (neutrons). The operators η^1 and $A^{1\dagger}$ are the quasi-particle scattering and double creation operators, respectively, of rank one. (See Chap. II and Appendix I.)

[22] M. G. Mayer, Phys. Rev. **75**, 1969 (1949), and O. Haxel, J. H. D. Jensen, and H. E. Suess, Phys. Rev. **75**, 1766 (1949).
[23] See A. Bohr and B. R. Mottelson, Ref. 5.

This operator must be evaluated in the states of one quasi-particle with various numbers of phonons

$$\psi_j = C_{j00}^j\alpha_j^\dagger\psi_0 + \sum_{j'} C_{j'12}^j[\alpha_{j'}^\dagger B^\dagger]_j\psi_0 + \sum_{j'J} C_{j'J2J}^j[\alpha_{j'}^\dagger[B^\dagger B^\dagger]_J]_j\psi_0\,, \quad (54)$$

which have been discussed in Chap. II. The η and $A^\dagger$ parts of the magnetic moment operator are of entirely different character, since the η operators do not change the number of quasi-particles, while the other terms create or destroy two quasi-particles. Although the $A^\dagger$ terms are almost entirely responsible for the M1 transitions between the collective states, and are treated in Chap. VII, they play a very minor part in the calculation of the magnetic dipole moments, and are neglected here. The η terms contribute both from the quasi-particle and the phonon parts of the wave functions. It is convenient to separate this operator approximately into two parts, one of which operates only on quasi-particles and the other on phonons.

$$\mu_{\rm op} \cong \sum_{j'j} 3^{-\frac{1}{2}}\langle j'||\mu||j\rangle(U_jU_{j'} + V_jV_{j'})(\eta_{j'j}^1)_{\rm qp} + g_R R_z = \mu_{\rm qp} + g_R R_z\,, \quad (60)$$

with

$$[(\eta)_{\rm qp}, B^\dagger] = 0\,, \quad (61a)$$

and

$$[R, \alpha^\dagger] = 0\,. \quad (61b)$$

This is possible because of the adiabatic character of the vibrational states, which enables quasi-particles to be distinguished from phonons to a good approximation as long as the first vibrational level is well into the gap. The operator R_z appearing in Eq. (60) is the collective angular momentum operator, which is diagonal in phonon number and has diagonal matrix elements in states $\alpha_{jm}^\dagger\psi_0$, $[\alpha_{j'}^\dagger B^\dagger]_{jm}\psi_0$, and $[\alpha_{j'}^\dagger[B^\dagger B^\dagger]_J]_{jm}\psi_0$, which are given in Appendix III, Eqs. (C1), (C2), and (C3). In Sec. B the phonon g factor g_R is derived, and the results of systematic calculations are presented, but in the calculation of the odd-mass nuclei we use $g_R = Z/A$, since the results are insensitive to this value.

The only nonzero matrix elements of the particle part of the magnetic moment operator $\mu_{\rm qp}$ defined by Eq. (60) are for states of no phonon diagonal in the quasi-particles, states of one phonon diagonal in the quasi-particles or with quasi-particle spin-orbit pairs, and states of two phonons diagonal in the quasi-particles or with quasi-particle spin-orbit pairs. Equation (C3) shows that the weak coupling limit for the magnetic dipole moment is just the single-particle (Schmidt) value μ_{lj}, and the only deviations from the shell–model results are produced by the collective

effects in this approximation. In I the coefficients were determined in perturbation theory. In this work we determine these coefficients by the method derived in Chap. II. However, the qualitative conclusions of I are unchanged, i.e., that the phonons themselves do not contribute very much to these moments, but that the major effect is due to the admixture of other quasi-particles; and that the predicted deviations from the single-particle values are much too small to account for the experimental results.

2. *Higher Seniority Contributions*

In the spherical region, the major cause for the deviation of the odd-mass magnetic dipole moments from the single-particle values for one shell-model configuration is the admixture of small amounts of other configurations of higher seniority, as Blin–Stoyle[24] and Arima and Horie[25,26] have demonstrated. Although the wave functions (54) deviate strongly from pure seniority one, neither the pairing nor the quadrupole force can account for these particular types of configuration admixtures. For this reason we calculate the additional contributions which arise from a δ-function interaction in the manner described in I.

Systematic calculations of this effect have been carried out by Freed and Kisslinger.[27] From the quasi-particle states are projected states of the proper number of particles

$$(\alpha^{\dagger}_{lj}\psi^{0}_{0})_{n_e n_o} = \sum_{n_1+n_2\cdots=n_e} \mathfrak{A}^{(e)}_{n_1 n_2\cdots}|j_1^{n_1}(0)j_2^{n_2}(0)\cdots\rangle + \sum_{n_1+n_2\cdots+p=n_o} \mathfrak{A}^{(o)}_{n_1 n_2\cdots p}|j_1^{n_1}(0)j_2^{n_2}(0)\cdots j^{p}(j)jm\rangle\,, \quad (62)$$

in which $n_e(n_o)$ is the number particles of the even (odd) type. The other notation is that of Ref. 27. The n_i are even, p is odd, $j_i^{n_i}(0)$ indicates the seniority zero state of n_i particles in the j_i level, and $j^p(j)$ is the seniority one state of particles in the j level. The admixture coefficients $a^{(e)}$ and $a^{(o)}$ are given by

$$|\mathfrak{A}^{(e)}_{n_i\cdots}|^2 = |\sum_c \mathfrak{A}^{(e)}_c|^{-2} \prod_{\text{even type}} U_i^{2j_i+1-n_i} V_i^{n_i} (j_i+\tfrac{1}{2})^{\frac{1}{2}n_i} \times [(\tfrac{1}{2}n_i)!(j_i+\tfrac{1}{2}-\tfrac{1}{2}n_i)!]^{-1}$$

$$|\mathfrak{A}^{(o)}_{n_i\cdots p}|^2 = |\sum_c \mathfrak{A}^{(o)}_c|^{-2} \prod_{\substack{\text{odd type}\\ i\neq j}} U_i^{2j_i+1-n_i} V_i^{n_i} (j_i+\tfrac{1}{2})^{\frac{1}{2}n_i} \times [(\tfrac{1}{2}n_i)!(j_i+\tfrac{1}{2}-\tfrac{1}{2}n_i)!]^{-1} \times U_j^{2j-p} V_j^{p-1} (j+\tfrac{1}{2})^{\frac{1}{2}(p-1)} [(\tfrac{1}{2}p-\tfrac{1}{2})!(j-\tfrac{1}{2}p)!]^{-1}\,. \quad (63)$$

The subscript c stands for a configuration $n_1, n_2, \cdots$ for the evens or $n_1, n_2 \cdots p$ for the odds. With the δ-function interaction between all particles which was the same used by Arima and Horie, [$V_{ij} = \frac{1}{8}(11 + \sigma_i\sigma_j)V_s\delta(\mathbf{r}_i - \mathbf{r}_j)$], to each of the even and odd configurations in Eq. (62) are admixed configurations of seniority two or three, respectively, which are important for the magnetic moments. These are configuration admixtures in which particles in spin–orbit doublets are coupled to angular momentum unity, the rank of the dipole moment operator. This is discussed in detail for pure configurations in Ref. 26.

As a result of these configuration admixtures, the magnetic moment of a quasi-particle of orbital angular momentum l and angular momentum j is altered from $\mu_{sp}(lj)$ to

$$\mu^{c}_{qp}(lj) = \mu_{sp}(lj) + \sum_{\text{even } c} |\mathfrak{A}^{(e)}_c|^2 \delta\mu^{(e)}_c + \sum_{\text{odd } c} |\mathfrak{A}^{(0)}_c|^2 \delta\mu^{(0)}_c\,. \quad (64)$$

In Eq. (64), the sums run over the configurations with even and odd numbers of particles. The procedure for calculating the changes in the magnetic moments due to the admixtures to the even and odd types of configurations, $\delta\mu^{(e)}_c$ and $\delta\mu^{(o)}_c$, respectively, is exactly the same as that described in Ref. 27, except that in the present work harmonic oscillator wave functions are used for the radial integrals $I(n_i r_i^2 n r^2) = \frac{1}{2}\int R^2_{n_i l_i} R^2_{nl} r^2 dr$. The third column of Tables I and II lists these quasi-particle moments for various states in the spherical nuclei with the same parameters for the pairing force and the single-particle energy levels as are used to obtain the energy systematics discussed in Chap. III.

Having calculated these quasi-particle moments, one simply combines these results with those of the previous part to obtain the magnetic dipole moment of an odd-mass nucleus. Separating the contribution from the zero-, one-, and two- phonon parts of the wave function, the final result is

$$\langle\psi_j|\mu_{op}|\psi_j\rangle = (C^j_{j00})^2 \mu^{c}_{qp}(lj) + \mu_1 + \mu_2\,, \quad (65)$$

[24] R. J. Blin-Stoyle, Proc. Phys. Soc. (London) 66, 1158 (1953).
[25] A. Arima and H. Horie, Progr. Theoret. Phys. (Kyoto) 12, 623 (1954).
[26] A. Arima, H. Horie, and H. Sano, Prog. Theoret. Phys. (Kyoto) 17, 567 (1957).
[27] N. Freed and L. Kisslinger, Nucl. Phys. 25, 611 (1961).

TABLE I. Magnetic moments of odd-proton nuclei. The isotope and state are listed in columns 1 and 2, the ground state being starred when known. Columns 3 and 4 list the quasi-particle (Schmidt) moments and the quasi-particle moment corrected by higher seniority configurations admixed by a δ-function force, respectively. Columns 5, 6, and 7 list the contributions from the zero-, one-, and two-phonon parts of the wave function. Columns 8 and 9 list the theoretical moments with $g_r = 0$ and $g_r = Z/A$, respectively. The last column is the experimental moments in nuclear magnetons. The experimental values were taken from a compilation kindly furnished by Dr. G. Fuller.

Isotope	State	μ_{sp}	μ^c_{qp}	μ_0	μ_1	μ_2	μ_{theor} $g_r = 0$	μ_{theor} $g_r = Z/A$	μ_{exp}
$_{29}Cu^{61}$	3/2*	3.79	1.33	0.96	−0.10	0.00	0.67	0.95	
Cu^{63}	3/2*	3.79	1.31	0.95	−0.11	0.00	0.67	0.84	
Cu^{65}	3/2*	3.79	1.27	0.90	−0.12	−0.01	0.60	0.78	
$_{31}Ga^{67}$	3/2*	3.79	2.32	1.46	0.15	0.07	1.47	1.68	1.90
Ga^{69}	3/2*	3.79	2.27	1.25	0.17	0.09	1.24	1.51	2.02
$_{33}As^{73}$	3/2*	3.79	1.97	0.98	0.97	0.10	1.89	2.05	
As^{75}	3/2*	3.79	2.19	0.99	0.88	0.14	1.77	2.01	1.439
As^{77}	3/2*	3.79	2.21	1.20	0.55	0.13	1.65	1.88	
$_{35}Br^{77}$	3/2*	3.79	2.15	0.93	0.85	0.20	1.86	1.98	
Br^{79}	3/2*	3.79	2.14	1.25	0.68	0.11	1.93	2.05	2.106
Br^{81}	3/2*	3.79	2.18	1.59	0.49	0.06	2.06	2.14	2.270
Br^{83}	3/2*	3.79	2.27	1.94	0.27	0.03	2.20	2.24	
$_{37}Rb^{81}$	3/2*	3.79	2.10	1.15	0.35	0.10	1.47	1.61	2.05
	5/2	0.86	1.32	0.75	0.68	0.09	1.30	1.51	
Rb^{83}	3/2	3.79	2.10	1.45	0.28	0.04	1.68	1.78	
	5/2*	0.86	1.33	0.91	0.50	0.04	1.31	1.45	1.42
Rb^{85}	3/2	3.79	2.09	1.61	0.25	0.02	1.82	1.89	
	5/2*	0.86	1.35	0.97	0.44	0.02	1.32	1.42	1.35
Rb^{87}	3/2*	3.79	2.21	1.87	0.20	0.01	2.05	2.09	2.75
	5/2	0.86	1.32	1.04	0.35	0.02	1.32	1.42	
$_{39}Y^{89}$	1/2*	−0.26	−0.26	−0.26	0.00	0.00	−0.26	−0.26	−0.137
	9/2	6.79	6.14	5.25	0.54	0.02	5.78	5.81	
$_{41}Nb^{91}$	1/2	−0.26	−0.26	−0.26	0.00	0.00	−0.26	−0.26	
	9/2*	6.79	5.94	5.76	0.16	0.00	5.91	5.92	
Nb^{93}	1/2	−0.26	−0.26	−0.20	−0.01	−0.01	−0.24	−0.22	
	9/2*	6.79	5.68	4.02	1.36	0.16	5.46	5.54	6.17
Nb^{95}	1/2	−0.26	−0.26	−0.19	−0.00	−0.01	−0.24	−0.20	
	9/2*	6.79	5.65	3.69	1.57	0.22	5.39	5.48	
$_{43}Tc^{97}$	9/2*	6.79	5.36	4.59	0.67	0.04	5.29	5.30	
Tc^{99}	9/2*	6.79	5.37	4.34	0.88	0.06	5.24	5.28	5.60
Tc^{101}	9/2*	6.79	5.33	3.50	1.47	0.02	5.08	5.17	
$_{45}Rh^{103}$	1/2*	−0.26	−0.26	−0.14	0.03	−0.02	−0.18	−0.13	−0.0883
	9/2	6.79	5.00	4.78	0.20	0.00	4.98	4.99	
Rh^{105}	1/2	−0.26	−0.26	−0.13	0.04	−0.02	−0.16	−0.11	
$_{47}Ag^{105}$	1/2*	−0.26	−0.26	−0.16	0.04	−0.01	−0.18	−0.13	±0.101
Ag^{107}	1/2*	−0.26	−0.26	−0.15	0.04	−0.02	−0.18	−0.13	−0.114
Ag^{109}	1/2*	−0.26	−0.26	−0.15	0.04	−0.02	−0.18	−0.13	−0.131
Ag^{111}	1/2*	−0.26	−0.26	−0.14	0.04	−0.02	−0.17	−0.11	−0.145
Ag^{113}	1/2*	−0.26	−0.26	−0.13	0.05	−0.02	−0.15	−0.10	
$_{49}In^{109}$	1/2	−0.26	−0.26	−0.20	0.00	0.00	−0.23	−0.20	
	9/2*	6.79	6.01	3.60	1.15	0.12	4.80	4.90	5.53
In^{111}	1/2	−0.26	−0.26	−0.20	0.00	0.00	0.23	−0.20	
	9/2*	6.79	6.03	3.67	1.13	0.12	4.85	4.92	5.33
In^{113}	1/2	−0.26	−0.26	−0.20	0.00	0.00	0.23	−0.20	−0.21
	9/2*	6.79	6.05	3.76	1.08	0.11	4.89	4.95	5.52
In^{115}	1/2	−0.26	−0.26	−0.20	0.00	0.00	−0.23	−0.20	
	9/2*	6.79	6.09	3.75	1.11	0.11	4.91	4.98	5.53
In^{117}	1/2	−0.26	−0.26	−0.20	0.00	0.00	−0.24	−0.21	
	9/2*	6.79	6.11	3.77	1.10	0.11	4.94	5.00	
In^{119}	1/2	−0.26	−0.26	−0.20	0.00	0.00	−0.24	−0.21	
	9/2*	6.79	6.03	3.82	1.02	0.10	4.87	4.93	
$_{51}Sb^{119}$	1/2	2.79	0.54	0.12	−0.01	0.02	0.26	0.12	
	5/2*	4.79	2.60	1.68	0.49	0.05	2.09	2.23	
	7/2	1.72	3.78	2.85	0.73	0.07	3.55	3.65	
Sb^{121}	1/2	2.79	0.62	0.11	0.04	0.02	0.31	0.16	
	5/2*	4.79	2.58	1.73	0.47	0.05	2.11	2.24	3.36
	7/2	1.72	3.80	2.96	0.67	0.06	3.60	3.69	
Sb^{123}	1/2	2.79	0.60	0.10	0.07	0.02	0.35	0.19	
	5/2	4.79	2.56	1.75	0.45	0.05	2.13	2.25	
	7/2*	1.72	3.83	3.03	0.64	0.05	3.64	3.72	2.55
Sb^{125}	1/2	2.79	0.58	0.09	0.11	0.02	0.38	0.22	
	5/2	4.79	2.56	1.79	0.43	0.40	2.16	2.29	
	7/2*	1.72	3.85	3.12	0.57	0.44	3.68	3.75	
$_{53}I^{125}$	1/2	2.79	1.59	0.22	0.08	0.10	0.50	0.40	
	5/2*	4.79	3.81	1.46	0.89	0.20	2.42	2.55	3.0
	7/2	1.72	2.77	1.47	1.02	0.25	2.50	2.73	
I^{127}	1/2	2.79	1.56	0.21	0.15	0.11	0.59	0.47	
	5/2*	4.79	3.50	1.65	0.85	0.09	2.42	2.60	2.809

TABLE I. *Continued*

Isotope	State	μ_{sp}	μ_{qp}^{c}	μ_0	μ_1	μ_2	μ_{theor} $g_r = 0$	μ_{theor} $g_r = Z/A$	μ_{exp}
	7/2	1.72	2.79	1.72	0.86	0.15	2.58	2.75	
I^{129}	1/2	2.79	1.55	0.20	0.25	0.11	0.71	0.57	
	5/2	4.79	3.50	1.92	0.77	0.12	2.61	2.80	
	7/2*	1.72	2.81	2.02	0.65	0.09	2.65	2.77	2.617
I^{131}	1/2	2.79	1.56	0.20	0.38	0.11	0.86	0.69	
	5/2	4.79	3.51	2.27	0.63	0.07	2.84	2.98	
	7/2*	1.72	2.82	2.32	0.43	0.03	2.72	2.79	2.738
I^{133}	1/2	2.79	1.57	0.20	0.50	0.10	1.02	0.81	
	5/2	4.79	3.52	2.66	0.48	0.05	3.09	3.18	
	7/2*	1.72	2.83	2.62	0.20	0.01	2.79	2.83	2.84
$_{55}Cs^{129}$	1/2*	2.79	1.73	0.26	0.07	0.10	0.53	0.44	1.47
	5/2	4.79	3.61	1.50	0.89	0.20	2.26	2.58	
	7/2	1.72	2.52	1.39	1.04	0.25	2.45	2.78	
Cs^{131}	1/2	2.79	1.73	0.25	0.18	0.10	0.67	0.55	
	5/2*	4.79	3.63	1.80	0.83	0.15	2.52	2.78	3.52
	7/2	1.72	2.53	1.96	0.54	0.14	2.49	2.64	
Cs^{133}	1/2	2.79	1.73	0.25	0.33	0.11	0.85	0.69	
	5/2	4.79	3.65	2.27	0.67	0.08	2.86	3.03	
	7/2*	1.72	2.53	2.33	0.20	0.03	2.51	2.56	2.58
Cs^{135}	1/2	2.79	1.76	0.23	0.70	0.07	1.22	1.01	
	5/2	4.79	3.69	3.18	0.27	0.01	3.40	3.46	
	7/2*	1.72	2.53	2.49	0.04	0.00	2.52	2.53	2.73
Cs^{137}	1/2	2.79	1.80	0.03	1.42	0.00	1.72	1.46	
	5/2	4.79	3.75	3.74	0.00	0.00	3.74	3.74	
	7/2*	1.72	2.53	2.52	0.00	0.00	2.52	2.52	2.84
$_{57}La^{137}$	5/2	4.79	3.77	3.36	0.21	0.01	3.52	3.51	
	7/2*	1.72	2.28	2.22	0.05	0.00	2.26	2.27	
La^{139}	5/2	4.79	3.84	3.83	0.01	0.00	3.84	3.84	
	7/2*	1.72	2.26	2.25	0.00	0.00	2.25	2.25	2.78
$_{59}Pr^{141}$	5/2*	4.79	4.02	4.02	0.00	0.00	4.02	4.02	4.0
	7/2	1.72	2.00	1.99	0.00	0.00	2.00	2.00	
Pr^{143}	5/2	4.79	3.83	3.10	0.29	0.05	3.32	3.44	
	7/2	1.72	2.18	1.61	0.47	0.05	2.04	2.12	
$_{61}Pm^{145}$	5/2	4.79	3.62	3.35	0.17	0.02	3.48	3.54	
	7/2	1.72	2.23	1.51	0.59	0.07	2.07	2.17	
Pm^{147}	5/2	4.79	3.64	2.92	0.36	0.08	3.21	3.36	(3.6)
	7/2*	1.72	2.21	1.11	0.83	0.18	1.95	2.12	(3.0)
Pm^{149}	5/2	4.79	3.65	1.51	0.75	0.29	2.08	2.55	
	7/2*	1.72	2.19	0.75	0.97	0.35	1.83	2.06	
$_{77}Ir^{191}$	3/2*	0.12	2.02	0.77	0.23	0.05	0.97	1.05	0.18
Ir^{193}	3/2*	0.12	1.02	0.82	0.20	0.04	0.99	1.05	0.19
$_{79}Au^{195}$	1/2	2.79	0.37	0.34	−0.08	−0.01	0.24	0.25	
	3/2*	0.12	0.80	0.61	0.30	0.01	0.84	0.93	
	11/2	7.79	5.30	2.46	2.12	0.49	4.95	5.07	
Au^{197}	1/2	2.79	0.33	0.31	−0.06	−0.01	0.24	0.25	
	3/2*	0.12	0.79	0.63	0.27	0.01	0.84	0.92	0.145
	11/2	7.79	5.29	2.61	2.03	0.43	4.97	5.08	
Au^{199}	1/2	2.79	0.32	0.31	−0.04	0.00	0.25	0.26	
	3/2*	0.12	0.78	0.64	0.24	0.01	0.82	0.89	0.24
	11/2	7.79	5.30	2.78	1.95	0.38	5.00	5.10	
$_{81}Tl^{199}$	1/2*	2.79	1.13	1.11	−0.02	0.00	1.08	1.09	1.57
Tl^{201}	1/2*	2.79	1.04	1.02	−0.01	0.00	1.00	1.01	1.58
Tl^{203}	1/2*	2.79	1.00	0.99	−0.01	0.00	0.97	0.98	1.61
Tl^{205}	1/2*	2.79	0.70	0.70	0.00	0.00	0.70	0.70	1.63

with

$$\mu_1 = \sum_{j'} (C^{j}_{j'12})^2 \left\{ \frac{j'(j'+1)+j(j+1)-6}{2(j+1)j'} \cdot \frac{\mu_{qp}(l'j')}{j'} + \frac{j(j+1)-j'(j'+1)+6}{2j+1} g_R \right\} + \sum_{l'} 2C^{j}_{l'+\frac{1}{2}12} C^{j}_{l'-\frac{1}{2}12} (U_{l'+\frac{1}{2}} U_{l'-\frac{1}{2}} + {}_{l'+\frac{1}{2}} V_{l'-\frac{1}{2}}) \times \frac{[(l+j+7/2)(l'-j+5/2)(l'+j-3/2)(j-l'+5/2)]^{\frac{1}{2}}}{2(j+1)(2l'+1)} \times (g_l - g_s) \tag{66}$$

and

$$\mu_2 = \sum_{j'J} (C^{j}_{j'2J})^2 \left\{ \frac{j(j+1)+j'(j'+1)-J(J+1)}{2(j+1)} \times \frac{\mu_{qp}(l'j')}{j'} + \frac{j(j+1)+J(J+1)-j'(j'+1)}{2(j+1)} g_R \right\}. \tag{67}$$

TABLE II. Magnetic moments of odd-neutron nuclei. [See the caption of Table I.]

Isotope	State	μ_{sp}	μ^c_{qp}	μ_0	μ_1	μ_2	μ_{theor} $g_r = 0$	μ_{theor} $g_r = Z/A$	μ_{exp}
$_{28}Ni^{59}$	3/2*	−1.91	−0.68	−0.40	0.54	0.11	−0.05	0.24	
	5/2	1.37	0.60	0.35	0.15	0.16	0.32	0.66	
Ni^{61}	3/2*	−1.91	−0.65	−0.51	0.20	0.05	−0.44	−0.25	±0.3
	5/2	1.37	0.80	0.64	0.15	0.09	0.69	0.88	±1.15
Ni^{63}	3/2*	−1.91	−0.68	−0.55	−0.14	0.00	−0.80	−0.69	
	5/2	1.37	0.90	0.72	0.26	0.03	0.90	1.02	
$_{30}Zn^{65}$	3/2	−1.91	−0.71	−0.45	−0.18	0.00	−0.67	−0.62	
	5/2	1.37	0.97	0.64	0.23	0.05	0.73	0.92	
Zn^{67}	3/2	−1.91	−0.67	−0.36	0.05	0.00	−0.40	−0.30	
	5/2*	1.37	0.79	0.52	0.18	0.05	0.52	0.75	0.876
$_{32}Ge^{71}$	1/2*	0.64	0.64	0.29	0.17	0.50	0.97	0.86	
	9/2	−1.91	−1.20	−0.46	−0.38	−0.07	−1.09	−0.90	
Ge^{73}	1/2	0.64	0.64	0.29	0.17	0.57	0.92	1.00	
	9/2*	−1.91	−1.03	−0.40	−0.30	−0.05	−0.93	−0.76	−0.879
Ge^{75}	1/2*	0.64	0.64	0.29	0.15	0.47	0.85	0.92	
$_{34}Se^{75}$	5/2*	1.37	0.86	0.12	0.36	0.28	0.01	0.77	
Se^{77}	1/2*	0.64	0.64	0.31	0.15	0.53	0.92	0.99	0.534
Se^{79}	1/2	0.64	0.64	0.36	0.12	0.40	0.83	0.88	
Se^{81}	1/2	0.64	0.64	0.42	0.08	0.28	0.75	0.79	
$_{36}Kr^{79}$	1/2	0.64	0.64	0.30	0.16	0.56	0.94	1.02	
Kr^{81}	1/2	0.64	0.64	0.39	0.11	0.34	0.79	0.84	
Kr^{83}	9/2*	−1.91	−0.39	−0.27	−0.03	0.01	−0.38	−0.30	−0.970
Kr^{85}	9/2*	−1.91	−0.35	−0.16	−0.03	0.02	−0.32	−0.17	±1.005
Kr^{87}	5/2*	−1.91	−0.92	−0.64	0.04	0.05	−0.71	−0.55	
$_{38}Sr^{87}$	9/2*	−1.91	−0.43	−0.38	−0.02	0.00	−0.43	−0.40	−1.093
Sr^{89}	5/2*	−1.91	−0.83	−0.82	0.01	0.00	−0.82	−0.81	
$_{40}Zr^{91}$	5/2*	−1.91	−0.91	−0.87	0.02	0.00	−0.88	−0.85	−1.303
Zr^{93}	5/2*	−1.91	−0.44	−0.40	0.05	0.02	−0.40	−0.32	
$_{42}Mo^{95}$	5/2*	−1.91	−0.44	−0.38	0.07	0.03	−0.37	−0.28	−0.914
$_{42}Mo^{97}$	5/2*	−1.91	−0.16	−0.14	−0.01	0.02	−0.22	−0.13	−0.933
$_{44}Ru^{97}$	5/2	−1.91	−0.44	−0.37	0.08	0.04	−0.36	−0.25	
Ru^{99}	5/2*	−1.91	−0.14	−0.11	0.01	0.06	−0.20	−0.04	−0.63
Ru^{101}	5/2*	−1.91	−0.09	−0.06	−0.03	0.06	−0.20	−0.03	−0.69
$_{46}Pd^{103}$	5/2	−1.91	−0.07	−0.05	−0.01	0.03	−0.16	−0.04	
Pd^{105}	5/2*	−1.91	−0.10	−0.06	0.05	0.02	−0.19	0.01	−0.57
Pd^{107}	5/2	−1.91	−0.14	−0.05	0.16	0.00	−0.31	0.10	
Pd^{109}	5/2	−1.91	−0.18	−0.05	0.18	−0.01	−0.38	0.12	
Pd^{111}	5/2	−1.91	−0.22	−0.05	0.18	0.02	−0.37	0.14	
$_{48}Cd^{107}$	1/2	−1.91	−0.40	−0.27	−0.01	0.05	−0.38	−0.22	
	3/2	1.15	0.57	0.16	0.13	0.08	0.29	0.37	
	5/2*	−1.91	−0.13	−0.09	0.00	0.02	−0.20	−0.07	−0.617
	11/2	−1.91	−0.21	0.22	0.30	0.11	0.48	0.62	
Cd^{109}	5/2*	−1.91	−0.17	−0.10	0.07	0.01	−0.26	−0.03	−0.829
Cd^{111}	1/2*	−1.91	−0.48	−0.34	−0.31	0.02	−0.64	−0.63	−0.595
	5/2	−1.91	−0.23	−0.10	0.13	0.00	−0.34	0.02	(0.73)
Cd^{113}	1/2*	−1.91	−0.50	−0.34	−0.33	0.01	−0.63	−0.66	−0.622
	3/2	1.15	0.60	0.23	0.37	0.12	0.38	0.72	
	5/2	−1.91	−0.26	−0.09	0.17	0.00	−0.38	0.08	
	11/2	−1.91	−0.39	0.17	0.19	0.06	0.31	0.42	
Cd^{115}	1/2*	−1.91	−0.49	−0.33	−0.26	−0.01	−0.51	−0.59	
$_{50}Sn^{111}$	7/2	1.49	0.72	0.69	0.07	0.01	0.74	0.78	
Sn^{113}	1/2	−1.91	−0.81	−0.69	−0.18	0.01	−0.88	−0.86	
	7/2	1.49	0.80	0.75	0.08	0.00	0.83	0.80	
Sn^{115}	1/2*	−1.91	−0.79	−0.68	−0.22	0.00	−0.89	−0.91	−0.918
Sn^{117}	1/2*	−1.91	−0.82	−0.69	−0.18	0.00	−0.84	−0.87	−1.000
	3/2	1.15	0.73	0.61	0.15	0.01	0.68	0.77	
	11/2	−1.91	−0.76	−0.63	−0.08	0.00	−0.75	−0.71	
Sn^{119}	1/2*	−1.91	−0.79	−0.66	−0.07	−0.01	−0.69	−0.74	−1.046
	3/2	1.15	0.73	0.66	0.10	0.00	0.72	0.76	(0.7)
	11/2	−1.91	−0.68	−0.63	−0.03	0.00	−0.67	−0.66	
Sn^{121}	1/2*	−1.91	−0.70	−0.58	0.07	−0.01	−0.49	−0.52	
	3/2	1.15	0.71	0.66	0.07	0.00	0.71	0.73	
	11/2	−1.91	−0.54	−0.53	0.00	0.00	−0.54	−0.54	
Sn^{123}	1/2	−1.91	−0.63	−0.48	0.22	−0.01	−0.27	−0.27	
	3/2	1.15	0.71	0.65	0.05	0.00	0.69	0.70	
	11/2	−1.91	−0.40	−0.40	0.00	0.00	−0.40	−0.40	
Sn^{125}	1/2	−1.91	−0.58	−0.41	0.31	0.00	−0.15	−0.09	
	3/2	1.15	0.71	0.65	0.01	0.00	0.66	0.66	
	11/2	−1.91	−0.26	−0.25	0.00	0.00	0.26	−0.26	
$_{52}Te^{121}$	1/2*	−1.91	−0.58	−0.35	−0.10	−0.04	−0.39	−0.49	
	3/2	1.15	0.65	0.42	0.36	0.02	0.66	0.80	
	11/2	−1.91	−0.49	−0.32	−0.08	0.00	−0.47	−0.39	
Te^{123}	1/2*	−1.91	−0.51	−0.31	0.19	−0.04	−0.09	−0.16	−0.736

TABLE II. *Continued*

Isotope	State	μ_{sp}	μ^c_{qp}	μ_0	μ_1	μ_2	μ_{theor} $g_r = 0$	μ_{theor} $g_r = Z/A$	μ_{exp}
Te^{125}	1/2*	−1.91	−0.47	−0.26	0.43	−0.02	0.13	0.16	−0.887
	3/2	1.15	0.64	0.48	0.15	0.01	0.56	0.64	
	11/2	−1.91	−0.22	−0.22	0.00	0.00	−0.22	−0.22	
Te^{127}	3/2*	1.15	0.64	0.51	0.04	0.01	0.52	0.57	
	11/2	−1.91	−0.11	−0.10	0.01	0.00	−0.11	−0.09	
Te^{129}	3/2*	1.15	0.66	0.52	0.01	0.02	0.50	0.56	
	11/2	−1.91	−0.05	−0.04	0.03	0.00	−0.05	−0.01	
$_{54}Xe^{127}$	1/2*	−1.91	−0.54	−0.24	0.47	−0.03	0.18	0.19	
	3/2	1.15	0.66	0.30	0.30	0.07	0.42	0.67	
	11/2	−1.91	−0.32	−0.32	0.00	0.00	−0.32	−0.32	
Xe^{129}	1/2*	−1.91	−0.51	−0.20	0.58	0.01	0.28	0.40	−0.777
Xe^{131}	3/2*	1.15	0.68	0.44	0.05	0.05	0.42	0.53	0.691
	11/2	−1.91	−0.15	−0.10	0.15	0.01	−0.15	−0.07	
Xe^{133}	3/2*	1.15	0.71	0.50	0.04	0.03	0.48	0.57	
	11/2	−1.91	−0.18	−0.12	0.01	0.01	−0.17	−0.10	
$_{56}Ba^{131}$	1/2*	−1.91	−0.58	−0.21	0.58	0.01	0.27	0.38	
	3/2	1.15	0.69	0.32	0.17	0.09	0.36	0.58	
Ba^{133}	1/2*	−1.91	−0.60	−0.19	0.57	0.04	0.23	0.43	
	3/2	1.15	0.70	0.40	0.08	0.07	0.39	0.54	
	11/2	−1.91	−0.26	−0.15	−0.02	0.01	−0.25	−0.16	
Ba^{135}	3/2*	1.15	0.73	0.55	0.03	0.02	0.53	0.61	0.837
Ba^{137}	1/2	−1.91	−0.84	−0.52	0.13	0.00	−0.54	−0.39	
	3/2*	1.15	0.78	0.77	0.00	0.00	0.77	0.77	0.936
	11/2	−1.91	−0.37	−0.37	0.00	0.00	−0.37	−0.37	
$_{58}Ce^{139}$	3/2*	1.15	0.79	0.79	0.00	0.00	0.79	0.79	±0.8
	11/2	−1.91	−0.48	−0.48	0.00	0.00	−0.48	−0.48	
$_{60}Nd^{141}$	3/2*	1.15	0.78	0.78	0.00	0.00	0.78	0.78	
Nd^{143}	7/2*	−1.91	−1.04	−1.04	0.00	0.00	−1.04	−1.04	−1.0
Nd^{145}	7/2*	−1.91	−1.07	−0.46	−0.11	0.05	−0.75	−0.52	−0.7
Nd^{147}	5/2*	1.37	0.96	0.13	−0.18	0.09	0.04	0.03	±0.6
$_{62}Sm^{147}$	7/2*	−1.91	−1.05	−0.51	−0.09	0.05	−0.76	−0.55	−0.8
Sm^{149}	7/2*	−1.91	−1.07	−0.40	−0.12	0.09	−0.72	−0.44	−0.6
$_{76}Os^{189}$	3/2*	−1.91	0.15	0.03	0.36	0.33	0.21	0.73	0.657
Os^{191}	3/2	−1.91	0.36	0.10	−0.06	0.33	0.03	0.38	
$_{78}Pt^{193}$	1/2*	0.64	0.64	0.21	0.00	0.09	0.31	0.30	
Pt^{195}	1/2*	0.64	0.64	0.24	−0.03	0.09	0.14	0.13	0.606
$_{80}Hg^{195}$	1/2*	0.64	0.64	0.27	−0.02	0.03	0.29	0.29	0.535
	13/2	−1.91	0.63	0.43	0.21	0.03	0.61	0.67	−1.039
Hg^{197}	1/2*	0.64	0.64	0.31	−0.05	−0.04	0.26	0.22	0.527
	13/2	−1.91	0.65	0.40	0.25	0.05	0.62	0.69	−1.04
Hg^{199}	1/2*	0.64	0.64	0.38	−0.05	0.00	0.39	0.32	0.530
Hg^{201}	3/2*	−1.91	0.95	0.69	0.23	0.02	0.89	0.95	−0.357
$_{82}Pb^{207}$	1/2*	0.64	0.64	0.64	0.00	0.00	0.64	0.64	0.590

3. *Results and Discussion*

In Tables I and II the experimental[28] and theoretical results are listed for the odd-proton and odd-neutron magnetic dipole moments, respectively, in units of nuclear magnetons. We use harmonic oscillator wave functions and take the quantity $V_s I$ as a dimensionless radial integral multiplied by $CA^{-\frac{1}{3}}$, in which C is a constant. The value of $C = 50$ MeV is used for all of the calculations. Some systematic improvement can be gained in the fitting of the data with some variation in the magnitude of the force in the various regions, as discussed below. In Appendix II we include sufficient information about the states to make possible a rapid calculation of special cases with different values of the parameter. In the tables the ground state is starred when known (column two), the fifth column lists the contribution from the no-phonon component $\mu_0 = (C^j_{j00})^2 \mu^c_{qp}(lj)$, and the other columns are defined in Eqs. (C4) and (65)–(67).

For the most part the largest portion of the dipole moments arise from the quasi-particle with no phonon, with the higher seniority corrections playing an important role. Therefore this aspect of the calculation is an average over the results using pure configurations, with the averaging determined by the pairing force. The two-phonon contributions are almost always quite small. Although the one-phonon contributions are frequently large this is usually due to the quasi-particles which are admixed with the phonon rather than the phonon itself. We have also

[28] G. Fuller (private communication).

given the results with the phonon g_R factor equal to zero—thereby keeping the contributions of the admixed quasi-particles but neglecting that of the phonon itself. In very few cases are the results changed very much and there is not sufficient systematic dependence upon the value of this collective g factor to estimate its magnitude from the odd-mass data.

For the odd-proton nuclei the theoretical results are in good agreement with the experimental data. The main errors seem to come from the treatment of the admixtures due to the δ force. For the Tl ground states, in which the phonon admixtures are negligible, a decrease in the force strength C of some 30% is needed to increase the theoretical values to about 1.6 nm. However, for the 3/2 states in Au and Ir it might be difficult to fit the experimental values unless the admixtures introduced by the long-range force are altered, for although a decrease in C reduces the magnitude of the magnetic moment of the 3/2 quasi-particle it increases those of the 1/2 and 5/2 quasi-particles, which are admixed by the phonons.

There is also a large inaccuracy in the calculated value of the 1/2 ground states in Cs^{129}. This is not unexpected since this is the rather unusual state arising in the zeroth order from the 5/2 quasi-particle coupled to one phonon and is therefore especially sensitive to the parameters (see Chap. III). In fact, only a moderate increase in the admixture of the 5/2 quasi-particle and one-phonon component of the state would be needed to increase the theoretical value to 1.4 nm, since the 5/2 quasi-particle has the largest moment of 3.61 nm for this isotope.

The results for the 1/2-states are of special interest. Although the configuration mixing due to a δ-function force is unable to alter these moments from the single-particle values, which is an important argument for the validity of these methods since the experimental values are also close to the single-particle values,[24] the configuration mixing due to the phonons does accomplish this. The best systematics are found in the Ag isotopes, from which one sees that the magnitude of the shifts from the single-particle value are in general agreement with the experimental results. This is the clearest case for which one can separate the effects of the long-range force from the short-range force for the magnetic dipole moments. There is no indication of a need for a quenched particle moment.

The numerical results for the odd-neutron isotopes are not in as good agreement with the experimental values as for the odd-proton cases. In the lighter isotopes the calculated results follow the experimental trends but vary too strongly from the single-particle values. However, a decrease of the constant C by about 20% would bring all of the theoretical results into satisfactory agreement for this region. For the isotopes above the deformed region a large change in the value of the strength of the δ force is called for. A choice of the constant C of 25 MeV instead of 50 MeV would bring the 13/2 and 3/2 states into approximate agreement with the experimental values without changing the 1/2 quasi-particle moments, which is consistent with the results for odd-proton nuclei in this region.

The large discrepancy in the moments of the 1/2+ states in Te and Xe is due to the large phonon plus 3/2 quasi-particle component. This could mean that the wrong spin-1/2 level is dropping down, a result which could follow from a relatively small change in the unperturbed states before the quadrupole force is included.

The general conclusion for the magnetic dipole moments is that there are a number of different effects which are important for at least some of the nuclei, and that one must include all of them to gain quantitative agreement with the systematic data. However, since the phonon contributions are often about equal to the decrease in the no-phonon contribution from the pure quasi-particle value, the final numerical result is often similar to the pure quasi-particle moment, although the interpretation is quite different. Thus these moments are rather insensitive to important nuclear structure considerations.

B. Magnetic Dipole Moment of One-Phonon States

In the preceding section we have used for the g factor of a phonon g_R a value of Z/A which is the approximate prediction of the collective model.[23] In this section we evaluate g_R in terms of particle quantities. It is the scattering terms η in the moment operator which lead to a nonzero moment. From Eq. (59) the magnetic dipole moment of a phonon is

$$\mu^{\mathrm{ph}} = \sum_{jj'} 3^{-\frac{1}{2}} \langle j' || \mu || j \rangle (U_j U_{j'} + V_j V_{j'}) \langle \psi_0 B | \eta^1_{j'j} | B^\dagger \psi_0 \rangle. \tag{68}$$

The matrix element in Eq. (68) is evaluated by taking the commutator

$$\begin{aligned} \langle \psi_0 | B \eta^1_{j'j} B^\dagger | \psi_0 \rangle &= \langle \psi_0 \eta^1_{j'j} B B^\dagger \psi_0 \rangle + \langle \psi_0 [B, \eta^1_{j'j}] B^\dagger \psi_0 \rangle \\ &\approx \langle \psi_0 \eta^1_{j'j} \psi_0 \rangle + \langle \psi_0 [B, \eta^1_{j'j}] B^\dagger \psi_0 \rangle , \end{aligned} \tag{69}$$

in which the Sawada approximation, $[B, B^\dagger] = 1$, has been applied in the first term. This first term, which involves the interaction between quasi-particles in

the ground state is generally considerably smaller than the second term, and is neglected henceforth. Applying the commutation rule for $[\eta^{1m}_{ab}, A^{\dagger 2m}_{cd}]$ [given in Appendix I, Eq. (A4)] and the analogous commutation rule for $[\eta^{1m}_{ab}, A^{2-m}_{cd}]$, one finds that

$$\mu^{\rm ph} = \sum_{jj'j''} 5^{\frac{1}{2}} \langle j'||\mu||j\rangle (U_jU_{j'} + V_jV_{j'}) C^{212}_{202} W(1j'2j'';j2) \times [r_\omega(j'j'')r_\omega(jj'') + s_\omega(j'j'')s_\omega(jj'')] , \quad (70)$$

in which the r_ω and s_ω are the coefficients which appear in the expansion of the phonon into quasi-particles [Eq. (34)]. Writing this out fully, one has

$$\mu^{\rm ph} = 8\cdot 5^{-\frac{1}{2}} C^{212}_{202} N^2_\omega \omega \sum_{jj'j''} \langle j'||\mu||j\rangle \times (U_jU_{j'} + V_jV_{j'}) W(1j'2j'';j2) \times (U_jV_{j''} + U_{j''}V_j)(U_{j'}V_{j''} + U_{j''}V_{j'}) \times \frac{(E_j + E_{j'} + 2E_{j''})\langle j||q||j''\rangle\langle j'||q||j''\rangle}{[(E_j + E_{j''})^2 - \omega^2][(E_{j'} + E_{j''})^2 - \omega^2]} . \quad (71)$$

N_ω is defined by Eq. (94).

The results of sample calculations for the parameters used in Chap. III are given in Table III.

TABLE III. Gyromagnetic ratio for the phonon. Since there are no experimental results for any of the nuclei studied, only the results for the 50-82 shell are presented.

Isotope	$g^{\rm a}_{\rm ph}$	Isotope	$g^{\rm a}_{\rm ph}$
$_{50}Sn^{112}_{62}$	0.01	$_{54}Xe^{126}_{72}$	0.26
Sn^{114}	−0.02	Xe^{128}	0.25
Sn^{116}	−0.09	Xe^{130}	0.28
Sn^{118}	−0.14	Xe^{132}	0.33
Sn^{120}	−0.15	Xe^{134}	0.38
Sn^{122}	−0.14	Xe^{136}	0.49
Sn^{124}	−0.10	$_{56}Ba^{130}_{74}$	0.34
$_{52}Te^{120}_{68}$	0.20	Ba^{132}	0.36
Te^{122}	0.17	Ba^{134}	0.41
Te^{124}	0.16	Ba^{136}	0.42
Te^{126}	0.18	Ba^{138}	0.52
Te^{128}	0.21	$_{58}Ce^{138}_{80}$	0.57
Te^{130}	0.09	Ce^{140}	0.95
		$_{60}Nd^{142}_{82}$	1.95

[a] The calculation includes only the particles in the outer shells. The core contribution would shift the g values toward 0.45.

VI. ELECTRIC QUADRUPOLE MOMENTS

Although the experimental data for quadrupole moments are less extensive and often less reliable than that for magnetic dipole moments, they offer new possibilities for information about nuclear structure. In the first place, even in the Mayer–Jensen coupling scheme, the quadrupole moment changes from a maximum positive value for one particle to a maximum negative value as one adds pairs of particles, so that the magnitude of the moment gives information about the filling of the particle levels. As was pointed out above, if one knows the occupation numbers of the particle levels in the pairing scheme, one completely specifies the wave function, so that in the absence of other effects the quadrupole moments provide quite direct evidence about the wave functions in our model. However, the other point in which there is a strong qualitative difference between the systematics of magnetic dipole and electric quadrupole moments, is large additions to the quadrupole moments which arise from the admixture of phonon states to quasi-particle states, so that the particle contributions are often considerably smaller than the collective ones.

A. Odd-Mass Nuclei

1. *Quasi-Particle and Collective contributions*

The expression for the quadrupole operator in terms of quasi-particles has been given in Chap. II, Eq. (17) [here we include the extra factor of $(16\pi/5)^{\frac{1}{2}}$ to conform to the usual definition]:

$$Q_0 = (4\pi^{\frac{1}{2}}/5) \sum_{j'j} \langle j'||q||j\rangle [\tfrac{1}{2}(U_jV_{j'} + U_{j'}V_j) \times (A^{2\dagger}_{j'j} + (-1)^m A^2_{j'j}) + (U_jU_{j'} - V_jV_{j'})\eta^2_{j'j}] . \quad (72)$$

For the evaluation of this operator in the states of odd-mass nuclei [see Eq. (54)], the η terms connect the parts of the wavefunction with equal numbers of phonons, while the $A^\dagger$ terms change the number of phonons. Let us first treat the latter terms.

Because of the nature of the collective states as quadrupole vibrational states, in case of competition between particle and collective parts of the wavefunction, we can expect the collective aspects to be much larger for the quadrupole operator. Therefore, in evaluating the $A^\dagger$ terms in Eq. (72) we can neglect the quasi-particle contributions compared to the phonon contributions with an accuracy which can be estimated by comparing the single-particle E2 transition rates to the experimental values, i.e., with an error of less than ten percent in most nuclei. Since the quasi-particle transitions are hindered for E2 transitions (see Chap. VII), the accuracy is probably considerably better than this in most cases. The most important part comes from the off-diagonal elements

between the one-phonon and zero-phonon states. The matrix element involved is

$$\langle\psi_0\alpha_{jm}|Q_0|[\alpha_{j'}^\dagger B^\dagger]_{jm}|\psi_0\rangle \cong (-1)^{j'-j}\langle\psi_0|\alpha_{jm}Q_0[B^\dagger\alpha_{j'}^\dagger]_{jm}|\psi_0\rangle\,. \quad (73)$$

This is most easily evaluated by recoupling the phonon operator to the quadrupole operator:

$$\langle\psi_0\alpha_{jm}|Q_0|[\alpha_{j'}^\dagger B^\dagger]_{jm}|\psi_0\rangle \cong (-1)^{j'-j}C^{2j'j}_{0mm} \times \textstyle\sum_s [(2j+1)(2S+1)]^{\frac{1}{2}}W(22jj';Sj) \times \langle\psi_0\alpha_{jm}\{[Q_0B^\dagger]_s\alpha_{j'}^\dagger\}_j\psi_0\rangle\,, \quad (74)$$

in notation indicating that the quadrupole operator is vector coupled to the phonon operator, which is in turn coupled to the j' quasi-particle to form a quantity of angular momentum j. One can take advantage of the fact that

$$\langle\psi_0\alpha_{jm}|B^\dagger \approx 0 \quad (75)$$

to replace the factor $[Q_0B^\dagger]^s$ by the commutator $[Q_0, B^\dagger]^s$, which we define by

$$[Q_0,B^\dagger]^S_M = \textstyle\sum_m [Q_0^m,B^{M-m\dagger}]C^{22S}_{m\,M-m\,M}\,. \quad (76)$$

Using the approximate commutation rules (26), this commutator is

$$[Q_0,B^\dagger]^S \cong \delta_{S0}\textstyle\sum_\xi\sum_{jj'} e^\xi_{\text{eff}}(U_jV_{j'}+V_jU_{j'})\langle j'||q||j\rangle \times \tfrac{1}{2}\,(r_\omega(j'j)+s_\omega(j'j))\,, \quad (77)$$

which is the result used to obtain the B(E2)'s. This result must be intimately connected to the B(E2)'s, since the same operator is involved, and the expression for the matrix element in question, with the above approximations (which, essentially, are the distinguishing of the quasi-particles for the phonons), is simply

$$\langle\psi_0\alpha_{jj}|Q_0|[\alpha_j^\dagger B^\dagger]_{jj}|\psi_0\rangle \cong \frac{1}{5^{\frac{1}{2}}}\left[\frac{j(2j-1)}{(j+1)(2j+3)}\right]^{\frac{1}{2}} \times [B(\text{E2})]^{\frac{1}{2}}\,. \quad (78)$$

These matrix elements give most of the contribution of the $A^\dagger$ terms in Eq. (72) and are the only ones included in our calculations.

In evaluating the η terms in Eq. (72), we make the same type of approximations as were used in the case of the magnetic moments (see Chap. V. A.1). However, we shall keep only the one-quasi-particle matrix elements of η since the one-phonon and two-phonon matrix elements are never more than about 25% of these terms. Moreover, (for the quadrupole moments) the purely collective contributions from the $A^\dagger$ (derived above) are usually considerably larger than the η contributions. The collective contributions to the one-phonon diagonal matrix elements are of the same magnitude as the quasi-particle contributions, and they are also ignored. The matrix element of the η terms in the state of one quasi-particle and no phonons is

$$Q_{\text{qp}} = \langle\psi_0\alpha_{jj}Q_0\alpha_{jj}^\dagger\psi_0\rangle = -e^\xi_{\text{eff}}(U_j^2-V_j^2)[(2j-1)/2(j+1)]\langle j|r^2|j\rangle\,, \quad (79)$$

which is the same result as derived in I. However, in addition to the pure quasi-particle results, there are contributions of about equal magnitude from the admixture of other configurations. This is treated below.

2. *Contributions from Configurations Admixed by a δ-Function Force*

Just as in the treatment of the magnetic dipole moments, there are certain configurations admixed by a δ-function force, or any other short-range force, which are not admixed by the pairing or quadrupole forces in the approximations used in this work, but which contribute to the quadrupole moments amounts of the same general magnitude as the single-particle contributions.

On the other hand, one has already included a certain amount of configuration mixing by introducing the effective charges e^ξ_{eff} in Eq. (31). These effective charges are presumably due to the polarization of the closed shells by the particles in the major shell being filled,[2] and are associated with configurations at the energy required to break a double closed shell. The configurations considered in this section are essentially associated only with the particles in the levels being filled, and are at energies of the magnitude of the gap, which is considerably smaller than the energy needed to break a closed shell (an essential assumption of this model). Still, the separation of these effects is not at all complete, and effects such as the blocking of some shell-model levels by adding particles outside the closed shells will also change the magnitude of the effective charge which arises from the closed shells. Thus the calculation of this section also gives an estimate of the magnitude of changes in the effective charges as one fills a major shell.

Referring to Eq. (62), for both the odd and even pure seniority-one and seniority-zero configurations, there are additions to the quadrupole moments. Let us refer to the state in which the odd number of particles are in the l_0j_0 level, with p odd particles in a particular configuration. For each level in which there is an even number of particles, i.e., $l_i \neq l_0$

whether of the even or odd type of particles, there are admixtures to the quadrupole moments of the form

$$\delta Q_{l_i \neq l_0} = [-(2j_0 + 1 - p)f]/(\Delta\epsilon_i + 2E_S) . \quad (80)$$

In Eq. (80) the factor f depends upon the single-particle values for the l's and j's, the occupation numbers, the force strength V_s, and the radial integrals. The explicit form is given in Ref. 26. In the energy denominator, when the admixed configurations involve elevating a particle to its spin-orbit partner, we use the parameters of Chap. III or $7(2l_i + 1)A^{-\frac{2}{3}}$ MeV. There are also admixtures for which $\Delta\epsilon_i$ is zero. These are simply the broken pair contributions of spin-2 which give the major effects for the additional quadrupole moments arising from the configuration mixing of the particles in the shell being filled. The quantity $2E_s$ is the energy for the lowest excitations which break a pair, and is used to represent the average energy to break a pair for each of the pure configurations. There are similar equations for the admixtures from the odd level [Ref. (26)], which are treated in the same manner.

Equation (80) shows that there is a slight complication for these admixtures to the moments compared to the analogous magnetic dipole moment calculation, since the admixtures of the even type depend upon p, the number of particles in the odd level. The physical interpretation is that the quadrupole moment for a half-filled subshell is zero, for a shell less than half-filled it is negative, and for more than half-filled it is positive. Thus, if for each p the $\delta Q_{l_i \neq l_0}$ are summed for the even type with occupation numbers n_1, $n_2 \cdots$, and this is referred to as $\delta Q^p_{n_1 n_2} \cdots$, the resulting change in the moment from the even configuration n_1, $n_2 \cdots$ is

$$\delta Q^{\text{even}}_{n_1 n_2 \cdots} = \sum_p P_p \delta Q^p_{n_1 n_2 \cdots} , \quad (81)$$

where P_p = probability of finding p particles in the j level. δQ^{odd}_c, the change in the quadrupole moment arising from an odd configuration, is calculated as in Ref. 26 with the modifications mentioned above. Therefore, we obtain as the electric quadrupole moment of a quasi-particle

$$Q^c_{\text{qp}}(lj) = -e^{\xi}_{\text{eff}} \left[\frac{16\pi}{5}\right]^{\frac{1}{2}} (U_j^2 - V_j^2) \frac{2j-1}{2(j+1)} \langle j|r^2|j\rangle + \sum_{\text{even } c} e^{\xi}_{\text{eff}} |\mathfrak{A}^{(e)}_c|^2 \delta Q^{\text{even}}_c + \sum_{\text{odd } c} e^{\xi}_{\text{eff}} |\mathfrak{A}^{(o)}_c|^2 \delta Q^{\text{odd}}_c . \quad (82)$$

Finally, combining Eqs. (78) and (82), the electric quadrupole moment is

$$\langle \psi_j | Q_{\text{op}} | \psi_j \rangle = (C^j_{j00})^2 Q^c_{\text{qp}}(lj) + \frac{8\pi}{5} C^j_{j12} C^j_{j00} \left[\frac{j(2j-1)}{(j+1)(2j+3)}\right]^{\frac{1}{2}} [B(\text{E2})]^{\frac{1}{2}} . \quad (83)$$

The results are given and compared to experiments[28] in tables IV and V for odd-proton and odd-

TABLE IV. Quadrupole moments of odd-proton nuclei. The isotope and state are listed in the first two columns, the ground state being starred when known. The next three columns contain the quasi-particle moment, and the moment corrected by wave functions admixed by a δ force for two effective charges. The phonon contribution is in column six, and the last two columns are the theoretical and experimental moments in units of 10^{-24} cm^2. The experimental values were taken from a compilation kindly furnished by Dr. Gladys Fuller.

Isotope	State	$e^p = 2, e^n = 1$ Q_{qp}	$e^p = 1, e^n = 0$ Q^c_{qp}	$e^p = 2, e^n = 1$ Q^c_{qp}	Q_{ph}	$e^p = 2, e^n = 1$ Q_{theor}	Q_{exp}
$_{31}Ga^{67}$	3/2*	−0.03	−0.02	−0.04	−0.17	−0.19	0.22
$_{31}Ga^{69}$	3/2*	−0.03	−0.02	−0.04	−0.16	−0.18	0.20
$_{31}Ga^{71}$	3/2*	−0.03	−0.02	−0.04	−0.16	−0.18	0.12
$_{33}As^{73}$	3/2*	0.02	0.02	0.09	0.26	0.33	
$_{33}As^{75}$	3/2*	0.01	0.02	0.07	0.18	0.21	0.31
$_{33}As^{77}$	3/2*	0.002	0.01	0.04	0.06	0.08	
$_{35}Br^{77}$	3/2*	0.06	0.05	0.17	0.51	0.58	
$_{35}Br^{79}$	3/2*	0.05	0.05	0.16	0.42	0.51	0.32
$_{35}Br^{81}$	3/2*	0.04	0.04	0.13	0.30	0.39	0.27
$_{35}Br^{83}$	3/2*	0.03	0.03	0.09	0.16	0.24	
$_{37}Rb^{85}$	5/2*	0.15	0.11	0.35	0.40	0.65	0.28
	3/2	0.09	0.08,	0.21	0.26	0.44	
$_{37}Rb^{87}$	5/2	0.18	0.12	0.25	0.34	0.54	
	3/2*	0.08	0.07	0.14	0.20	0.32	0.14
$_{39}Y^{89}$	9/2	−0.24	−0.15	−0.31	−0.28	−0.56	
$_{41}Nb^{93}$	9/2*	−0.19	−0.12	−0.28	−0.42	−0.62	−0.13
$_{41}Nb^{95}$	9/2*	−0.19	−0.12	−0.31	−0.58	−0.78	
$_{43}Tc^{97}$	9/2*	−0.09	−0.05	−0.09	−0.53	−0.61	
$_{43}Tc^{99}$	9/2*	−0.08	−0.04	−0.09	−0.71	−0.77	+0.3
$_{43}Tc^{101}$	9/2*	−0.08	−0.04	−0.10	−1.07	−1.13	
$_{45}Rh^{101}$	9/2	0.02	0.03	0.17	0.32	0.49	
$_{45}Rh^{103}$	9/2	0.03	0.03	0.20	0.46	0.65	
$_{49}In^{109}$	9/2*	0.25	0.14	0.62	0.52	0.97	1.20

TABLE IV. *Continued*

Isotope	State	$e^p = 2, e^n = 1$ Q_{qp}	$e^p = 1, e^n = 0$ Q^c_{qp}	$e^p = 2, e^n = 1$ Q^c_{qp}	Q_{ph}	$e^p = 2, e^n = 1$ Q_{theor}	Q_{exp}
$_{49}In^{111}$	9/2*	0.25	0.14	0.62	0.53	0.97	1.18
$_{49}In^{113}$	9/2*	0.25	0.14	0.62	0.54	0.98	1.0
$_{49}In^{115}$	9/2*	0.25	0.14	0.62	0.56	1.01	1.1
$_{49}In^{117}$	9/2*	0.26	0.14	0.61	0.55	1.01	
$_{49}In^{119}$	9/2*	0.26	0.14	0.64	0.52	1.01	
$_{51}Sb^{119}$	5/2*	−0.31	−0.12	−0.06	−0.41	−0.45	−0.2
	7/2	−0.27	−0.10	+0.02	−0.46	−0.46	
$_{51}Sb^{121}$	5/2*	−0.31	−0.12	−0.07	−0.39	−0.43	−0.26
	7/2	−0.27	−0.10	−0.01	−0.43	−0.44	
$_{51}Sb^{123}$	5/2	−0.31	−0.12	−0.07	−0.37	−0.42	
	7/2*	−0.27	−0.10	−0.04	−0.40	−0.43	
$_{51}Sb^{125}$	5/2	−0.31	−0.12	−0.07	−0.34	−0.40	
	5/2*	−0.28	−0.11	−0.06	−0.36	−0.41	
$_{53}I^{125}$	5/2*	−0.25	−0.16	−0.60	−0.75	−1.00	−0.89
	7/2	−0.17	−0.11	−0.45	−0.88	−1.05	
$_{53}I^{127}$	5/2*	−0.26	−0.17	−0.61	−0.70	−0.99	−0.79
	7/2	−0.17	−0.11	−0.43	−0.81	−1.08	
$_{53}I^{129}$	5/2	−0.26	−0.17	−0.59	−0.63	−0.96	
	7/2*	−0.17	−0.11	−0.39	−0.67	−0.95	−0.55
$_{53}I^{131}$	5/2	−0.26	−0.17	−0.54	−0.52	−0.87	
	7/2*	−0.17	−0.11	−0.35	−0.49	−0.76	−0.40
$_{55}Cs^{131}$	5/2*	−0.21	−0.14	−0.48	−0.80	−1.04	
	7/2*	−0.04	−0.02	−0.04	−0.46	−0.49	
$_{55}Cs^{133}$	5/2	−0.21	−0.14	−0.45	−0.68	−0.96	
	7/2*	−0.04	−0.02	−0.04	−0.27	−0.31	−0.003
$_{55}Cs^{135}$	5/2	−0.22	−0.15	−0.41	−0.39	−0.74	
	7/2*	−0.04	−0.02	−0.04	−0.08	−0.12	0.049
$_{55}Cs^{137}$	5/2	−0.22	−0.15	−0.30	−0.03	−0.33	
	7/2*	−0.03	−0.02	−0.03	−0.005	−0.03	0.05
$_{57}La^{127}$	5/2	−0.15	−0.10	−0.28	−0.38	−0.66	
	7/2*	0.08	0.05	0.19	0.21	0.38	
$_{57}La^{139}$	5/2	−0.16	−0.10	−0.21	−0.04	−0.25	
	7/2*	0.08	0.05	0.12	0.02	0.14	0.23
$_{59}Pr^{141}$	5/2*	−0.08	−0.05	−0.09	−0.14	−0.10	−0.07
	7/2	0.18	0.13	0.25	0.03	0.28	
$_{59}Pr^{143}$	5/2*	−0.08	−0.05	−0.13	−0.48	−0.58	
	7/2	0.18	0.13	0.41	0.92	1.22	
$_{61}Pm^{145}$	5/2	0.03	0.03	0.08	0.16	0.23	
	7/2	0.26	0.18	0.54	0.96	1.33	
$_{61}Pm^{147}$	5/2	0.31	0.17	0.37	0.21	0.51	
	7/2*	0.27	0.19	0.70	1.27	1.62	±0.95
$_{61}Pm^{149}$	5/2	0.03	0.03	0.11	0.04	0.09	
	7/2*	0.27	0.19	0.80	1.55	1.82	
$_{77}Ir^{191}$	3/2*	0.01	0.005	−0.05	0.20	0.16	1.0
$_{77}Ir^{193}$	3/2*	0.01	0.005	−0.05	0.19	0.15	1.0
$_{79}Au^{195}$	3/2*	0.12	0.09	0.53	0.68	1.08	
$_{79}Au^{197}$	3/2*	0.13	0.09	0.57	0.62	1.07	0.56
$_{79}Au^{199}$	3/2*	0.13	0.09	0.55	0.55	1.00	
$_{81}Tl^{199}$	3/2	0.26	0.15	0.54	0.12	0.62	
$_{81}Tl^{201}$	3/2	0.26	0.15	0.57	0.11	0.65	
$_{81}Tl^{203}$	3/2	0.26	0.15	0.53	0.07	0.58	
$_{81}Tl^{205}$	3/2	0.26	0.17	0.44	0.03	0.47	

neutron nuclei, respectively. The third column in the tables gives the uncorrected quasi-particle quadrupole moments, Eq. (79), the fourth and fifth columns give the corrected moments for two choices of the effective charges, and Q_{theor} is the total result using effective charge of 1 for the neutron and 2 for the proton. In these tables one can see that although the phonon contribution often dominates, in many cases the single-particle parts are as large or larger than Q_{ph}, and that the higher seniority terms are very important for the quasi-particle quadrupole moments, Q_{qp}. In many of the cases in which the calculated result is too large, the use of the experimental value for the $B(E2)$'s improves the comparison with experiment.

B. Electric Quadrupole Moment of One-Phonon State

In exactly the same manner as the magnetic dipole moment of the one-phonon state was found (Chap. V), one can calculate the electric quadrupole moment

TABLE V. Quadrupole moments of odd-neutron nuclei. (See the caption for Table IV.)

Isotope	State	$e^p = 2, e^n = 1$ Q_{qp}	$e^p = 1, e^n = 0$ Q^e_{qp}	$e^p = 2, e^n = 1$ Q^e_{qp}	Q_{ph}	Q_{theor}	Q_{exp}
$_{30}Zn^{65}$	3/2	0.02	0.04	0.09	0.30	0.35	
Zn^{65}	5/2*	0.035	0.05	0.14	0.50	0.59	
$_{30}Zn^{67}$	3/2	0.047	0.04	0.17	0.38	0.47	
	5/2*	0.072	0.05	0.22	0.55	0.66	0.18
$_{32}Ge^{73}$	9/2*	−0.076	−0.05	−0.21	−0.91	−0.99	−0.2
$_{34}Se^{75}$	5/2*	0.10	0.11	0.42	0.24	0.30	1.1
$_{34}Se^{79}$	7/2*						0.8
$_{36}Kr^{83}$	9/2*	0.063	0.10	0.31	0.67	0.89	0.22
$_{36}Kr^{85}$	9/2*	0.12	0.13	0.41	0.71	0.89	0.30
$_{38}Sr^{87}$	9/2*	0.12	0.05	0.25	0.31	0.53	
$_{38}Sr^{89}$	5/2*	−0.094	−0.06	−0.26	−0.054	−0.31	
$_{40}Zr^{91}$	5/2*	−0.094	−0.05	−0.25	−0.079	−0.34	
$_{40}Zr^{93}$	5/2*	−0.027	−0.01	−0.05	−0.12	−0.22	
$_{42}Mo^{95}$	5/2*	−0.029	−0.02	−0.07	−0.17	−0.28	
$_{42}Mo^{97}$	5/2*	+0.038	0.05	0.16	+0.29	+0.36	
$_{44}Au^{99}$	5/2*	0.032	0.05	0.16	0.31	0.37	
$_{44}Ru^{101}$	5/2*	0.073	0.06	0.26	0.80	0.82	
$_{46}Pd^{105}$	5/2*	0.085	0.06	0.30	0.76	0.91	
$_{48}Cd^{107}$	5/2*	0.078	0.04	0.24	0.63	0.79	0.78
$_{48}Cd^{109}$	5/2*	0.095	0.04	0.29	0.58	0.75	0.80
$_{48}Cd^{111}$	5/2*	0.11	0.05	0.31	0.48	0.62	
$_{52}Te^{123}$	3/2	−0.03	−0.02	−0.12	−0.33	−0.42	
	11/2	−0.03	+0.01	0.03	−0.60	−0.63	
$_{52}Te^{129}$	3/2	0.03	0.01	0.07	0.19	0.25	
	11/2	0.08	0.14	0.36	0.61	0.84	
$_{54}Xe^{129}$	3/2	0.007	−0.005	−0.003	0.19	0.19	
	11/2	0.06	0.10	0.35	1.1	1.3	
$_{54}Xe^{131}$	3/2*	0.03	0.08	0.32	0.37	−0.12	
	11/2	0.10	0.13	0.46	0.99	1.29	
$_{54}Xe^{133}$	3/2*	0.06	0.04	0.18	0.31	0.44	
	11/2	0.15	0.15	0.56	0.78	1.16	
$_{56}Ba^{135}$	3/2*	0.06	0.05	0.19	0.33	0.47	
	11/2	0.15	0.16	0.56	0.84	1.25	
$_{56}Ba^{137}$	3/2*	0.06	0.08	0.26	0.01	0.26	
	11/2	0.22	0.18	0.63	0.06	0.68	
$_{58}Ce^{139}$	3/2*	0.06	0.08	0.25	0.03	0.28	
	11/2	0.22	0.15	0.57	0.12	0.69	
$_{58}Ce^{141}$	7/2*	−0.23	−0.17	−0.49	−0.03	−0.54	
$_{60}Nd^{141}$	3/2*	0.06	0.10	0.29	0.02	0.31	
	11/2	0.22	0.16	0.59	0.07	0.66	
$_{60}Nd^{145}$	7/2*	−0.23	−0.13	−0.53	−0.03	−0.56	±1.0
	5/2	−0.19	−0.11	−0.45	0.0	0.005	
$_{60}Nd^{143}$	7/2*	−0.20	−0.12	−0.52	−0.94	−1.06	
	5/2	−0.19	−0.11	−0.49	−0.15	−0.20	
$_{60}Nd^{147}$	7/2	−0.17	−0.11	−0.49	−1.08	−1.23	
	5/2*	−0.19	−0.11	−0.52	−0.31	−0.38	
$_{62}Sm^{147}$	7/2*	−0.20	−0.12	−0.52	−0.94	−1.19	<0.7
$_{62}Sm^{149}$	7/2*	−0.18	−0.11	−0.50	−1.10	−1.29	<0.7
$_{76}Os^{189}$	3/2*	−0.03	−0.02	−0.10	−0.34	−0.36	+0.6
$_{76}Os^{191}$	3/2	−0.001	−0.005	−0.004	0.05	0.05	
$_{78}Pt^{193}$	3/2	−0.002	−0.01	−0.012	0.01	0.01	
	5/2	−0.09	−0.06	−0.29	−0.94	−1.09	
$_{78}Pt^{195}$	3/2	0.035	0.02	0.14	0.54	0.64	
	5/2	−0.055	−0.03	−0.14	−0.72	−0.82	
$_{78}Pt^{197}$	3/2	+0.073	0.04	0.29	0.64	0.85	
	5/2	−0.001	0.02	0.05	0.02	0.05	
$_{80}Hg^{197}$	3/2	0.03	0.00	0.13	0.26	0.37	
	13/2	0.24	0.04	0.59	1.18	1.55	1.53
$_{80}Hg^{199}$	3/2	0.07	0.01	0.28	0.46	0.68	
	13/2	0.26	0.03	0.61	1.19	1.53	
$_{80}Hg^{201}$	3/2*	0.11	0.01	0.37	0.44	0.71	0.50
	13/2	0.28	0.03	0.59	1.08	1.43	

of a phonon. The result is

$$Q^{ph} = \langle \psi_0 B Q_0 B^\dagger \psi_0 \rangle = 8 \cdot 5^{-\frac{1}{2}} C^{222}_{202} N^2_\omega \sum_{jj'j''} \langle j' || q || j \rangle \times (U_j U_{j'} - V_j V_{j'}) W(2j'2j''; j2)(U_j V_{j''} + U_{j''} V_j) \times (U_{j'} V_{j''} + U_{j''} V_{j'}) \langle j || q || j'' \rangle \langle j' || q || j'' \rangle \times \frac{E_j + E_{j'} + 2E_{j''}}{[(E_j + E_{j''})^2 - \omega^2][(E_{j'} + E_{j''})^2 - \omega^2]}. \quad (84)$$

There is not the regularity to be expected for these moments that is expected with the magnetic dipole moments. That this is true is apparent from the

factors $(U_jU_{j'} - V_jV_{j'})$, which produce cancellation and wide variation in the results. Since there are no experimental data, we do not carry out the numerical calculations.

VII. ELECTROMAGNETIC TRANSITIONS

Since the electromagnetic field is so well understood and electromagnetic radiation from nuclei has been carefully worked out, the data on the gamma transitions provide important information about many aspects of nuclear structure. In addition to the purely spectroscopic information obtained from the general character of the multipole radiations, many of the details of the nuclear wave functions can be learned from the transition rates. Moreover, because this type of experimental information is so extensive, it is often possible to pick out particular transitions in a number of nuclei which stress particular parts of nuclear wave functions, thereby providing systematic studies of various aspects of nuclear structure.

A. Odd-Mass Isotopes

The pairing correlations play an important role in the electromagnetic transitions. Because a quasi-particle is composed of particles plus "holes" in the shell-model states, the transition between two quasi-particles states involves both particle and hole transitions, or, in other words, the transition involves particle states and time-reversed particle states. This is the origin of the result given in I that the matrix element of single-particle operator $O = \sum_{12}\langle 1|O|2\rangle b_1^\dagger b_2$ in one quasi-particle state is related to the single-particle matrix elements by

$$\langle\psi_0^0\alpha_{j_fm_f}|\sum_{12}\langle 1|\mathcal{O}|2\rangle b_1^\dagger b_2|\alpha_{j_im_i}^\dagger\psi_0^0\rangle = (U_{j_f}U_{j_i} - (-1)^T V_{j_f}V_{j_i})\langle j_fm_f|\mathcal{O}|j_im_i\rangle\,, \quad (85)$$

where T is the time-reversal property of the operator, i.e., $T = 0$ or 1, if the operator does not change sign or does change sign, respectively, under time reversal. For electromagnetic transitions the result is that the matrix elements of the electric and magnetic 2^L-pole transition operators in quasi-particle states are related to the single-particle matrix elements by

$$\langle\psi_0^0\alpha_{j_fm_f}|\mathfrak{M}(\mathrm{EL})|\alpha_{j_im_i}^\dagger\psi_0^0\rangle = (U_fU_i - V_fV_i) \times\langle j_fm_f|\mathfrak{M}(\mathrm{EL})|j_im_i\rangle\,, \quad (86a)$$

$$\langle\psi_0^0\alpha_{j_fm_f}|\mathfrak{M}(\mathrm{ML})|\alpha_{j_im_i}^\dagger\psi_0^0\rangle = (U_fU_i + V_fV_i) \times\langle j_fm_f|\mathfrak{M}(\mathrm{ML})|j_im_i\rangle\,, \quad (86b)$$

since the magnetic operators change sign while the electric ones do not. This effect was studied for single closed-shell nuclei in some detail, and gives an accurate estimate of some of the transition rates, since for those isotopes, the effect of the long-range force on the one-quasi-particle states is not important.

In order to carry out a quantitative study of the systematics of the isomeric transitions for all of the spherical nuclei, it is necessary to include the effect of the phonon admixtures. For the transitions of high multipolarity, such as the E3 and M4 transitions, it is a good approximation to neglect the terms in the single-particle operators which change the number of phonons. In that case the most important effect of the long-range force is to deplete the amount of one-quasi-particle state in the wavefunction. In this approximation, the relationship between the single-particle lifetime, $\tau_{i\to f}^{\mathrm{sp}}$ and the lifetime in states [Eq. (54)] is

$$1/\tau_{i\to f} = D(1/\tau_{i\to f}^{\mathrm{sp}})\,, \quad (87)$$

with this retardation factor D being approximately

$$D = (U_iU_f \mp V_iV_f)^2(C_{j_f00}^{j_f}C_{if00}^{if})^2\,. \quad (88)$$

In Eq. (88) the upper sign holds for electric and the lower one for magnetic transitions. The coefficients C_{j00}^j are the no-phonon components of the wave functions of an odd-mass system of spin j, obtained from Eq. (47).

The most useful data for systematic studies of electromagnetic transitions in the one-quasi-particle states are those of the isomeric transitions, especially the M4 and E3 transitions. Let us first consider the M4's. The single-particle transition rates have been calculated by Moszkowski and others. For M4 transitions the theoretical single-particle transition probability is approximately[29]

$$P_{\mathrm{theor}}^{\mathrm{sp}} \cong C(\mathrm{M4})A^2(\Delta E)^9S(j_i,4,j_f)\,, \quad (89)$$

with $C(\mathrm{M4})$ a constant proportional to the radius parameter, r_0, to the sixth power, and equal to 1.56×10^{-5} or 2.86×10^{-5} for neutrons or protons, respectively, for a choice of $r_0 = 1.1\times10^{-13}$ cm. $S(j_f,4,j_i)$ is the "statistical factor" and A is the mass number. The experimental values for the transition probability P_{exp} is found in terms of the experimental half-life, $T_{\frac{1}{2}}$, conversion coefficient α, and the fraction of M4 involved in the transition F,

$$P_{\mathrm{exp}} = F/1.44T_{\frac{1}{2}}(1+\alpha)\,. \quad (90)$$

The experimental results are given in terms of the reduction factor

$$D_{\mathrm{exp}} = P_{\mathrm{exp}}/P_{\mathrm{theor}}^{\mathrm{sp}}\,. \quad (91)$$

[29] S. Moszkowski, in *Gamma and Beta Spectroscopy* edited by E. Siegbahn (Interscience Publishers, Inc., New York, 1955).

Results are given for the M4 transitions in our regions in which the half-lives have been measured. In most cases F is known from experiment, but in a few cases it is estimated from theoretical considerations. In a number of cases the internal conversion coefficients have not been measured and the calculations of Rose[30] have been used. If only the K and L conversion coefficients are known, the total conversion coefficient is taken to be $\alpha = \alpha_K(1 + 1.3\,\alpha_L/\alpha_K)$.

transitions in the Pt, Hg, and Pb isotopes. In the Pb isotopes the most important effects are due to the pairing correlations. As one removes particles from Pb^{207} the vibration does become a little softer, tending to reduce the calculated transition rates a bit faster than when the phonon effect is neglected, but the experimental information shows the constancy expected from the pairing effects. In any case, the fact that the Pb^{207} D_{exp} is less than that of Pb^{203} is hard to understand.

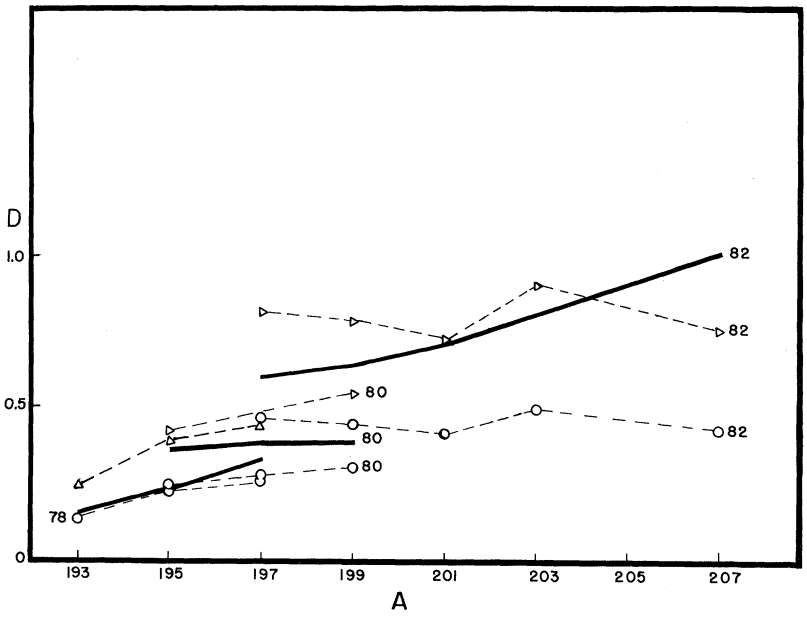

FIG. 37. Reduction factors for M4 13/2 + -5/2 − odd-neutron transitions. The theoretical results are given by the solid line, while the experimental ratio of the transition probability to the single-particle value is given as triangles or circles connected by dashed lines with the assumption of a radius parameter of 1.0 and 1.1 F, respectively. The sequences are labeled by the proton numbers.

The most striking feature of the systematics of M4 transition rates is their constancy, which was first pointed out by Goldhaber and Sunyar,[31] for none of the measured rates differs from the single-particle estimate by more than a factor of about ten. Equation (88) shows that the pairing part of the reduction factor is $(U_iU_f + V_iV_f)^2$, which tends to be constant. Since the magnitude of the one-quasi-particle component in the states being considered is usually at least fifty percent, the theoretical reduction factor D also tends to be constant. Let us now look in detail at the several regions to see if not only the constancy produced by the pairing correlations shows up, but also the effects of phonon admixtures.

Figure 37 contains the information about the isomeric transition between the $i_{13/2}$ and $f_{5/2}$ odd-neutron

Following the Hg isotopes from mass 195 to 199, both the 13/2 and 5/2 states are filling, and the pairing part of the reduction factor increases. This is partially offset by the phonon factor, which decreases, resulting in a slowly increasing D, which is in agreement with experiment. In the case of the Pt isotopes, the pairing factor is increasing at nearly the same rate in isotopes 193, 195, and 197 as the Hg isotopes, for the same neutron numbers are involved, but in this case the phonon factor is quite strongly increasing. As a result, the theoretical reduction increases in the Pt isotopes much more strongly than in the Hg, a fact which seems to be supported by the experimental evidence.

There is a great deal of experimental information concerning the neutron $h_{11/2}$ and $d_{3/2}$ levels from the M4 transitions in the Sn, Te, Xe, and Ba isotopes as shown in Fig. 38. In going from smaller to larger mass numbers in these isotopes, one is proceeding from 67 to 81 neutrons in the 50–82 neutron major

[30] M. E. Rose, *Internal Conversion Coefficients* (North-Holland Publishing Company, Amsterdam, 1958).
[31] M. Goldhaber and A. W. Sunyar, Phys. Rev. **83**, 906 (1951).

shell. Since the first fourteen particles in this shell mainly occupy the $g_{7/2}$ and $d_{5/2}$ levels, one is essentially going from unfilled $h_{11/2}$ and $d_{3/2}$ levels to filled ones. However, due to the fact that these two levels are rather closely spaced, the factor $(U_{11/2}U_{3/2} + V_{11/2}V_{3/2})$ stays quite close to unity. Therefore almost any variation in the theoretical results must come from the changes in the phonon admixtures. In the sequence of six isotopes $Te^{123-133}$, experimental results show a general increase of the D_{exp} factor. In the theoretical calculation there are two competing effects, since the $C^{3/2}_{3/2\,00}$ coefficient increases from about 0.8 at Te^{121} to unity at Te^{133}, while the $C^{11/2}_{11/2\,00}$ has a maximum at mass numbers 125 and 133. Although the detailed variation predicted by the theory does not seem to show up, the general tendency for the transition revealed by the Y, Nb, Tc, and In isotopes. Since the protons are involved, the pairing factor remains almost constant and just helps to determine the general magnitude for each element, so the variations in each element are mainly due to the phonon. One striking result is the strong maximum in the three Y isotopes at the 50-neutron closed shell. This can be explained by the fact that the phonon admixtures increase as one leaves the single closed-shell case, as the theoretical curve shows. For the four Nb isotopes, one is adding neutrons to the 50 closed shell, starting with the single closed-shell Nb^{91} case. Therefore, the theoretical results display a decreasing magnitude for this D factor, which is in agreement except for the very uncertain Nb^{93} point. In the three Tc isotopes with mass numbers 93–97, this

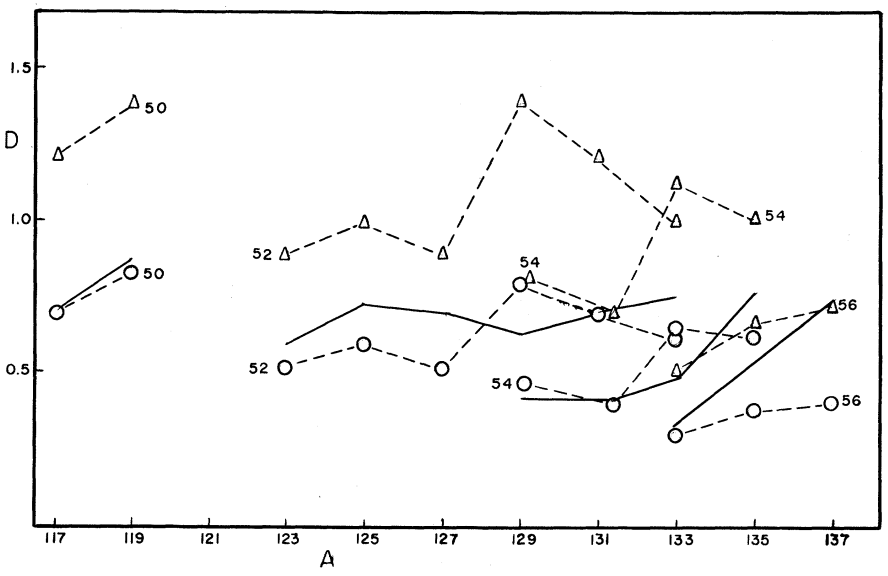

FIG. 38. Reduction factors for M4 $h_{11/2}$-$d_{3/2}$ odd-neutron transitions. The notation is the same as in Fig. 37.

nuclei to become stiffer to vibration and thus contain less phonon admixture as one approaches the 82-neutron number leads to a general increase of the theoretical D factor which is consistent with the experiments.

The theoretical results for the sequence of isotopes Xe 129–135 show a similar dip at the 131 mass number, due to the minimum in the $C^{11/2}_{11/2\,00}$ coefficient, with a general increase thereafter to the case of 81 neutrons. The experimental results are in good agreement, even having a minimum at Te^{131}. Finally, the three isotopes Ba^{133-7} have an experimental reduction factor which increases sharply, which is in agreement with the strong phonon changes which occur with 56 protons.

Figure 39 presents the study of the $p_{1/2}$–$g_{9/2}$ proton effect is seen quite clearly in both the theoretical and experimental reduction factors. Finally, for the In isotopes, the pairing factor is constant and the phonon admixture is also almost completely unchanged as the neutrons increase from 64–68, so the D_{theor} remain constant in $In^{113-117}$, in agreement with D_{exp}.

Another interesting thing in this region is a pairing force effect for the three single closed-shell $N = 50$ isotopes Y^{89}, Nb^{91}, and Tc^{93}. The minimum in the reduction factor seems to come from the change in the gap at 41 particles, as was discussed in I. Finally, there is a little information concerning the neutron $p_{1/2}$–$g_{9/2}$ M4 transition. Figure 40 shows that one can just conclude that the experimental and theoretical results are consistent.

Figures 37–40 show that, for a choice of the radius parameter somewhere between 1.0 and 1.1 F, the magnitude of the experimental vs theoretical reduction factors is in agreement. We can conclude that this extensive information on M4 transitions seems to give good evidence for the accuracy of the wave functions which result from this method.

The experimental data on E3 transitions is not so extensive as the M4 data, and it turns out not nearly as useful for this work. The main reason is that the best systematics concern the transition between the 7/2+ state and the 1/2− state for isotopes in which the odd particle is in the 28–50 shell. These are just the cases with which this method seems to be least

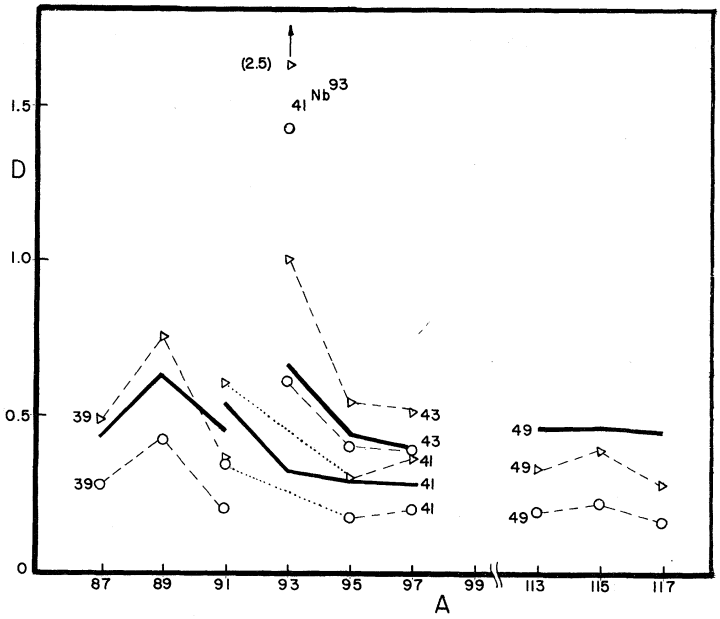

FIG. 39. Reduction factors for M4 $p_{1/2}$-$g_{9/2}$ odd-proton transitions. The notation is the same as in Fig. 37.

able to deal, at least without including the three quasi-particle states (see Chap. III). Therefore we do not attempt to calculate these transition rates.

The only systematic data which we can treat involve the neutron $h_{11/2}$–$d_{5/2}$ E3 transitions in $Pd^{109-111}$, Cd^{111}, and Xe^{127}. This is an interesting sequence, for the neutron Fermi level is crossing between the two levels at about $N = 63$. Therefore, one can expect a sharp reduction in the D factor at this point, since the factor $(UU - VV)$ goes approximately to zero there. The very small transition rates[31] compared to the single-particle values for Cd^{111} and Pd^{111} seem to be correlated with this theoretical prediction. None of the E3 transitions between the 7/2+ and 1/2− states mentioned in the preceding paragraph have these very strong reductions, indirectly supporting the conjecture that those states contain other admixtures than the pairing picture would predict.

There are numerous other lifetimes measured in the spherical odd-mass isotopes. Although there is not so much in the way of systematics, there are some interesting cases. Of special interest are some of the E2 transition rates. Here one has the tendency for the reduction of the contributions from the single quasi-particle states, but enhancements arising from the phonon admixtures. Thus, e.g., recent experiments on Sb^{123} which show an enhanced E2 transition give evidence that $g_{7/2}$ and $d_{5/2}$ states contain considerable admixtures of phonon states.[32]

B. Even–Even Isotopes

1. *One-Phonon-to-Ground-State Transition*

The most extensive data on electromagnetic interactions in the even–even nuclei are on the $B(E2)$ values for the transition from the lowest 2+ state to the ground state. In Chap. II this was defined as

$$B(E2)_{2+\to 0+} = |\langle\psi_0|\hat{Q}|B^\dagger\psi_0\rangle|^2 . \tag{92}$$

Since in all of our calculations we take the three long-range-force parameters as equal, $\chi_p = \chi_n = \chi_{np}$, the $B(E2)$ can be written in the simplified form,

$$B(E2) = \frac{4}{5}N_\omega^2\left[\sum_\xi \frac{e_{\text{eff}}^\xi (U_jV_{j'} + V_jU_{j'})^2(2j'+1)(C_{0\frac{1}{2}\frac{1}{2}}^{2j'j})^2\langle j'||\hat{r}||j\rangle\cdot 2(E_j+E_{j'})}{(E_j+E_{j'})^2-\omega^2}\right]^2, \tag{93}$$

[32] G. Scharff-Goldhaber (private communication).

where

$$N_\omega^2 = \frac{4\pi}{8\omega}\Big[\sum_{12}\frac{E_1+E_2}{[(E_1+E_2)^2-\omega^2]^2}(U_1V_2+U_2V_1) \times (2j_1+1)(C^{2j_1j_2}_{0\frac{1}{2}\frac{1}{2}})^2\langle 1|r^2|2\rangle\Big]^{-1} \quad .(94)$$

The theoretical values of the B(E2)'s seem to be in reasonably good agreement with the experimental

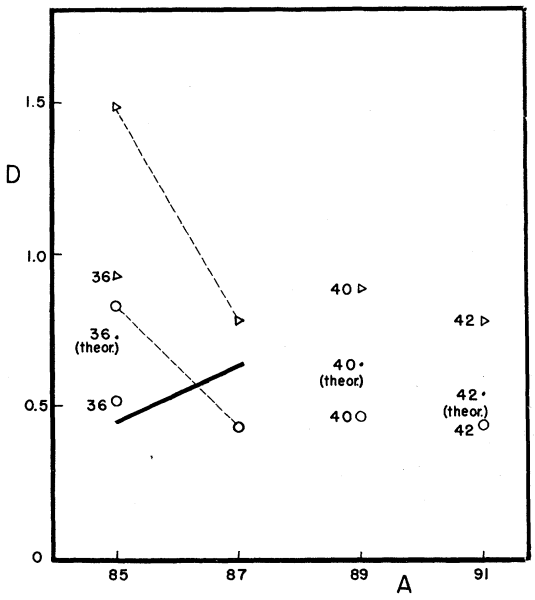

FIG. 40. Reduction factors for $p_{1/2}$-$g_{9/2}$ odd-neutron transitions. The notation is the same as in Fig. 37.

data.[33] There is a general tendency for the calculated B(E2)'s given in Table VI to become increasingly larger than the experimental ones as the vibration gets softer and one approaches the deformed regions.

2. *The Crossover 2+-Two-Phonon-to-Ground-State Transition*

There have been many measurements in recent years of the B(E2)'s for the transition from the second phonon 2+ state (referred to hereafter as the 2′ state) to the 0+ ground state. In the linearized QRPA theory we have applied here this transition is forbidden, which is in agreement with the small B(E2)(2′ → 0) value compared to the B(E2)(2 → 0). However, one of the promising features of this method is the relative ease with which some corrections can be made. For these transitions it is rather straightforward to carry out the necessary corrections to the QRPA approximation.

[33] The B(E2) and B(E2) crossovers are taken from an unpublished compilation by Y. Yoshizawa.

TABLE VI. B(E2) Values for ground-state transitions in even-even nuclei. The column labeled $B(E2)_{\text{theor}}$ lists the calculated $B(E2)_{0+\to 2+}$ values using the same parameters used to calculate the energies in Figs. 2(a), (b). In the few cases for which the calculated energy (of Fig. 2) is far below the experimental value, the B(E2) is listed in parenthesis for a lower $\bar{X}$ chosen to fit the energy. The experimental values are listed in units of $e^2 \times 10^{-48}$ cm^4, and compared with the single-particle value of $3 \times 10^{-5}\, e^2 \times 10^{-48}\, A^{4/3}$ cm^4.

Isotope	$B(E2)_{\text{theor}}$	$B(E2)_{\text{exp}}$	× sp	Source
$_{28}$Ni^{58}	0.017	0.072	11	a
Ni^{60}	0.051	0.091	13	a
Ni^{62}	0.100	0.083	12	a
Ni^{64}	0.092	0.087	12	
$_{30}$Zn^{64}	0.264	0.170	21	a
Zn^{66}	0.245	0.145	18	a
Zn^{68}	0.164	0.125	16	a
$_{32}$Ge^{70}	0.458	0.172	18	a
Ge^{72}	0.476	0.230	24	a
Ge^{74}	0.609	0.317	33	a
Ge^{76}	0.729	0.263	28	a
Ge^{78}	0.451			
$_{34}$Se^{74}	0.696	0.21	21	
Se^{76}	(0.919)	0.480	48	a
Se^{78}	(0.770)	0.385	38	a
Se^{80}	(0.594)	0.283	28	a
Se^{82}	0.327	0.213	21	a
$_{36}$Kr^{78}	1.784	0.51	51	
Kr^{80}	(0.812)	0.34	34	
Kr^{82}	(0.550)	0.18	18	
Kr^{84}	0.313	0.15	15	
$_{38}$Sr^{86}	0.205			
Sr^{88}	0.143	0.13	12	b
$_{40}$Zr^{90}	0.141			
Zr^{92}	0.080	0.79	65	
Zr^{94}	0.216			
$_{42}$Mo^{94}	0.166	0.27	21	
Mo^{96}	0.360	0.30	23	
Mo^{98}	0.683	0.27	21	
Mo^{100}	0.915	0.61	47	
$_{44}$Ru^{96}	0.279	0.25	19	
Ru^{98}	0.563	0.48	37	
Ru^{100}	0.947	0.57	41	
Ru^{102}	(1.424)	0.73	52	
$_{46}$Pd^{104}	(1.006)	0.55	37	
Pd^{106}	(1.261)	0.65	44	
Pd^{108}	(1.603)	0.74	50	
Pd^{110}	(2.009)	0.86	58	
$_{48}$Cd^{106}	0.447	0.47	31	
Cd^{108}	0.571	0.54	35	
Cd^{110}	0.687	0.50	33	
Cd^{112}	0.758	0.54	35	
Cd^{114}	0.799	0.58	38	
Cd^{116}	0.809	0.60	40	
$_{50}$Sn^{112}	0.350	0.18	11	
Sn^{114}	0.381	0.20	12	
Sn^{116}	0.399	0.21	12	
Sn^{118}	0.414	0.23	14	
Sn^{120}	0.416	0.22	13	
Sn^{122}	0.365	0.25	15	
Sn^{124}	0.273	0.21	12	
$_{52}$Te^{120}	1.183	0.55	29	
Te^{122}	1.307	0.65	35	
Te^{124}	1.080	0.39	21	
Te^{126}	0.729	0.53	28	
Te^{128}	0.468	0.41	22	
Te^{130}	0.289	0.34	18	
$_{54}$Xe^{128}	(1.654)			
Xe^{130}	1.174	0.48	24	
Xe^{132}	0.592	0.32	16	
Xe^{134}	0.344			
Xe^{136}	0.198			
$_{56}$Ba^{132}	(1.814)	0.73	36	
Ba^{134}	0.929			
Ba^{136}	0.509			
Ba^{138}	0.294	0.30	14	

TABLE VI. *Continued*

Isotope	$B(E2)_{theor}$	$B(E2)_{exp}$	× sp	Source
$_{58}Ce^{138}$	0.631			
Ce^{140}	0.392	0.36	17	b
Ce^{142}	0.828	0.59	27	
$_{60}Nd^{142}$	0.361	0.34	15	c
Nd^{144}	0.908	0.44	19	c
Nd^{146}	2.101	0.84	37	
$_{62}Sm^{146}$	0.900			
Sm^{148}	2.189	0.89	37	
Sm^{150}	(4.0)	1.32	56	
$_{64}Gd^{148}$	0.974			
Gd^{150}	1.872			
$_{76}Os^{188}$	(11.8)	2.80	85	
Os^{190}	(9.3)	2.55	78	
$_{78}Pt^{194}$	(5.2)	1.94	59	d
Pt^{196}	4.086	1.27	37	d
Pt^{198}	3.060	1.35	39	
$_{80}Hg^{196}$	1.250			
Hg^{198}	1.355	1.13	32	
Hg^{200}	0.982	0.85	24	
Hg^{202}	0.749	0.59	17	
Hg^{204}	0.461			
$_{82}Pb^{200}$	0.337			
Pb^{202}	0.280			
Pb^{204}	0.216	0.17	5	e
Pb^{206}	0.101	0.13	4	e

[a] P. H. Stelson and F. K. McGowan, Nucl. Phys. **32**, 652 (1962).
[b] S. Ofer and A. Schwarzschild, Phys. Rev. Letters **3**, 384 (1959).
[c] O. Nathan and V. I. Popov, Nucl. Phys. **21**, 631 (1960).
[d] F. K. McGowan and P. H. Stelson Phys. Rev. **122**, 1274 (1961).
[e] O. Nathan Nucl. Phys. **30**, 332 (1962).
Other experimental data was obtained from a compilation kindly furnished by Dr. Yasukaza Yoshizawa.

The crossover $B(E2)$ is defined,

$$B(\underset{0\to 2'}{E2}) = |\langle\psi_0||\hat{Q}||F[B^\dagger B^\dagger]^2/\sqrt{2}\psi_0\rangle|^2 . \quad (95)$$

F is a normalization constant which takes into account the deviation of the $B^\dagger$ operators from bosons for the two-phonon states. This factor can be quite different from unity when the vibrational states are low in energy. Since the numbers of quasi-particles differ in the zero- and two-phonon states by zero, four, etc., the $A^\dagger$ parts of the quadrupole operator cannot lead to the transitions. Therefore, the η parts of the operator, which do not contribute to the $B(E2)$'s $(0 \to 2^+)$, are entirely responsible for the transitions, which we can thus expect to be of the order of single-particle magnitude. We need the matrix element $\langle\psi_0\{\eta^2_{j'j}[B^\dagger B^\dagger]^2\}^0\psi_0\rangle$ in which the operators have been vector-coupled to total angular momentum zero. Applying the commutation rule given in Appendix I, Eq. (A4), plus the condition $B\psi_0 \cong 0$, one readily finds that

$$\langle\psi_0\{\eta^2_{j'j}[B^\dagger B^\dagger]^2\}^0\psi_0\rangle = 10\cdot 5^{\frac{1}{2}} \sum_{j_1} r_\omega(jj_1)s_\omega(j'j_1) \times W(2j'2j_1;j2) . \quad (96)$$

Therefore, the reduced lifetime for the direct crossover transition is

$$B(\underset{0\to 2'}{E2}) = [\sum_\xi \sum_{jj'} 10Fe^\xi_{eff}(U_jU_{j'} - V_jV_{j'}) \times \langle j'||r^2Y^2||j\rangle 2^{-\frac{1}{2}} \sum_{j_1} r_\omega(jj_1)s_\omega(j'j_1) \times W(2j'2j_1;j2)]^2 . \quad (97)$$

The results shown in Table VII are calculated by choosing $F = 1$ and taking the effective charges of the proton and neutron to be $e^p_{eff} = 2e$ and $e^n_{eff} = e$ (column two), and for comparison $e^p_{eff} = e$ and $e^n_{eff} = 0$ (column three). From Eq. (97) it is evident that the theoretical results are sensitive to the parameters both because of the cancellations due to the factors $(U_jU_{j'} - V_jV_{j'})$ and because of the interference between neutrons and protons, which is illustrated by the comparison of columns two and three. The theoretical values are frequently an order-of-magnitude smaller than the experimental results.[33] One important reason for this is the error in the choice of unity for the normalization factor F, which can change the results by a factor of two according to rough estimates. However, since these transitions are of single-particle magnitude, an accurate estimate of these $B(E2)$'s requires the use of more detailed properties of the wave functions, and an investigation of other effects which might be important in some cases.

TABLE VII. $B(E2)_{0+\to 2'}$ crossover rate. The same single-particle estimate is used as in Table VI. Effective charges $e^p = 2$, $e^n = 1$, and $e^p = 1$, $e^n = 0$ used to compute $B(E2)_{theor}$ in units of $e^2 \times 10^{-48}$ cm^4.

Isotope	$B(E2)_{theor}$ $e^p=1, e^n=0$	$B(E2)_{theor}$ $e^p=2, e^n=1$	$B(E2)_{exp}$[a]	$\frac{B(E2)_{exp}}{B(E2)_{sp}}$
$_{32}Ge^{70}$	0.0026	0.0016	0.007	0.8
Ge^{72}	0.0048	0.0035	0.0017	0.2
Ge^{74}	0.0058	0.0064	0.022	3.
Ge^{76}	0.0042	0.0115	0.004	0.4
$_{34}Se^{74}$	0.0000	0.0023	0.005	0.5
Se^{76}	0.0031	0.0015	0.010	1.
Se^{78}	0.0018	0.0046	0.010	1.
Se^{80}	0.0016	0.0030	0.019	2.
Se^{82}	0.0011	0.0101	0.008	0.8
$_{36}Kr^{78}$	0.0000	0.0102		
Kr^{80}	0.0000	0.0002		
Kr^{82}	0.0000	0.0008		
Kr^{84}	0.0001	0.0026		
Kr^{86}	0.0005	0.0019		
$_{38}Sr^{86}$	0.0008	0.0007		
Sr^{88}	0.0009	0.0037		
$_{40}Zr^{90}$	0.0006	0.0024		
Zr^{92}	0.0005	0.0006		
Zr^{94}	0.0008	0.0008		
Zr^{96}	0.0022	0.0070		
$_{42}Mo^{94}$	0.0005	0.0006	0.005	0.5
Mo^{96}	0.0009	0.0008	0.011	0.9
Mo^{98}	0.0015	0.0040	0.014	1.
Mo^{100}	0.0048	0.0191	0.013	1.
$_{44}Ru^{98}$	0.0001	0.0001	0.005	0.4
Ru^{100}	0.0003	0.0002	0.015	1.
Ru^{102}	0.0005	0.0014	0.017	1.

TABLE VII. *Continued*

Isotope	$B(E2)_{theor}$ $e^p = 1, e^n = 0$	$B(E2)_{theor}$ $e^p = 2, e^n = 1$	$B(E2)_{exp}$[a]	$\frac{B(E2)_{exp}}{B(E2)_{sp}}$[a]
Ru^{104}	0.0010	0.0040	0.010	0.8
$_{46}Pd^{106}$	0.0007	0.0034	0.014	1.
Pd^{108}	0.0010	0.0041	0.007	0.5
Pd^{110}	0.0012	0.0039	0.010	0.6
$_{48}Cd^{110}$	0.0019	0.0071	0.020	1.
Cd^{112}	0.0022	0.0077	0.010	0.6
Cd^{114}	0.0025	0.0067	0.007	0.4
Cd^{116}	0.0026	0.0051	0.011	0.7
$_{50}Sn^{114}$	0.0000	0.0001		
Sn^{116}	0.0000	0.0012		
Sn^{118}	0.0000	0.0022		
Sn^{120}	0.0000	0.0019		
Sn^{122}	0.0000	0.0011		
Sn^{124}	0.0000	0.0004		
$_{52}Te^{122}$	0.0000	0.0045	0.019	1.
Te^{124}	0.0000	0.0026	0.016	1.
Te^{126}	0.0000	0.0010	0.005	0.3
Te^{128}	0.0000	0.0002	0.012	0.7
Te^{130}	0.0000	0.0001	0.011	0.6
$_{54}Xe^{128}$	0.0006	0.0002		
Xe^{130}	0.0004	0.0008		
Xe^{132}	0.0002	0.0011		
Xe^{134}	0.0001	0.0007		
$_{56}Ba^{130}$	0.0043	0.127		
Ba^{132}	0.0025	0.0072		
Ba^{134}	0.0016	0.0068		
Ba^{136}	0.0035	0.0017		
$_{58}Ce^{138}$	0.0015	0.0073		
Ce^{140}	0.0000	0.0001		
Ce^{142}	0.0049	0.0244		
$_{60}Nd^{144}$	0.0039	0.0192		
Nd^{146}	0.0080	0.0470		
Nd^{148}	0.0164	0.106		
Nd^{150}	0.0767	0.512		
$_{62}Sm^{146}$	0.0019	0.0104		
Sm^{148}	0.0029	0.0203		
Sm^{150}	0.0073	0.0577		
Sm^{152}	0.054	0.437		
$_{76}Os^{186}$	0.0136	0.0856		
Os^{188}	0.0107	0.0702	0.20	6.
Os^{190}	0.0074	0.0480	0.18	5.
Os^{192}	0.0053	0.0325	0.21	6.
$_{78}Pt^{192}$	0.0004	0.0003		
Pt^{194}	0.0003	0.0003	0.009	0.3
Pt^{196}	0.0002	0.0004		
Pt^{198}	0.0001	0.0007		
$_{80}Hg^{196}$	0.0044	0.0155		
Hg^{198}	0.0043	0.0160		
Hg^{200}	0.0046	0.0206		
Hg^{202}	0.0022	0.0140		
Hg^{204}	0.0019	0.0186		

[a] The experimental results were obtained from a compilation kindly furnished by Dr. Y. Yoshizawa.

For the region $28 \leqslant Z \leqslant 40$; $28 \leqslant N \leqslant 50$, the theoretical $B(E2)(0 \rightarrow 2')$ values were also calculated including the $f_{7/2}$ protons and neutrons from the shell below. These results are not included in the table, but there was a large difference in the results indicating the sensitivity of the calculations to the parameters, especially in this region. Since these transitions are essentially of single-particle type, the results can be expected to depend much more upon the details of the nuclear structure than those for the one-phonon $B(E2)(0 \rightarrow 2+)$. In particular, with more systematic empirical data we expect that there will be more scatter in the experimental values for these transition rates than for the transition rates found for the one-phonon to the ground-state transitions. Of course, this simple treatment of the two-phonon states cannot be expected to be very accurate. Moreover the general tendency for the $B(E2)$'s to be so small in this calculation indicates that the corrections are quite large, and that in fact the treatment of the second phonon state as $B^\dagger B^\dagger \psi_0$ is not very accurate.

3. *The* M1 *Admixture in the Two-Phonon* $2+$ *to One-Phonon Transition*

From the magnetic-moment operator, Eq. (59), one can see that in the matrix element needed to calculate the M1 transition between the two-phonon $2+$ $(2')$ state and the one-phonon state,

$$\langle \psi_0 | B\mu_{op}[B^\dagger B^\dagger]^2 | \psi_0 \rangle , \tag{98}$$

only the η terms contribute. However, the calculation of this matrix element is rather intricate. In this case the commutation rules Eq. (A3) and (A4) along with the condition $B\psi_0 = 0$ are *not* sufficient to evaluate the matrix element, and one is required to make statements about the magnitude of rather complicated terms. Because of the accurate data it is important to carry out this calculation, this is not done here. Also we do not calculate the change in the value of the cascade $B(E2)$'s of the $2' \rightarrow 2 \rightarrow 0$ transitions from the QRPA value.

4. *Transitions in Two-Quasi-Particle States*

As soon as one leaves the single-closed-shell isotopes, there is actually very little information about transitions in the quasi-particle states beyond those studied in I. With new experimental apparatus and techniques, one can look forward to the possibility of systematic studies in the future. One interesting case has been recent measurements of a highly forbidden E2 transition in Sn^{118} and Sn^{120} in states which should be rather pure-quasi-particle states, showing the particle-hole cancellations predicted by the pairing corrections.[34]

VIII. BETA DECAY

Nuclear beta-decay rates have been used in the past to help determine nuclear spins and parities, and moreover, when the spins are known and the type of decay determined, the rates may be related to the nuclear state involved.

[34] H. H. Bolotin, A. C. Li, and A. Schwarzschild, Phys. Rev. **124**, 213 (1961), and H. Ikegami and T. Udagawa, Phys. Rev. **124**, 1518 (1961).

A. Beta-Decay Matrix Elements—Odd Mass

In the same fashion as with electromagnetic transitions, the effect of pairing correlations on the β-decay nuclear matrix elements may easily be determined. The simplest case to consider is a transition between two one-quasi-particle states. This will be a transition between an odd-proton and an odd-neutron nucleus, and will thus be between a neutron one-quasi-particle state and a proton one-quasi-particle state. The β operator O_β for the nuclear matrix element is of single-particle type $(b_p^\dagger b_n)$ or $(b_n^\dagger b_p)$ depending on whether $N \rightarrow P$ or $P \rightarrow N$ in the transition. The initial state is of the type $\alpha_n^\dagger|\psi_0\rangle$ or $\alpha_p^\dagger|\psi_0\rangle$, depending on whether the neutron or proton number is odd in the initial state. The final state is then of opposite type. The matrix element M may be evaluated in terms of the single-particle matrix element M_{sp} by performing the quasi-particle transformation on the operator $b^\dagger b$. [See Eq. (9)].

Four cases may be distinguished depending on the nuclear species involved:

(1) $N \rightarrow P$ odd jumping, (odd N even Z) $\rightarrow (N-1, Z+1)$, $M = U_n U_p M_{sp}$

(2) $P \rightarrow N$ odd jumping, (even N odd Z) $\rightarrow (N+1, Z-1)$, $M = U_n U_p M_{sp}$

(3) $N \rightarrow P$ even jumping, (even N odd Z) $\rightarrow (N-1, Z+1)$, $M = \mp V_n V_p M_{sp}$

(4) $P \rightarrow N$ even jumping, (odd N even Z) $\rightarrow (N+1, Z-1)$, $M = \mp V_n V_p M_{sp}$

In (3) and (4) the sign is plus or minus depending on whether the operator is odd or even under time reversal. These expressions differ from the reduction factors derived for electromagnetic transition owing to the fact that here (1) and (3) [or (2) and (4)] correspond to different transitions, while in the electromagnetic case, where the same particle merely changes levels, the corresponding (1) and (3) [or (2) and (4)] both contribute to the same transition, i.e., the even jumping and odd jumping both contribute to the same transition.

An absolute comparison of these reduction factors with experimental data would be quite difficult for medium to heavy nuclei. However, for a group of one-quasi-particle transitions all between the same quasi-particle levels, the entire dependence of the nuclear matrix element on the particular nuclear species (i.e., on A) should be contained in the reduction factors, the single-particle matrix element being common except for small changes due to the slow change in the shell-model well shape with A. Then for such a group of transitions (of allowed type), the comparative life (ft) value is proportional to M^{-2} so we should have, aside from the statistical factor (see below),

$$ft \propto (U_n U_p)^{-2} \text{ cases (1), (2), odd jumping,} \quad (99)$$

$$ft \propto (V_n V_p)^{-2} \text{ cases (3), (4), even jumping.} \quad (100)$$

One such group occurs in nuclei $115 \leqslant A \leqslant 141$ between the proton $d_{5/2}$ level and the neutron $d_{3/2}$ level (see Fig. 41.) The figure shows experimental log

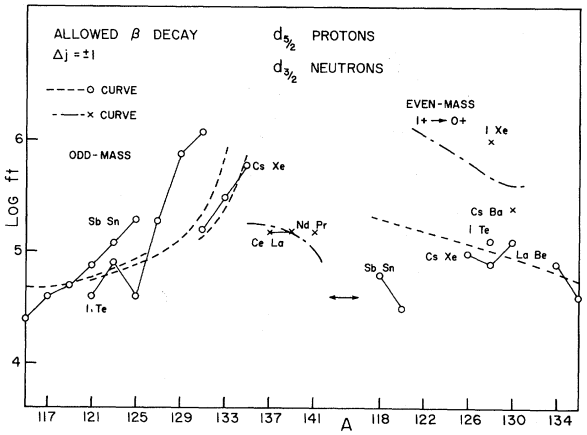

FIG. 41. Allowed transitions involving a $d_{5/2}$ proton and a $d_{3/2}$ neutron, odd mass and even mass. The o and × points are the experimental log ft values including the statistical factor for odd-jumping and even-jumping transitions, respectively, for the odd-mass points and for $P \rightarrow N$ and $N \rightarrow P$ transitions respectively for the odd-odd $\rightarrow$ even-even transitions. The dashed o curve and dot-dashed × curve are the corresponding theoretical curves log C/R^2, where R is the appropriate reduction factor $U_n U_p$ and $V_p V_n$, respectively, for the odd-mass cases and $V_n U_p$ and $U_n V_p$, respectively, for the even-mass cases. An arrow indicates the value log C chosen to fit both the even- and odd-mass data.

ft values minus log $\frac{1}{3}(2Ji+1)$ and compares them with the theoretical reduction factors log $C/(U_p U_n)^2$ and log $C/(V_p V_n)^2$. The normalization C is chosen for each level pair to fit the data for both the odd-mass and even-mass transitions (see Sec. B below). On each plot, a small arrow marks log C. The statistical factor $\frac{1}{3}(2J_i+1)$ is chosen so make the corresponding factor for the 1+-to-0+ transitions discussed below equal to unity. Most of the experimental ft values correspond to odd-jumping transitions. This is in general accord with the upward trend of log ft with increasing A, since filling levels means decreasing U's, and thus decreasing M and increasing ft. The few even-jumping transitions which occur for large-mass isotopes exhibiting this transition have lower ft values than the neighboring odd-jumping transitions. This is reasonable since both shells are nearly filled for these isotopes, i.e., $V > U$ and M even jumping $> M$ odd jumping.

For other level pairs there is much less systematic information. For $57 \leqslant A \leqslant 67$ there are a few cases of $p_{3/2}$–$p_{3/2}$ transitions (see Fig. 42). It is difficult to see the effect of the reduction factors with so few cases. Also, the excitation energy is high in some of the cases, involving a particle from the next shell, so there may well be appreciable three-quasi-particle and phonon admixtures to the wave function in those cases.

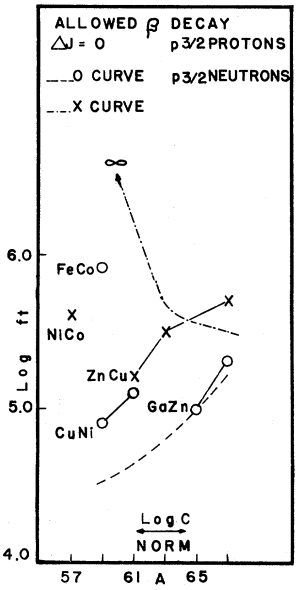

FIG. 42. Allowed transitions involving a $p_{3/2}$ neutron and proton, odd mass. The points and curves are as described in Fig. 41 odd-mass part.

For $69 \leqslant A \leqslant 87$ there are about a dozen cases of a transition between a proton $p_{3/2}$ level and the neutron $p_{1/2}$ level (see Fig. 43). For these, the trend, with one exception, is (with increasing A) increasing ft value for odd-jumping cases and decreasing ft value for even jumping as expected. For the exception, a particularly fast even-jumping case ${}_{32}Ge^{71}_{39}(\frac{1}{2}-)$ ${}_{31}Ga^{71}_{40}(\frac{3}{2}-)$ $\log ft = 4.3$, the low ft value may be due to exceptional purity (small phonon admixture) of the wave functions owing to the proximity of the nearly magic neutron number 40. The agreement here is only qualitative, but the normalization was chosen to fit the corresponding even-mass cases as well (see below).

Finally there are for $101 \leqslant A \leqslant 111$ a few cases of a transition between a $g_{9/2}$ proton and a $g_{7/2}$ neutron (see Fig. 44). The normalization of the theoretical curves was chosen as a compromise to fit these data and the more numerous even A (see following) cases.

These comparisons are valid only if the phonon component (or other three-or-more quasi-particle components) of the wave functions may be ignored or assumed to have an effect independent of mass number. Otherwise, the matrix elements to this part of the wave function must be included. However, such a calculation can not be done without essentially making an absolute evaluation of the matrix elements to various single-particle levels as the different levels will come in with different reduction factors.

There is also some systematic data for unique 1st-forbidden transitions. For $89 \leqslant A \leqslant 97$ there are a few transitions between a proton $p_{1/2}$ level and a neutron $d_{5/2}$ level (see Fig. 45). Even if the ft value can be used as a measure of the relative magnitudes of the matrix element, there are too few data to see a trend.

For $123 \leqslant A \leqslant 137$ there are a few transitions between a proton $g_{7/2}$ level and a neutron $h_{11/2}$ level (see Fig. 45). Once again there are too few data to believe the trend shown by the experimental points, although the even-jumping cases here are all lower than the odd-jumping cases.

B. Beta-Decay Matrix Elements—Even Mass

The large majority of even-mass decays proceed from the ground state of an odd–odd nucleus to the

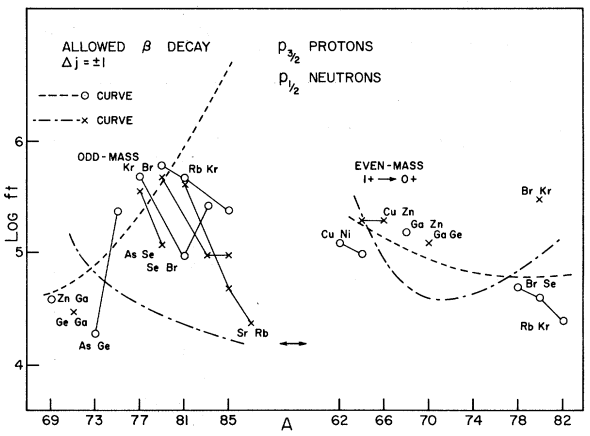

FIG. 43. Allowed transitions involving a $p_{3/2}$ proton and a $p_{1/2}$ neutron, odd mass and even mass. See caption of Fig. 41 for details.

0+ ground state or the 2+-or-higher vibrational state or a two-quasi-particle state of an adjacent even–even nucleus. By far the most abundant systematic data are for a transition from a 1+ state by allowed β decay to both the 0+ ground state and first excited 2+ state. For 27 transitions from $62 \leqslant A \leqslant 136$ the average log ft value is 4.9 for the 0+ transition and 5.5 for the 2+ transition. The spread of values is quite small (rms = 0.4 for 0+ case).

The initial state in this case is primarily a two-quasi-particle state of the type $(\alpha_n^\dagger\alpha_p^\dagger)^{1+}|\psi_0\rangle$ or a combination of such states. For the 0+ ground-state transition, the final state is primarily the quasi-particle vacuum $|\psi_0\rangle$. Thus we must distinguish two cases

$$(1)\ N \rightarrow P \text{ odd–odd} \rightarrow \text{even–even } M = U_n V_p M_{sp} \tag{101}$$

$$(2)\ P \rightarrow N \text{ odd–odd} \rightarrow \text{even–even } M = V_n U_p M_{sp} \tag{102}$$

where $M_{sp} = (1/\sqrt{3})\langle p||\sigma||n\rangle$. The operator here is the spin operator σ, and the neutron and proton levels must be spin-orbit partners. If in any cases the two-quasi-particles forming 1+ were not spin-orbit partners, i.e., having the same l value, the transition would be l forbidden and presumably have a larger ft value. There are three groups of nuclei corresponding to different probable levels for the neutron and proton (see Figs. 43, 44, and 41.)

	Proton Level	Neutron Level	Average log ft
$62 \leqslant A \leqslant 82$	$p_{3/2}$	$p_{1/2}$	4.95
$104 \leqslant A \leqslant 118$	$g_{9/2}$	$g_{7/2}$	4.73
$118 \leqslant A \leqslant 136$	$d_{5/2}$	$d_{3/2}$	4.98

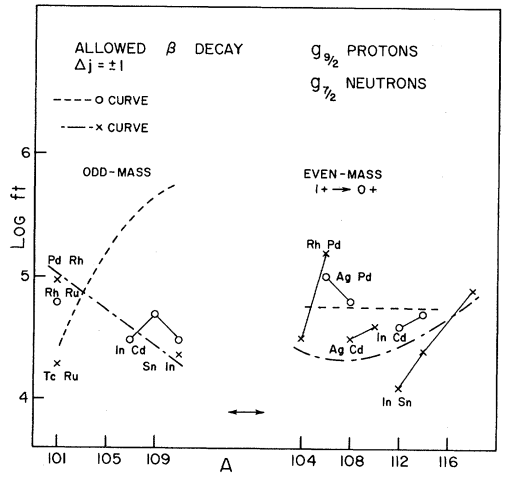

FIG. 44. Allowed transitions involving a $g_{9/2}$ proton and a $g_{7/2}$ neutron, odd mass and even mass. See caption of Fig. 41 for details.

The reduction factor UV does not vary greatly as U is a decreasing, and V an increasing function of A. The single-particle matrix element of σ does depend on the l value $\langle l,l+\frac{1}{2}||\sigma||l,l-\frac{1}{2}\rangle \propto \{[l(l+1)]/(2l+1)\}^{\frac{1}{2}}$ being larger for large l. Thus, the $g_{7/2} - g_{9/2}$ transitions should be fastest as they are. This argument makes the dubious assumption of the same overlap for neutron and proton wave functions for each set of quantum numbers. It also assumes pure quasi-particle wave functions. The constancy of the ft's indicates that any deviation from this picture must have a uniform effect independent of mass.

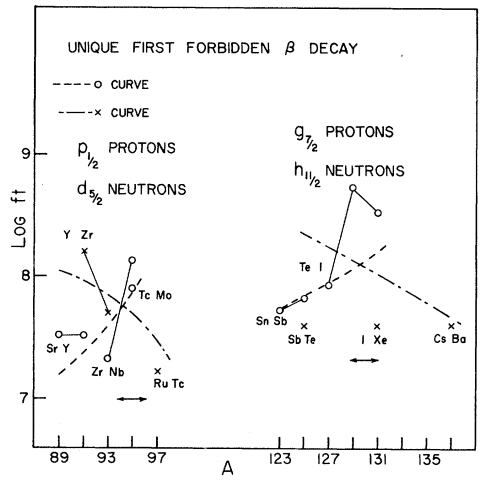

FIG. 45. Unique transitions involving a $p_{1/2}$ proton and a $d_{5/2}$ neutron, and unique transitions involving a $g_{7/2}$ proton and an $h_{11/2}$ neutron odd mass. For details see the caption of Fig. 41, odd-mass part.

Exactly the same reduced single-particle matrix element of σ occurs for these $1+ \rightarrow 0+$ transitions as in the one-quasi-particle $\rightarrow$ one-quasi-particle transitions previously described for the same N and P states as those making up the 1+ level. Thus, the theoretical reduction factor curves for corresponding single-particle states are plotted with the same normalization in the odd–even $\rightarrow$ even–odd cases as in the corresponding odd–odd $\rightarrow$ even–even plots. This same normalization works fairly well in both the even- and odd-mass cases implying that the reduced single-particle matrix elements are the same in the two cases. This is a nice verification of the quasi-particle picture for odd-mass nuclei and the proton and neutron-two-quasi-particle picture for odd–odd cases. It shows that the odd–odd quasi-particles are similar to the more familiar odd-mass quasi-particles.

The "Experimental Single Shell Model Particle Estimate" may be obtained by setting the reduction factor equal to unity. The value is marked on each figure by an arrow. This lifetime is about ten times the value obtained (from the neutron and O^{14} decay rates) on the assumption of perfect overlap between the neutron and proton orbital wave functions. The difference is largest for the heaviest nuclei. This dis-

crepancy may be due to lack of overlap between the pure n and p shell model states, the omission of coupling to phonons, and the omission of neutron–proton short-range forces.[35]

The matrix element $1+ \rightarrow 2+$ phonon state may easily be written in the QRPA approximation, but terms with different reduction factors for different quasi-particle levels are involved requiring an accurate knowledge of the n–p overlap of the different wave functions. For the 1-phonon transition for an $N \rightarrow P$ case, the matrix element is

$$M = \langle \psi_0 B | \sum_{\mathrm{p'n'}} \langle \mathrm{p'}|\sigma|\mathrm{n'}\rangle (U_{\mathrm{p'}}U_{\mathrm{n'}}\alpha^{\dagger}_{\mathrm{p'}}\alpha_{\mathrm{n'}} + V_{\mathrm{p'}}V_{\mathrm{n'}}\alpha^{\dagger}_{\mathrm{n'}}\alpha_{\mathrm{p'}}) \times |(\alpha^{\dagger}_{\mathrm{n}}\alpha^{\dagger}_{\mathrm{p}})^{1+}\psi_0\rangle . \quad (103)$$

Since n′, p′ are spin-orbit partners and for the cases considered there is also a large amplitude for n and p to be spin-orbit partners, the main contribution to the matrix element comes from those terms of the phonon amplitude with two identical protons or neutrons (in the initial p- or n- quasi-particle state) coupled to 2+. This will be but a fraction of the phonon amplitude, leading to a reduction of the matrix element compared to the ground state transition. The angular-momentum recoupling makes a further reduction.

The allowed transition to the two-phonon 2+ state may also be computed. This involves corrections to the Sawada commutation rules for the phonon operators and should thus be expected to give larger *ft* values than those for the one-phonon transition. This is in agreement with the experimental observations for higher-energy 2+ states.

All of the calculations for Figs. 41–45 have been made with the assumption of pure quasi-particle states. It is not easy to see *a priori* how the phonon interactions change the results because this depends upon which quasi-particles are admixed. However, a tendency might be expected for the isotopes closer to the closed shells to have smaller *ft* values in some cases, which seems to be borne out in some of the data.

IX. CONCLUSIONS

For nuclei with proton numbers besween 28 and 82, with the exception of the well-known deformed nuclei, we have calculated the low-energy states in a shell model with a pairing force between the neutrons and protons separately and a quadrupole force between all pairs of particles. The Bardeen approximation has been used to introduce the quasi-particles, which approximately diagonalize the pairing interaction, and the quasi-particle random phase or dilute quasi-particle approximation has been used to introduce the phonons, which approximately account for the interaction between the quasi-particles due to the quadrupole interaction. Studies are then carried out to see if the low-energy properties can be at least semiquantitatively understood in terms of these basic types of excitations.

In the even–even nuclei, the only states for which there are systematic experimental data are the collective states. For these nuclei one can approximately trace the extremely rapid drop of the first 2+ (one-phonon) state as one goes from the single-closed-shell cases until the energy of these vibrational levels is about one-fourth of the gap. At about this point the vibrations seem unstable in the theory and the accuracy is lost due to the large average number of quasi-particles mixed into the ground state. As one adds particles above the $N = 82$ closed shell, there is a very rapid drop in the phonon energy until at about neutron number 86 the spherical shape becomes unstable. Thus, for any reasonable choice of parameters, the deformation is expected to appear rather suddenly at around mass number 150. The transition into the deformed region above mass number 190 is much more gradual, so that one can make the theory predict, e.g., either that all of the Pt nuclei and, say, Os^{190} and Os^{192} are spherical, or that all of the Os nuclei are unstable and only the heaviest Pt nuclei are spherical, with moderate changes in the parameters.

Other possible regions of instability of spherical shape occur for either protons or neutrons near the middle of the $g_{9/2}$ shell and for the neutron deficient Xe and Ba isotopes. In these cases the tendency for deformation does not seem so strong, and with reasonable changes in the parameters one could find consistency with a spherical shape.

For the odd-mass isotopes the two basic excitations, the quasi-particles and the phonons, both appear in the states which we consider. Although for the single-closed-shell isotopes the quasi-particle states are the only ones for which there is systematic information, the states with one-phonon excitation enter the picture rather quickly when one has both neutrons and protons outside of the closed shells. For nuclei with mass numbers $100 \leqslant A \leqslant 150$ and $190 \leqslant A \leqslant 208$, the effects, often large, of the quadrupole interaction upon the quasi-particle spectrum improve the agreement with experiment in almost every case. The positions of levels which arise from pure quasi-particle states, and the energy at which

[35] The last point has been considered by L. Silverberg (private communication).

one begins to see states which arise from one-phonon and one-quasi-particle states (in the absence of the quasi-particle–phonon interaction) occur at approximately the energies given by experiment, within the accuracy expected by the simple forces and approximations used in this work. The coupling scheme seems to be maintained especially well for the isotopes from $_{50}$Sn to $_{60}$Nd and one can follow a number of interesting details of the spectra.

In the region below the Sn isotopes, the general coupling scheme seems to be completely adequate only for cases in which at least one kind of particle is near the 28, 38, 40, or 50 closed shell. The most striking discrepancy is the appearance of low-lying 7/2+ states in nuclei which in a pure shell model would be described as having three or five particles or holes in the $g_{9/2}$ level. This suggests that either the three quasi-particle states are playing an important role, or that the strong quadrupole interaction makes necessary a quite different coupling scheme. In many cases for $Z < 50$ and $N \geqslant 50$, such as the Ag isotopes, the other levels can be accounted for within the accuracy of the methods, but at this point one is very uncertain about the accuracy of the wave functions for these levels.

There is also evidence for the need of a neutron–proton interaction in addition to the quadrupole interaction. In the even isotopes this is suggested by the fact that the phonon energies for the single-closed-shell isotopes cannot be fitted with the same quadrupole parameters as apply for the cases with both neutrons and protons. The clearest evidence in the odd-mass isotopes is found in the cases with one and three particle away from the single closed shells, and in general tendencies for motion of certain effective single-particle levels with changes in the mass number. In addition, for the isotopes between Ni and Sr, the inclusion of a neutron–proton short-range force seems to be even more important because of the tendency for neutrons and protons to be in the same j levels.

Although there is a large body of accurate data on the magnetic dipole moments, one does not seem to be able to gain from this much systematic information about the details of the wave functions for spherical nuclei. One can see the effects of the seniority three admixtures, introduced by the short-range force, moving the values of the quasi-particle moments away from the single-particle values; but the results are rather insensitive to rather large admixtures of phonons. However, one interesting result is that the phonon admixtures can account for the deviation of the $p_{1/2}$ nuclei from the single-particle values, which is not possible with a δ-function interaction.

There are fewer systematic accurate data for the quadrupole moments and much more uncertainty in the calculation due to the large effects of the quadrupole force and the strong dependence upon the parameters. Using the no-phonon and one-phonon parts of the wave functions, the general systematic experimental trends of these moments are followed by the theoretical calculations, indicating that the most important physical effects seem to be accounted for. As more data accumulate, more nearly accurate calculations with further studies of the dependence upon the parameters would be useful.

The transition rates for the one-phonon E2 transitions are generally consistent with an effective charge of $2e$ for the proton and $1e$ for the neutron, but tend to become too large as the vibrations become softer. The crossover transitions from the two-phonon 2+ states are much more sensitive to the parameters, depending upon the microscopic makeup of the collective states in terms of the shell-model particles. However, further studies are needed in order to calculate accurately these as well as other effects such as the M1–E2 admixtures in terms of the microscopic structure.

The other electromagnetic transitions for which there are good systematic data, and which apparently can be easily interpreted, are the M4 transitions in odd-mass nuclei. For these the effects of the pairing correlations in mixing particle and hole transitions tend to maintain the single-particle transition rates and are in agreement with the systematic trends. One can also see the influence of the phonon interactions which can account for the further systematic reductions in the transition rates which are found as one leaves the single closed shells. In addition, there is a large body of systematic data on the β transitions involving only the σ operator, and the effects of the pairing correlations are in agreement with the systematic trends. By further calculations of transition rates with the states composed of quasi-particles and bosons, one will know in greater detail the accuracy of the coupling scheme which has been used in this work.

ACKNOWLEDGMENTS

One of the authors, L. S. K., wishes to thank the following laboratories for their hospitality during the course of part of this work: 1. University of Colorado, Institute for Theoretical Physics; 2. Radiation Laboratory, University of California; 3. Weizmann Institute, Rehovoth, Israel, where he was supported

by an E. J. fellowship, 1962–3; 4. Institute of Theoretical Physics, Copenhagen, Denmark. The other author, R. A. S., did part of this work while at the Aspen Institute of Physics, Aspen, Colorado. We wish to acknowledge helpful discussions with Dr. A. Bohr, Dr. B. Mottelson, and Dr. L. Silverberg.

We should also like to acknowledge the assistance of Mrs. M. Ratner in carrying out the numerical calculations, and the Case Institute of Technology for allowing us to use their computing facilities.

APPENDIX I

In this appendix we give the expressions for quasi-particles vector-coupled to form tensor operators with the usual (Condon–Shortley) phases. The double quasi-particle creation operator of rank L is defined as

$$A_{j_2j_1}^{LM\dagger} = \{ \sum_{\substack{m_1>0\\ m_2>0}} (-1)^{l_1+1} \alpha_{j_2m_2}^{\dagger} \alpha_{j_1m_1}^{\dagger} + \sum_{\substack{m_1<0\\ m_2>0}} (-1)^{j_1+m_1} \alpha_{j_2m_2}^{\dagger} \beta_{j_1-m_1}^{\dagger} + \sum_{\substack{m_1>0\\ m_2<0}} (-1)^{l_1+l_2+j_2+m_2} \beta_{j_2-m_2}^{\dagger} \alpha_{j_1m_1}^{\dagger} + \sum_{\substack{m_1<0\\ m_2<0}} (-1)^{l_2+j_1+j_2+m_1-m_2} \beta_{j_2-m_2}^{\dagger} \beta_{j_1-m_1}^{\dagger} \} C_{m_2m_1M}^{j_2j_1L}. \tag{A1}$$

The quasi-particle "scattering" operator of rank L is defined as

$$\eta_{j_2j_1}^{LM} = \{ \sum_{\substack{m_1>0\\ m_2>0}} (-1)^{l_1} \alpha_{j_2m_2}^{\dagger} \beta_{j_1m_1} + \sum_{\substack{m_1<0\\ m_2>0}} (-1)^{j_1+m_1} \alpha_{j_2m_2}^{\dagger} \alpha_{j_1-m_1} + \sum_{\substack{m_1>0\\ m_2<0}} (-1)^{l_1+l_2+j_2-m_2} \beta_{j_2-m_2}^{\dagger} \beta_{j_1m_1} + \sum_{\substack{m_1<0\\ m_2<0}} (-1)^{l_2+j_1+j_2+m_1-m_2} \beta_{j_2-m_2}^{\dagger} \alpha_{j_1-m_1} \} C_{m_2m_1M}^{j_2j_1L}. \tag{A2}$$

The commutation rules which are satisfied by these operators are

$$[A_{12}^{LM}, A_{34}^{L'M'\dagger}] = \delta_{LL'}\delta_{MM'}(\delta_{13}\delta_{24} - (-1)^{l_1+l_2+j_1+j_2}\delta_{14}\delta_{23}) + \text{terms in } \eta\,, \tag{A3}$$

and

$$[\eta_{12}^{SM'}, A_{34}^{LM\dagger}] = \sum_{S'} [(2L+1)(2S+1)]^{\frac{1}{2}} C_{MM'}^{LSS'} \times [\delta_{23} A_{14}^{S'M+M'\dagger} W(Sj_1Lj_4; j_2S') + (-1)^{l_1+j_1+l_3+j_3+1-L} \delta_{24} A_{13}^{S'M+M'\dagger} W(Sj_1Lj_3; j_2S')]\,. \tag{A4}$$

It is also possible to work directly with quasi-particles defined in terms of Condon–Shortley phases.[36]

APPENDIX II

In this appendix tables are given for the solution of the pairing equations, Eq. (4), and for the lowest few wave functions resulting from matrix diagonalization of the odd A, odd nucleon interacting with the phonon Eq. (47). A table is presented for the odd particles being in each of the major shells $28 \leqslant N \leqslant 50$, $50 \leqslant N \leqslant 82$, and $82 \leqslant N \leqslant 126$. (Tables VIII–XVI).

Within each shell the single-particle energies are given a smooth A dependence of the following form:

$$\epsilon_j(A) = \epsilon_j^0(A_0)(A_0/A)^{\frac{1}{3}} + \alpha_j(A_0/A)^{\frac{2}{3}}[1 - (A/A_0)^{\frac{1}{3}}] + \Delta\mathcal{E}_j(Z,N)\,. \tag{B1}$$

The first term gives the general $A^{-\frac{1}{3}}$ compression while the second term applies to spin orbit pairs. If in the shell both $j = l \pm \frac{1}{2}$ states are present,

$$\alpha_{l+\frac{1}{2}} = -(\epsilon_{l-\frac{1}{2}}^0(A_0) - \epsilon_{l+\frac{1}{2}}^0(A_0))l/(2l+1)\,, \tag{B2}$$

$$\alpha_{l-\frac{1}{2}} = +(\epsilon_{l-\frac{1}{2}}^0(A_0) - \epsilon_{l+\frac{1}{2}}^0(A_0))(l+1)/(2l+1)\,. \tag{B3}$$

If only one of the levels is present in the shell,

$$\alpha_{l+\frac{1}{2}} = -7A_0^{-\frac{2}{3}}l\,, \tag{B4}$$

or

$$\alpha_{l-\frac{1}{2}} = +7A_0^{-\frac{2}{3}}(l+1)\,. \tag{B5}$$

In addition in some regions, a special N- or Z- dependent shift was given to a level. This is indicated by the term $\Delta\mathcal{E}_j(Z, N)$. In order that the single-particle levels may easily be reconstructed by means of these formulas, or roughly by interpolation, the values of $\epsilon_j(A)$ are given for the beginning and end of each region. Furthermore, the special shifts $\Delta\mathcal{E}_j$ will be explicitly indicated for each region. The value of $G = \text{const} \times A^{-1}$ is also listed for each region.

In the tables, the first column lists the isotope species with its Z and N values and the next column the mass number. Columns 3 and 4 list the λ and Δ from which E_j, U_j, V_j, etc., may be computed. The remaining columns list the no-phonon and one-phonon amplitudes [see Eq. (54)] of the wave function of the lowest state or states of spin j listed in column 5.

[36] Ben Bayman (unpublished notes).

TABLE VIII. $28 \leq Z \leq 40$, $31 \leq N \leq 49$, $G = 24/A$. The single-particle neutron levels are (ϵ_j in MeV):

$f_{7/2}$	$p_{3/2}$	$f_{5/2}$	$p_{1/2}$	$g_{9/2}$	
−4.00	0.00	0.00	3.00	4.00	$A_0 = 58$
−3.27	0.11	−0.26	2.37	3.68	$A = 89$

Isotope	A	λ_n	Δ_n	j	C^j_{j00}	$C^j_{7/2\,12}$	$C^j_{5/2\,12}$	$C^j_{3/2\,12}$	$C^j_{1/2\,12}$	$C^j_{9/2\,12}$
28 Ni 31	59	−0.69	1.33	3/2	0.77	[a]	−0.20	0.36	0.37	
				5/2	0.76	[a]	0.39	0.18	−0.35	
28 Ni 33	61	−0.14	1.51	3/2	0.88	[a]	−0.06	0.20	0.37	
				5/2	0.89	[a]	0.10	0.05	−0.35	
28 Ni 35	63	0.45	1.48	3/2	0.90	[a]	0.17	−0.30	0.24	
				5/2	0.89	[a]	−0.35	−0.14	−0.20	
30 Zn 35	65	0.52	1.64	3/2	0.79	0.34	0.14	−0.35	0.19	
				5/2	0.81	0.14	−0.42	−0.25	−0.18	
30 Zn 37	67	1.27	1.38	3/2	0.73	0.31	0.19	−0.49	0.04	
				5/2	0.73	0.12	−0.53	−0.32	−0.03	
32 Ge 39	71	2.17	1.30	9/2	0.61					0.68
				1/2	0.68		0.36	0.50		
32 Ge 41	73	2.95	1.28	9/2	0.62					0.68
				1/2	0.67		0.39	0.48		
32 Ge 43	75	3.48	1.29	1/2	0.68		0.39	0.47		
32 Ge 45	77	3.90	1.19	1/2	0.69		0.39	0.45		
34 Se 41	75	2.94	1.22	5/2	0.38	0.07	−0.32	−0.22	0.67	
34 Se 43	77	3.46	1.24	1/2	0.70		0.38	0.46		
34 Se 45	79	3.88	1.16	1/2	0.75		0.37	0.42		
34 Se 47	81	4.23	0.95	1/2	0.81		0.34	0.38		
36 Kr 43	79	3.43	1.21	1/2	0.68		0.39	0.47		
36 Kr 45	81	3.85	1.13	1/2	0.79		0.35	0.40		
36 Kr 47	83	4.20	0.92	9/2	0.83					−0.52
36 Kr 49	85	3.71	0.00	9/2	0.66					−0.70
38 Sr 49	87	3.69	0.00	9/2	0.94					−0.33
40 Zr 49	89	3.67	0.00	9/2	0.99					−0.10

[a] For Ni the $f_{7/2}$ level was not included and G was increased to $26/A$.

TABLE IX. $36 \leq Z \leq 50$, $51 \leq N \leq 75$, $G = 23/A$. The single-particle neutron levels are (ϵ_j in MeV):

$d_{5/2}$	$g_{7/2}$	$s_{1/2}$	$h_{11/2}$	$d_{3/2}$	
−0.14	2.75	1.44	2.60	3.32	$A = 87 (Z = 37)$
0.00	0.80	1.30	2.50	2.80	$A_0 = 120$

Compared to the A_0 values the $g_{7/2}$ level is given a special shift $\Delta\epsilon_{7/2} = 0.14\,(50 - Z)$ MeV.

Isotope	A	λ_n	Δ_n	j	C^j_{j00}	$C^j_{7/2\,12}$	$C^j_{5/2\,12}$	$C^j_{3/2\,12}$	$C^j_{1/2\,12}$	$C^j_{11/2\,12}$
36 Kr 51	87	−0.14	0.00	5/2	0.83	−0.05	0.42	0.08	−0.28	
38 Sr 51	89	−0.13	0.00	5/2	0.99	−0.02	0.11	0.03	−0.07	
40 Zr 51	91	−0.12	0.00	5/2	0.98	−0.03	0.16	0.04	−0.12	
40 Zr 53	93	−0.26	0.81	5/2	0.95	−0.05	0.15	0.08	−0.24	
42 Mo 53	95	−0.26	0.81	5/2	0.93	−0.06	0.19	0.08	−0.27	
42 Mo 55	97	0.16	1.01	5/2	0.93	−0.06	−0.24	0.08	−0.23	
44 Ru 53	97	−0.27	0.81	5/2	0.92	−0.07	0.21	0.08	−0.28	
44 Ru 55	99	0.16	1.01	5/2	0.89	−0.09	−0.23	0.11	−0.33	
44 Ru 57	101	0.57	1.13	5/2	0.78	−0.05	−0.57	0.10	−0.09	
44 Ru 59	103	0.96	1.25	5/2	0.59	0.09	−0.56	0.01	0.42	
46 Pd 57	103	0.44	1.13	5/2	0.85	−0.05	−0.47	0.08	−0.14	
46 Pd 59	105	0.83	1.26	5/2	0.76	0.06	−0.56	0.05	0.21	
46 Pd 61	107	1.14	1.31	5/2	0.61	0.12	−0.51	0.02	0.47	
46 Pd 63	109	1.44	1.32	5/2	0.53	0.11	−0.47	0.01	0.56	
46 Pd 65	111	1.69	1.32	5/2	0.49	0.10	−0.46	−0.01	0.57	
48 Cd 59	107	0.70	1.27	5/2	0.84	0.05	−0.51	0.06	0.06	
				7/2	0.82	0.38	−0.03	−0.32		
48 Cd 61	109	1.01	1.30	5/2	0.76	0.12	−0.50	0.04	0.32	
				7/2	0.91	0.15	−0.08	−0.30		
				1/2	0.85		0.24	−0.39		
				3/2	−0.57	0.48	0.06	−0.33	−0.48	
48 Cd 63	111	1.31	1.31	5/2	0.66	0.14	−0.45	0.01	0.49	
				11/2	0.71					0.63
				1/2	0.85		0.36	−0.32		
				3/2	−0.61	0.38	0.05	−0.34	−0.53	
48 Cd 65	113	1.59	1.32	5/2	0.56	0.13	−0.42	−0.01	0.58	
				11/2	0.72					0.62
				1/2	0.83		0.45	−0.24		

TABLE IX. (*Continued*)

				3/2	0.62	−0.25	−0.04	0.37	0.56	
48 Cd 67	115	1.86	1.30	1/2	0.81		0.51	−0.12		
				11/2	0.75					0.60
50 Sn 59	109	0.58	1.21	1/2	0.93		−0.04	−0.34		
50 Sn 61	111	0.88	1.24	1/2	0.93		0.12	−0.32		
				7/2	0.98	−0.01	−0.06	−0.18		
50 Sn 63	113	1.18	1.25	1/2	0.93		0.24	−0.27		
				7/2	0.97	−0.18	−0.08	−0.13		
50 Sn 65	115	1.49	1.23	1/2	0.91		0.33	−0.20		
				3/2	0.85	−0.15	−0.01	0.36	0.32	
				11/2	0.87					0.47
50 Sn 67	117	1.79	1.22	1/2	0.91		0.38	−0.10		
				3/2	0.92	−0.01	0.03	0.36	0.16	
				11/2	0.91					0.40
50 Sn 69	119	2.07	1.20	1/2	0.92		0.38	−0.01		
				3/2	0.95	0.08	0.06	0.29	−0.01	
				11/2	0.96					0.26
50 Sn 71	121	2.34	1.17	1/2	0.91		0.37	0.14		
				3/2	0.96	0.13	0.08	0.20	−0.09	
				11/2	0.99					0.11
50 Sn 73	123	2.57	1.11	1/2	0.87		0.35	0.31		
				3/2	0.97	0.16	0.08	0.09	−0.15	
				11/2	0.99					0.06
50 Sn 75	125	2.79	1.03	1/2	0.84		0.30	0.43		
				3/2	0.97	0.16	0.07	−0.03	−0.15	
				11/2	0.98					0.18

APPENDIX III

We list in this appendix the matrix elements which are used in Chap. V for the calculation of the magnetic dipole moments.

(1) Matrix elements of the phonon angular momentum R_z:

$$\langle\psi_0\alpha_j|R_z|\alpha_j^\dagger\psi_0\rangle = 0\,, \tag{C1}$$

$$\langle\psi_0[\alpha_{j'}B]_{jm}|R_z|[\alpha_{j''}^\dagger B^\dagger]_{jm}\psi_0\rangle = \frac{m}{2}\frac{[6+j(j+1)-j'(j'+1)]}{j(j+1)}\delta_{j'j''}\,, \tag{C2}$$

$$\langle\psi_0[\alpha_{j'}(BB)^{J'}]_{jm}|R_z|[\alpha_{j''}^\dagger(B^\dagger B^\dagger)^J]_{jm}\psi_0\rangle = \frac{m}{2}\frac{[J(J+1)+j(j+1)-j'(j'+1)]}{j(j+1)}\delta_{j'j''}\delta_{JJ'}\,. \tag{C3}$$

(2) Matrix elements of the particle part of the magnetic moment operator:

$$\langle\alpha_{lj}|\mu_{\rm qp}|\alpha_{lj}^\dagger\rangle = \mu_{\rm sp}(lj) = jg_j = j\left\{\frac{[\frac{3}{4}+j(j+1)-l(l+1)]g_s+[l(l+1)+j(j+1)-\frac{3}{4}]g_l}{2j(j+1)}\right\}, \tag{C4}$$

$$\langle\psi_0[\alpha_{j'}B]_{jm}|\mu_{\rm qp}|[\alpha_{j'}^\dagger B^\dagger]_{jm}\psi_0\rangle = m\frac{[j(j+1)+j'(j+1)-6]}{2j(j+1)}g_{j'}\,, \tag{C5}$$

$$\langle\psi_0[\alpha_{ll\pm\frac{1}{2}}B]_{jm}|\mu_{\rm qp}|[\alpha_{ll\mp\frac{1}{2}}^\dagger B^\dagger]_{jm}\psi_0\rangle$$
$$= m\frac{[(l+j+\frac{7}{2})(l-j+\frac{5}{2})(l+j-\frac{3}{2})(j-l+\frac{5}{2})]^{\frac{1}{2}}}{2j(j+1)(2j+1)}(U_{l+\frac{1}{2}}U_{l-\frac{1}{2}}+V_{l+\frac{1}{2}}V_{l-\frac{1}{2}})(g_l-g_s)\,, \tag{C6}$$

$$\langle\psi_0[\alpha_{j'}(BB)^J]_{jm}|\mu_{\rm qp}|[\alpha_{j'}^\dagger(B^\dagger B^\dagger)^J]_{jm}\psi_0\rangle = m\frac{[j'(j'+1)+j(j+1)-J(J+1)]}{2j(j+1)}g_j\,, \tag{C7}$$

$$\langle\psi_0[\alpha_{ll\pm\frac{1}{2}}^\dagger(BB)^J]_{jm}|\mu_{\rm qp}|[\alpha_{ll\mp\frac{1}{2}}^\dagger(B^\dagger B^\dagger)^J]_{jm}\psi_0\rangle$$
$$= m(U_{l+\frac{1}{2}}U_{l-\frac{1}{2}}+V_{l+\frac{1}{2}}V_{l-\frac{1}{2}})\frac{[(J+l+j+\frac{3}{2})(J+l-j+\frac{1}{2})(j+l-J+\frac{1}{2})(J+j-l+\frac{1}{2})]^{\frac{1}{2}}}{(2l+1)j(j+1)}(g_l-g_s)\,. \tag{C8}$$

TABLE X. $52 \leq Z \leq 60$, $69 \leq N \leq 81$, $G = 23/A$. The single-particle neutron levels are (ϵ_j in MeV):

$d_{5/2}$	$g_{7/2}$	$s_{1/2}$	$h_{11/2}$	$d_{3/2}$	
0.00	0.80	1.30	2.50	2.80	$A_0 = 120$
0.06	0.69	1.23	2.44	2.57	$A = 141$

Isotope	A	λ_n	Δ_n	j	C^j_{j00}	$C^j_{7/2\,12}$	$C^j_{5/2\,12}$	$C^j_{3/2\,12}$	$C^j_{1/2\,12}$	$C^j_{11/2\,12}$
52 Te 69	121	2.06	1.17	1/2	0.77		0.56	0.03		
				3/2	0.80	0.18	0.13	0.48	−0.19	
				11/2	0.81					0.55
52 Te 71	123	2.32	1.15	1/2	0.77		0.52	0.23		
				3/2	0.81	0.24	0.13	0.33	−0.33	
				11/2	0.96					0.27
52 Te 73	125	2.56	1.09	1/2	0.74		0.44	0.43		
				3/2	0.87	0.26	0.12	0.12	−0.33	
				11/2	0.99					−0.11
52 Te 75	127	2.77	1.01	1/2	0.68		0.35	0.58		
				3/2	0.90	0.25	0.11	−0.09	−0.28	
				11/2	0.94					−0.34
54 Xe 73	127	2.54	1.07	1/2	0.66		0.49	0.43		
				3/2	0.68	0.30	0.15	0.06	−0.51	
				11/2	0.98					−0.17
54 Xe 75	129	2.75	0.99	1/2	0.61		0.39	0.59		
				3/2	0.76	0.30	0.13	−0.16	−0.41	
				11/2	0.85					−0.49
54 Xe 77	131	2.95	0.87	1/2	0.57		0.30	0.68		
				3/2	0.80	0.26	0.11	−0.31	−0.31	
				11/2	0.80					−0.55
54 Xe 79	133	3.13	0.70	1/2	0.54		0.23	0.74		
				3/2	0.85	0.22	0.09	−0.36	−0.23	
				11/2	0.82					−0.53
54 Xe 81	135	2.63	0.00	1/2	0.64		0.00	0.77		
				3/2	0.99	0.00	0.00	0.00	0.00	
				11/2	0.99					0.00
56 Ba 75	131	2.74	0.97	1/2	0.60		0.42	0.58		
				3/2	0.68	0.31	0.14	−0.19	−0.46	
				11/2	0.80					−0.56
56 Ba 77	133	2.93	0.86	1/2	0.56		0.32	0.68		
				3/2	0.76	0.28	0.12	−0.34	−0.34	
				11/2	0.76					−0.59
56 Ba 79	135	3.11	0.69	1/2	0.56		0.22	0.74		
				3/2	0.87	0.21	0.09	−0.33	−0.22	
				11/2	0.85					−0.50
56 Ba 81	137	2.61	0.00	1/2	0.79		0.05	0.61		
				3/2	0.99	0.03	0.01	−0.04	−0.03	
				11/2	0.99					−0.09
58 Ce 81	139	2.59	0.00	3/2	0.99	0.04	0.02	−0.04	−0.04	
				11/2	0.99					−0.10
60 Nd 81	141	2.57	0.00	3/2	0.99	0.03	0.01	−0.03	−0.03	
				11/2	0.99					−0.08

TABLE XI. $58 \leq Z \leq 62$, $83 \leq N \leq 87$, $G = 22/A$. The single-particle neutron levels are (ϵ_j in MeV):

$h_{9/2}$	$f_{7/2}$	$i_{13/2}$	$p_{3/2}$	$f_{5/2}$	$p_{1/2}$	
−0.84	−0.12	0.63	1.60	2.18	2.76	$A = 141$
−0.90	0.00	0.72	1.45	1.78	2.35	$A_0 = 207$

(the figure used a calculation with $\epsilon_{h9/2}$ one MeV higher).

Isotope	A	λ_n	Δ_n	j	C^j_{j00}	$C^j_{9/2\,12}$	$C^j_{7/2\,12}$	$C^j_{5/2\,12}$	$C^j_{3/2\,12}$	$C^j_{1/2\,12}$
58 Ce 83	141	−0.84	0.00	7/2	0.99	0.00	0.00	0.00	0.00	
60 Nd 83	143	−0.84	0.00	7/2	0.99	0.00	0.00	0.00	0.00	
60 Nd 85	145	−1.39	0.72	7/2	0.66	−0.15	0.56	0.07	−0.29	
				5/2	−0.32	0.74	0.18	−0.20	−0.13	0.12
				3/2	−0.44		0.66	0.12	−0.30	−0.16
60 Nd 87	147	−1.19	0.89	7/2	0.58	−0.10	0.55	0.08	−0.37	
				5/2	−0.37	0.57	0.25	−0.28	−0.25	0.21
				3/2	−0.44		0.60	0.13	−0.35	−0.20
62 Sm 85	147	−1.38	0.71	7/2	0.70	−0.16	0.55	−0.07	−0.27	
				5/2	−0.32	0.77	0.17	−0.19	−0.12	0.11
				3/2	−0.46		0.68	0.12	−0.28	−0.15
62 Sm 87	149	−1.18	0.87	7/2	0.61	−0.10	0.56	0.08	−0.35	
				5/2	−0.37	0.62	0.25	−0.26	−0.23	0.19
				3/2	−0.45		0.62	0.13	−0.33	−0.19

TABLE XII. $76 \leq Z \leq 82$, $111 \leq N \leq 125$, $G = 22/A$. The single-particle neutron levels are the same as in Table XI.

Isotope	A	λ_n	Δ_n	j	C^j_{j00}	$C^j_{7/2\,12}$	$C^j_{5/2\,12}$	$C^j_{3/2\,12}$	$C^j_{1/2\,12}$	$C^j_{13/2\,12}$
76 Os 113	189	1.28	0.87	3/2	0.45	0.22	−0.18	0.18	0.57	
76 Os 115	191	1.46	0.80	9/2	0.11	−0.01	0.80			
78 Pt 115	193	1.46	0.80	1/2	−0.58		0.60	0.46		
				3/2	0.81	0.28	−0.13	0.00	0.37	
				5/2	0.72	0.05	0.42	0.11	−0.40	
				13/2	0.65					−0.66
78 Pt 117	195	2.64	0.72	1/2	0.62		−0.61	−0.43		
				3/2	0.85	0.30	0.00	−0.29	0.22	
				5/2	0.85	0.06	0.29	0.01	−0.35	
				13/2	0.66					−0.66
78 Pt 119	197	2.81	0.63	1/2	0.73		−0.59	−0.29		
				3/2	0.85	0.26	0.11	−0.40	0.07	
				5/2	0.95	0.06	−0.01	−0.13	−0.21	
				13/2	0.70					−0.64
80 Hg 115	195	1.46	0.80	1/2	−0.65		0.57	0.46		
				3/2	0.95	0.19	−0.09	0.01	0.20	
				5/2	0.89	0.03	0.32	0.09	−0.25	
				13/2	0.82					−0.53
80 Hg 117	197	1.64	0.71	1/2	0.70		−0.58	−0.37		
				3/2	0.94	0.22	0.00	−0.19	0.14	
				5/2	0.94	0.04	0.20	0.00	−0.23	
				13/2	0.78					−0.57
80 Hg 119	199	1.81	0.63	1/2	0.77		−0.57	−0.23		
				3/2	0.88	0.23	0.11	−0.36	0.07	
				5/2	0.97	0.05	0.00	−0.10	−0.19	
				13/2	0.74					−0.60
80 Hg 121	201	1.98	0.53	1/2	0.95		−0.28	0.06		
				3/2	0.85	0.20	0.22	−0.39	−0.03	
				5/2	0.95	0.05	−0.23	−0.15	−0.07	
				13/2	0.76					−0.59
80 Hg 123	203	2.17	0.38	1/2	0.97		0.14	0.16		
				3/2	0.82	0.16	0.31	−0.35	−0.24	
				5/2	0.91	0.05	−0.36	−0.13	0.08	
				13/2	0.81					−0.54
82 Pb 115	197	1.46	0.79	3/2	0.99	0.12	−0.04	0.01	0.10	
				5/2	0.98	0.02	0.14	0.04	−0.13	
				13/2	0.97					−0.26
82 Pb 117	199	1.64	0.71	3/2	0.99	0.11	0.00	−0.06	0.05	
				5/2	0.99	0.02	0.07	0.00	−0.09	
				13/2	0.97					−0.24
82 Pb 119	201	1.81	0.62	3/2	0.99	0.09	0.03	−0.09	0.02	
				5/2	0.99	0.02	0.00	−0.02	−0.05	
				13/2	0.98					−0.20
82 Pb 121	203	1.98	0.52	3/2	0.99	0.08	0.06	−0.10	−0.01	
				5/2	0.99	0.02	−0.05	−0.03	−0.02	
				13/2	0.98					−0.17
82 Pb 123	205	2.17	0.38	1/2	0.99		0.02	0.03		
				3/2	0.99	0.05	0.07	−0.09	−0.05	
				5/2	0.99	0.01	−0.08	−0.03	0.01	
				7/2	−0.03	0.00	0.99	−0.01		
				9/2	0.04	0.00	0.99			
				13/2	0.99					−0.13
82 Pb 125	207	2.35	0.00	1/2	0.99		0.00	0.00		

TABLE XIII. $29 \leq Z \leq 39$, $34 \leq N \leq 50$, $G = 24/A$. The single-particle proton levels are (ϵ_j in MeV):

$f_{7/2}$	$f_{5/2}$	$p_{3/2}$	$p_{1/2}$	$g_{9/2}$			
−4.15	0.87	−0.08	2.18	2.95	$Z = 30$	$N = 34$	
−4.60	−0.60	0.00	1.80	2.80	$Z = 40$	$N = 50$	$A_0 = 90$.

A special shift $\Delta\varepsilon_{7/2} = \Delta\varepsilon_{5/2} = -0.11\,(N - 40)$ is included so that $\epsilon^0_{7/2}(A_0) = -3.50$ and $\epsilon^0_{5/2}(A_0) = +0.50$.

Isotope	A	λ_p	Δ_p	j	C^j_{j00}	$C^j_{7/2\,12}$	$C^j_{5/2\,12}$	$C^j_{3/2\,12}$	$C^j_{1/2\,12}$
29 Cu 34	63	−0.08	0.00	3/2	0.85	[a]	−0.20	0.33	0.28
29 Cu 36	65	−0.08	0.00	3/2	0.84	[a]	−0.21	0.32	0.30
31 Ga 36	67	−0.40	1.47	3/2	0.79	0.21	−0.18	0.19	0.40
31 Ga 38	69	−0.38	1.42	3/2	0.74	0.21	−0.18	0.20	0.44
33 As 40	73	0.20	1.52	3/2	0.71	0.35	−0.05	−0.27	0.37
33 As 42	75	0.09	1.45	3/2	0.67	0.32	−0.04	−0.19	0.44
33 As 44	77	−0.02	1.38	3/2	0.74	0.27	−0.04	−0.07	0.44
35 Br 42	77	0.59	1.48	3/2	0.66	0.35	0.10	−0.51	0.15
35 Br 44	79	0.46	1.29	3/2	0.77	0.28	0.13	−0.44	0.19

TABLE XIII. (*Continued*)

35 Br 46	81	0.33	1.30	3/2	0.85	0.23	0.14	−0.33	0.20
35 Br 48	83	0.20	1.20	3/2	0.92	0.19	0.12	−0.19	0.19
37 Rb 48	85	0.77	1.04	3/2	0.88	0.17	0.17	−0.38	0.05
				5/2	0.85	0.06	−0.45	−0.22	−0.01
37 Rb 50	87	0.68	0.93	3/2	0.92	0.16	0.14	−0.30	0.06
				5/2	0.89	0.06	−0.40	−0.19	−0.01
39 Y 50	89	1.47	0.95	1/2	0.99		0.11	0.12	

[a] For Cu the $f_{7/2}$ level was not included and G increased to $26/A$.

TABLE XIV. $37 \leq Z \leq 49$, $50 \leq N \leq 70$, $G = 26/A$. The single-particle proton levels are (ϵ_j in MeV):

$f_{5/2}$	$p_{3/2}$	$p_{1/2}$	$g_{9/2}$	
0.00	0.60	1.80	3.40	$A_0 = 90$
−0.10	0.58	1.60	2.30	$A = 115$

A special shift $\Delta\epsilon_{9/2} = -0.055\,(N - 50)$ is included.

Isotope	A	λ_p	Δ_p	j	C^j_{j00}	$C^j_{5/2\,12}$	$C^j_{3/2\,12}$	$C^j_{1/2\,12}$	$C^j_{9/2\,12}$
37 Rb 50	87	1.35	0.96	3/2	0.97	0.12	−0.21	0.03	
39 Y 50	89	1.84	0.86	1/2	0.99	0.09	0.09		
41 Nb 50	91	2.54	0.88	1/2	0.98	0.13	0.15		
				9/2	0.98				0.17
41 Nb 52	93	2.46	0.88	1/2	0.88	0.29	0.34		
				9/2	0.84				0.50
41 Nb 54	95	2.37	0.88	1/2	0.85	0.32	0.37		
				9/2	0.81				0.55
43 Tc 52	95	2.94	0.98	9/2	0.96				0.28
43 Tc 54	97	2.83	0.97	9/2	0.93				0.37
43 Tc 56	99	2.71	0.97	9/2	0.90				0.42
43 Tc 58	101	2.60	0.96	9/2	0.81				0.55
45 Rh 56	101	3.05	0.91	1/2	0.76	0.37	0.43		
				9/2	0.99				−0.17
45 Rh 58	103	2.93	0.90	1/2	0.73	0.38	0.45		
				9/2	0.98				−0.21
45 Rh 60	105	2.82	0.89	1/2	0.69	0.40	0.46		
				9/2	0.95				−0.29
47 Ag 58	105	3.23	0.75	1/2	0.77	0.36	0.43		
47 Ag 60	107	3.11	0.75	1/2	0.76	0.36	0.44		
47 Ag 62	109	2.99	0.74	1/2	0.75	0.37	0.44		
47 Ag 64	111	2.87	0.73	1/2	0.73	0.38	0.45		
47 Ag 66	113	2.75	0.73	1/2	0.70	0.39	0.46		
49 In 62	111	2.60	0.00	1/2	0.87	0.29	0.35		
				9/2	0.85				−0.49
49 In 64	113	2.48	0.00	1/2	0.88	0.29	0.35		
				9/2	0.86				−0.48
49 In 66	115	2.36	0.00	1/2	0.87	0.29	0.35		
				9/2	0.86				−0.49
49 In 68	117	2.24	0.00	1/2	0.87	0.29	0.35		
				9/2	0.86				−0.48
49 In 70	119	2.12	0.00	1/2	0.89	0.27	0.33		
				9/2	0.87				−0.47

TABLE XV. $51 \leq Z \leq 61$, $64 \leq N \leq 88$, $G = 231A$. The single-particle proton levels are (ϵ_j in MeV):

$g_{7/2}$	$d_{5/2}$	$h_{11/2}$	$d_{3/2}$	$s_{1/2}$	
0.26	0.78	2.29	3.45	3.59	$A = 115$
0.00	0.80	2.10	2.60	2.95	$A_0 = 207$

Isotope	A	λ_p	Δ_p	j	C^j_{j00}	$C^j_{7/2\,12}$	$C^j_{5/2\,12}$	$C^j_{3/2\,12}$	$C^j_{1/2\,12}$
51 Sb 64	115	0.26	0.00	7/2	0.87	0.43	0.12	−0.15	
				5/2	0.81	−0.18	0.47	0.10	−0.19
51 Sb 66	117	0.25	0.00	7/2	0.86	0.43	0.12	−0.16	
				5/2	0.80	−0.19	0.48	0.10	−0.19
51 Sb 68	119	0.24	0.00	7/2	0.87	0.43	0.11	−0.15	
				5/2	0.80	−0.19	0.47	0.10	−0.19
51 Sb 70	121	0.23	0.00	7/2	0.88	0.41	0.11	−0.14	
				5/2	0.82	−0.19	0.46	0.09	−0.17
51 Sb 72	123	0.23	0.00	7/2	0.89	0.40	0.10	−0.13	
				5/2	0.83	−0.20	0.45	0.09	−0.16
51 Sb 74	125	0.22	0.00	7/2	0.90	0.38	0.10	−0.12	
				5/2	0.84	−0.20	0.44	0.08	−0.15
53 I 72	125	−0.15	0.69	7/2	0.73	0.52	0.20	−0.22	

TABLE XV. (*Continued*)

				5/2	0.64	−0.18	0.57	0.11	−0.25
				1/2	−0.37		0.71	0.29	
53 I 74	127	−0.15	0.68	7/2	0.79	0.49	0.18	−0.20	
				5/2	0.69	−0.18	0.56	0.10	−0.22
				1/2	−0.37		0.74	0.27	
53 I 76	129	−0.14	0.67	7/2	0.85	0.44	0.14	−0.17	
				5/2	0.73	−0.18	0.54	0.10	−0.19
53 I 78	131	−0.14	0.65	7/2	0.91	0.36	0.11	−0.14	
				5/2	0.80	−0.18	0.49	0.09	−0.17
55 Cs 74	129	0.10	0.81	7/2	0.74	0.27	0.37	−0.28	
				5/2	0.64	−0.11	0.56	0.12	−0.29
				1/2	−0.39		0.71	0.31	
55 Cs 76	131	0.10	0.79	7/2	0.88	0.22	0.25	−0.23	
				5/2	0.71	−0.11	0.55	0.11	−0.25
				1/2	−0.38		0.74	0.28	
55 Cs 78	133	0.10	0.77	7/2	0.96	0.14	0.13	−0.16	
				5/2	0.79	−0.11	0.50	0.10	−0.20
				1/2	−0.38		0.78	0.24	
55 Cs 80	135	0.10	0.76	7/2	0.99	0.06	0.05	−0.09	
				5/2	0.93	−0.08	0.32	0.07	−0.12
55 Cs 82	137	0.10	0.74	7/2	0.99	0.01	0.01	−0.01	
				5/2	0.99	−0.01	0.05	0.01	−0.02
57 La 80	137	0.35	0.82	7/2	0.99	−0.13	−0.02	−0.08	
				5/2	0.94	−0.03	0.27	0.08	−0.14
				1/2	−0.40		0.85	0.18	
57 La 82	139	0.35	0.80	7/2	0.99	−0.02	0.00	−0.02	
				5/2	0.99	−0.01	0.04	0.01	−0.03
59 Pr 82	141	0.60	0.82	7/2	0.99	−0.04	0.00	−0.01	
				5/2	0.99	0.00	0.02	0.01	−0.02
59 Pr 84	143	0.60	0.80	5/2	0.90	0.03	0.27	0.13	−0.25
				7/2	0.86	−0.47	−0.04	−0.10	
61 Pm 84	145	0.88	0.77	5/2	0.96	−0.09	−0.08	0.11	−0.19
				7/2	0.82	−0.52	−0.09	−0.07	
61 Pm 86	147	0.88	0.75	5/2	0.90	0.12	−0.10	0.15	−0.30
				7/2	0.71	−0.63	−0.08	−0.08	
61 Pm 88	149	0.88	0.74	5/2	0.64	0.08	−0.01	0.21	−0.50
				7/2	0.58	−0.68	−0.06	−0.09	

TABLE XVI. $77 \leq Z \leq 81$, $114 \leq N \leq 126$, $G = 23/A$. The single-particle proton levels are the same as in Table XV.

Isotope	A	λ_p	Δ_p	j	C^j_{j00}	$C^j_{7/2\ 12}$	$C^j_{5/2\ 12}$	$C^j_{3/2\ 12}$	$C^j_{1/2\ 12}$	$C^j_{11/2\ 12}$
77 Ir 114	191	2.72	0.49	1/2	0.72		0.17	−0.63		
				3/2	0.87	0.22	0.12	−0.08	0.35	
77 Ir 116	193	2.71	0.48	1/2	0.75		0.16	−0.61		
				3/2	0.89	0.20	0.11	−0.08	0.33	
79 Au 116	195	2.89	0.38	1/2	0.95		0.18	0.22		
				3/2	0.87	0.14	0.09	−0.42	−0.11	
				5/2	−0.15	0.00	0.04	0.86	−0.29	
				11/2	0.68					−0.65
79 Au 118	197	2.88	0.37	1/2	0.96		0.16	0.19		
				3/2	0.89	0.13	0.09	−0.40	−0.10	
				5/2	−0.14	0.00	0.03	0.86	−0.29	
				11/2	0.70					−0.64
79 Au 120	199	2.86	0.37	1/2	0.97		0.15	0.16		
				3/2	0.90	0.12	0.08	−0.38	−0.09	
				5/2	−0.13	0.00	0.03	0.87	−0.30	
				11/2	0.72					−0.62
81 Tl 118	199	2.99	0.00	1/2	0.99		0.07	0.12		
				3/2	0.97	0.06	0.04	−0.16	−0.16	
				5/2	0.11	0.00	−0.02	−0.06	0.98	
				11/2	0.98					−0.22
81 Tl 120	201	2.98	0.00	1/2	0.99		0.06	0.12		
				3/2	0.97	0.05	0.04	−0.16	−0.16	
				5/2	0.09	0.00	−0.01	−0.05	0.98	
				11/2	0.98					−0.21
81 Tl 122	203	2.97	0.00	1/2	0.99		0.05	0.09		
				3/2	0.98	0.04	0.03	−0.13	−0.14	
				5/2	0.06	0.00	−0.01	−0.03	0.99	
				11/2	0.99					−0.17
81 Tl 124	205	2.96	0.00	1/2	0.99		0.02	0.05		
				3/2	0.99	0.02	0.01	−0.07	−0.09	
				5/2	0.03	0.00	0.00	0.01	0.99	
				11/2	0.99					−0.09
81 Tl 126	207	2.95	0.00							